

ELECTRONIC STRUCTURE OF PI-ELECTRON  
MOLECULES: HYDROCARBONS, QUINONES,  
THERMOCHROMIC ETHYLENES (NMR, ESR)

by

Peter Jeremy Schultz

Thesis submitted to the Graduate Faculty of the  
Virginia Polytechnic Institute and State University  
in partial fulfillment of the requirements for the degree of

DOCTOR OF PHILOSOPHY

in

Chemistry

APPROVED:

\_\_\_\_\_  
Chairman, John C. Schug

\_\_\_\_\_  
A. F. Clifford

\_\_\_\_\_  
T. C. Ward

\_\_\_\_\_  
J. G. Dillard

\_\_\_\_\_  
J. P. Wightman

June, 1972

Blacksburg, Virginia

## II. ACKNOWLEDGMENTS

The author expresses his deep appreciation to Dr. John C. Schug for his guidance and instruction of more than the research reported here. The author also expresses his appreciation to the members of the chemistry faculty at Virginia Polytechnic Institute and State University and fellow graduate students who took an interest in this problem. In particular, discussions with Dr. Michael Ogliaruso were enlightening. Acknowledgment is also due to the National Aeronautics and Space Administration for their support of this research.

#

III. TABLE OF CONTENTS

	Page
I. TITLE	i
II. ACKNOWLEDGMENTS	ii
III. TABLE OF CONTENTS	iii
IV. LIST OF TABLES	vi
V. LIST OF FIGURES	vii
VI. INTRODUCTION	1
VII. THEORETICAL METHOD	13
A. The Electronic Energy	13
B. The LCAO Approximation	22
C. The Pi-Electron Approximation	24
D. Basic Parameters	26
VIII. THEORETICAL CALCULATIONS: HYDROCARBONS, QUINONES	28
A. Hydrocarbons	30
1. Benzene	30
2. Naphthalene and Anthracene	33
3. <u>Trans</u> -Stilbene and <u>Cis</u> -Stilbene	34
4. Dihydrophenanthrene Intermediate	36
B. <u>p</u> -Quinones and Anthrone	38
1. <u>p</u> -Benzoquinone	39
2. 9,10 Anthraquinone	40
3. <u>p</u> -Naphthaquinone and Anthrone	42
C. Discussion	44

	Page
IX. THEORETICAL CALCULATIONS: THERMOCHROMIC ETHYLENES	49
A. Compounds and Bridged Structures	51
1. 10,10'-Bianthronylidene	51
2. 10,10'-Bixanthenylidene	53
3. Diphenylmethylenanthrone	53
4. Bifluorenylidene	54
B. Other Structures	55
1. Helianthrone and Mesonaphthobianthrone	55
2. Dihydrobianthrone and Dihydrohelianthrone	56
3. 10,10'-Bianthronylidene Double Bridge Structure	57
4. Protonated Structures	57
5. Betaines	57
C. Discussion	58
X. EXPERIMENTAL	61
A. Spectra Simulator Programs	62
B. Instrumentation	62
C. Materials and Purification	63
D. Anthrone	64
E. Anthraquinone	66
F. 10,10'-Bianthronylidene and 2,7'-Dimethyl- 10,10'-Bianthronylidene	67
G. 10,10'-Bianthranyl	71
H. 10,10'-Bixanthenylidene	73
I. Diphenylmethylenanthrone	75

	Page
J. Summary	76
XI. CONCLUSION	80
XII. BIBLIOGRAPHY	135
XIII. VITA	138

#### IV. LIST OF TABLES

	Page
I. Benzene Calculations; Mono-Excited CI	83
II. Benzene Calculations; Doubly Excited CI	84
III. Naphthalene Calculations; Mono-Excited CI	85
IV. Anthracene Calculations; Mono-Excited CI	86
V. Naphthalene Calculations; Doubly Excited CI	87
VI. Anthracene Calculations; Doubly Excited CI	88
VII. Stilbene Calculations	89
VIII. Dihydrophenanthrene Calculations	90
IX. <u>p</u> -Benzoquinone Calculations	91
X. Anthraquinone Calculations	93
XI. <u>p</u> -Naphthaquinone Calculations	95
XII. Anthrone Calculations	96
XIII. 10,10'-Bianthronylidene Calculations	97
XIV. 10,10'-Bixanthenylidene Calculations	98
XV. Diphenylmethyleneanthrone Calculations	99
XVI. Bifluorenylidene Calculations	100
XVII. Helianthrone Calculations	101
XVIII. Dihydrobianthrone, Dihydrohelianthrone, and Mesonaphthobianthrone Calculations	102
IXX. Double Bridge Structure of 10,10'-Bianthronylidene	103
XX. Protonated Compounds	104
XXI. Protonated Bridge Structures	105
XXII. Bond Resonance Integral Values	106

## V. LIST OF FIGURES

	Page
1. Effect of $\gamma_{CC}$ on energy levels of benzene.	107
2. Effect of $\beta_{CC}$ on energy levels of benzene.	108
3. <u>Trans</u> -stilbene, <u>cis</u> -stilbene, and dihydrophenanthrene intermediate.	109
4. <u>p</u> -Quinones and anthrone.	110
5. 10,10'-Bianthronylidene structures.	111
6. 10,10'-Bixanthenylidene structures.	112
7. Diphenylmethylenanthrone structures.	113
8. Bifluorenylidene structures.	114
9. Helianthrone structures and mesonaphthobianthrone.	115
10. 10,10'-Bianthranyl and 10,10'-bianthranyl radical.	116
11. Dihydrobianthrone and hydrobianthrone radical.	117
12. NMR spectrum of anthrone in $D_2SO_4$ ; sweep width 9.00 ppm.	118
13. NMR spectrum of anthraquinone in $CDCl_3$ ; sweep width 1.85 ppm.	119
14. NMR spectrum of 10,10'-bianthronylidene in $CDCl_3$ ; sweep width 1.85 ppm.	120
15. NMR spectrum of 2,7'-dimethyl-10,10'-bianthronylidene melt in $CDCl_3$ ; sweep width 9.00 ppm.	121
16. NMR spectrum of regenerated 2,7'-dimethyl-10,10'-bianthronylidene in $CDCl_3$ ; sweep width 9.00 ppm.	122
17. ESR spectrum of hydrobianthrone radical in $CHCl_3$ at $-75^\circ C$ ; sweep width 40 gauss.	123
18. ESR spectrum of hydrobianthrone radical in pyridine; sweep width 20 gauss.	124
19. Simulation of ESR spectrum of hydrobianthrone radical; length 15.535 gauss.	125

	Page
20. NMR spectrum of 10,10'-bixanthenylidene in CDCl <sub>3</sub> ; sweep width 1.85 ppm.	126
21. Simulation of NMR spectrum of 10,10'-bixanthenylidene in CDCl <sub>3</sub> , room temperature.	127
22. NMR spectrum of 10,10'-bixanthenylidene in decalin at 176°C; sweep width 1.85 ppm.	128
23. Simulation of NMR spectrum of 10,10'-bixanthenylidene in decalin at 176°C.	129
24. NMR spectrum of diphenylmethylenanthrone in CDCl <sub>3</sub> ; sweep width 1.85 ppm.	130
25. NMR spectrum of diphenylmethylenanthrone in CDCl <sub>3</sub> ; sweep width 0.92 ppm.	131
26. NMR spectrum of diphenylmethylenanthrone melt; sweep width 9.00 ppm.	132
27. NMR spectrum of diphenylmethylenanthrone in decalin at 100°C; sweep width 0.92 ppm.	133
28. NMR spectrum of diphenylmethylenanthrone in decalin at 180°C; sweep width 0.92 ppm.	134

## VI. INTRODUCTION

The Pariser-Parr-Pople (PPP) method has been widely applied to the calculation of ground and excited state properties of hydrocarbons with pi-electron systems.<sup>43,47,53</sup> The extension to molecules containing heteroatoms has received increasing attention.<sup>17,43</sup> The success of these calculations encourages the belief that the general approach is useful. The method has been most successful in generally predicting observed trends of a specific property within a series of closely related structures, e.g., the polyacenes.<sup>47</sup> Reasonable results have been reported in predicting a number of properties, e.g., charge distributions, ionization potentials, and pi-electron excitation energies for substituted benzene compounds.<sup>48</sup> However the method has failed seriously when widely differing molecules were considered, e.g., the pi-electron excitation energies of conjugated carbonyl compounds were uniformly too high.<sup>12</sup>

Inherent within the method is the use of configuration interaction (CI) in representing the electronic states of a particular molecule. Basically, the CI treatment is a means of introducing electron correlation into the molecular orbital wavefunction. The importance of configuration interaction has been reviewed and further studied by Allinger and Stuart.<sup>2</sup> The CI procedure commonly includes interactions only among singly excited configurations. Relatively few results have been reported which make use of doubly excited configurations, probably

since the mathematical formulation is lengthy and hence time-consuming. The number of excited states increases formidably on including configurations which represent the simultaneous excitation of two electrons. For example, 45 doubly excited states are included for a six pi-electron system such as benzene whereas only nine singly excited states are possible. In the present work molecules with from 10 to 30 pi-electrons (e.g., naphthalene and 10,10'-bianthrnylidene, respectively) were studied using singly and doubly excited states and it was impossible to include all of the configurations. Consequently several molecules with known electronic absorption spectra were analyzed to help determine how many configurations are needed and how they should be distributed between the singly and doubly excited states. This was necessary in order to confidently predict spectra which are not known experimentally or to gain information about observed absorption bands whose assignments are in doubt. A CI matrix with 80 total configurations of excitation energies up to 11.0 eV, one-half of them representing each type, was found to be satisfactory.

Reports of calculations involving doubly excited states have concentrated on their effects but have not studied the method particularly from the standpoint of fitting calculated results to experiment, e.g., in the case of benzene.<sup>29,30</sup> Good results have been obtained for benzene, naphthalene, and anthracene with the PPP method when only singly excited states were used.<sup>43</sup> These compounds were studied with the extended CI procedure to

see whether comparable results could be obtained.

Some important conclusions have been made concerning the use of the extended CI method and the results obtained from it previous to this study. For example:

(1) Theoretically (PPP) the singlet state of the croconate anion is found to be the ground state in agreement with experiment.<sup>46</sup>

The calculation including only singly excited configurations produced a triplet ground state.<sup>46</sup>

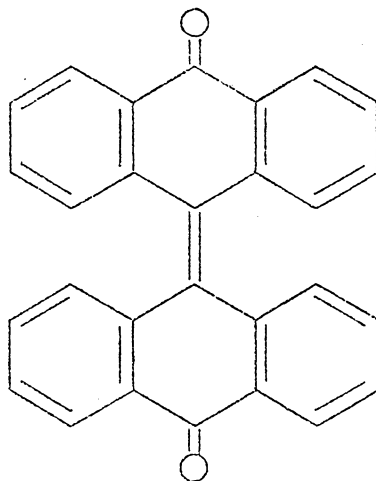
(2) Improved coincidence between the theoretical and observed values for the transition energies and transition moments of pyridine, phenol, aniline, pyrrole, and furan was obtained by Hirota and Nagakura.<sup>17</sup> After selecting optimized values for the parameters employed in the PPP method, they made comparisons between the results obtained using singly excited configurations (MCI) with those including doubly excited configurations (DCI). They found that the inclusion of doubly excited states removed some difficulties in the application of the PPP method to molecules containing heteroatoms.<sup>17</sup>

(3) The character of the singlet spectrum of benzene changed significantly on including higher excited configurations.<sup>29</sup>

(4) Allinger and Stuart reported that it is not necessary to include all of the doubly excited configurations.<sup>2</sup> They found that those configurations with excitation energies greater than 20 eV above the ground configuration could be excluded without affecting the resulting transition energies by more than 0.2 eV.

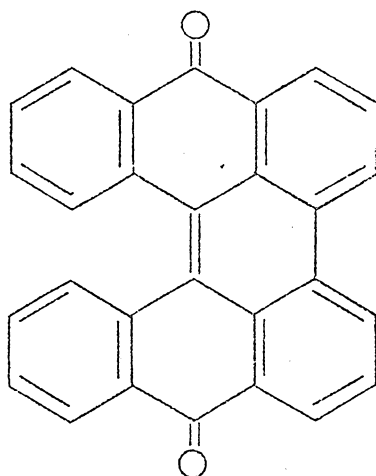
This would still require a large number of doubly excited configurations (e.g., over 200 for naphthalene) which presents a grave problem even for the large, high-speed computer.<sup>2</sup>

The interest in extended CI calculations arose from our studies of thermochromic ethylenes. The compound which has received the most attention is 10,10'-bianthrnylidene which is shown below.



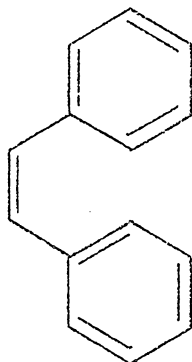
Most of the structures studies are shown in Figures 3-11 (pgs. 109 - 117 ). Significant relationships between them will be pointed out and they are referred to frequently throughout the text. The compounds 10,10'-bianthrnylidene, 10,10'-bixanthylydene (Fig. 6-A), and diphenylmethylenanthrone (Fig. 7-A) are thermochromic ethylenes which on heating in solution produce green, blue-green, and red-orange colors, respectively. These compounds contain an "ethylenic" linkage ( $\text{>C}=\text{C}<$ ) joining aromatic

six-membered ring systems. 10,10'-Bianthrnylidene and related structures such as helianthrone, which is shown below, are quinones.



Calculated results of the absorption spectra employing only singly excited configurations in the CI procedure were poor for smaller quinones<sup>12</sup> such as anthraquinone (Fig. 4-D). Thus it was felt that it would be inappropriate to apply that technique to the more complicated systems. In addition, the thermochromic ethylenes studied are fused stilbenes<sup>52</sup> containing structural units identical to

cis-stilbene which is shown below. Trans-stilbene (Fig. 3-A) and



cis-stilbene have been treated theoretically, with and without configuration interaction.<sup>4,33</sup> Neither calculation reproduced the experimental fact that the lowest singlet transition of trans-stilbene appears at a longer wave length than the corresponding transition of the cis-isomer; the results for cis-stilbene were even less satisfactory.<sup>4</sup> Basically, the disagreement between theory and experiment described above for the quinones and cis-stilbene is undesirable when one wishes to study the absorption spectra of related structures, namely, the thermochromic ethylenes. The extended CI method applied to the thermochromic ethylenes gave good results for anthraquinone and cis-stilbene.

The thermochromic ethylenes are very interesting compounds because of the reversible color changes which can be produced. There are three phenomena to be considered which certain compounds

exhibit: thermochromism, piezochromism, and photochromism; the reversible change in color brought about by change in temperature and in pressure and by irradiation, respectively. Colored modifications have been observed by using a number of different procedures depending on the compound under investigation. These included:

- (1) Diphenylmethylenanthrone formed a ruby red liquid when melted.<sup>14</sup>
- (2) 10,10'-Bianthrnylidene<sup>41</sup> formed a green modification and 10,10'-bixanthenylidene<sup>41</sup> formed blue-green crystals when their respective solids were sublimed onto a cold surface.
- (3) Vivid colors were produced by heating solutions of the thermochromic ethylenes.<sup>14,24,54</sup>
- (4) Solid 10,10'-bianthrnylidene became green when it was subjected to high pressures.<sup>27</sup>
- (5) Solutions of 10,10'-bianthrnylidene<sup>26</sup> and 10,10'-bixanthenylidene<sup>24</sup> at low temperature became deeply colored upon irradiation with ultraviolet light.
- (6) Quenching a concentrated sulfuric acid solution of 10,10'-bianthrnylidene in ice water produced a highly colored precipitate.<sup>28</sup> The colored precipitate was shown to be identical to the thermochromic form produced in heated solutions by comparing electronic spectra data.<sup>22</sup> Very often the color is eradicated and the original compound (normal form) recovered unchanged either by bringing the sample to room temperature or,

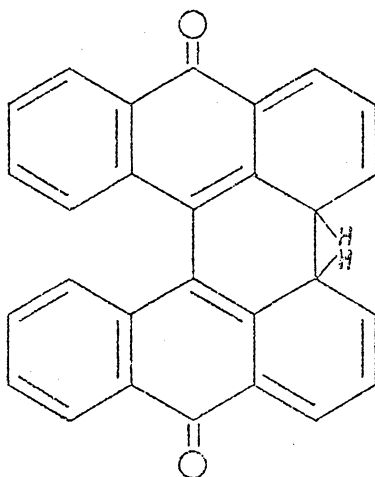
in the case of piezochromism or the sublimed solid, by dissolving the product in an organic solvent at room temperature. A recent history of the experimental studies of these systems has been given by J. C. Steichen.<sup>51</sup>

In the case of 10,10'-bianthronylidene, thermochromism in the solid was shown to be due to the presence of impurities.<sup>23</sup> The thermo- and photochromic forms which are produced in solution are considered to be the same on the basis of the identity of the wavelengths and shape of the long-wave length band maxima at 680 nm (1.82 eV).<sup>5</sup> The photochromism of 10,10'-bianthronylidene has been investigated at low temperatures<sup>5,26</sup>; its photolysis at ambient temperatures has also been studied.<sup>11</sup> The situation is complicated by the fact that upon irradiation in solution at room temperature permanent photoproducts are formed. Flash photolysis studies<sup>11</sup> indicated that helianthrone (shown above) was formed from an excited singlet state (not the photochromic state) of 10,10'-bianthronylidene and mesonaphthobianthrone (Fig. 9-C) was similarly formed from helianthrone. A general reaction scheme which represents reversible and irreversible changes that are more or less justified in the photochemistry of 10,10'-bianthronylidene has been presented by Becker and Earhart.<sup>5</sup>

The ground states of 10,10'-bianthronylidene<sup>15</sup> and 10,10'-bixanthylenylidene<sup>41</sup> are known to be "doubly-bent" structures with an angle of 40° between the central rings which are in a "boat" conformation. Proposed structures for the photochromic form

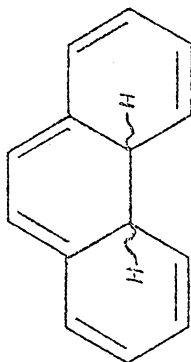
include:

- (1) The conformer of the normal form with the central rings in a "chair" conformation has been proposed by Kortum and coworkers.<sup>25</sup>
- (2) A betaine-like structure (Fig. 5-C) which is characterized by the opposite ionic charges in each half of the molecule has not gained wide acceptance.<sup>18,54</sup> It was shown that the rate at which the color is eradicated on irradiation by long wave length light was the same in either neutral or acid medium.<sup>18</sup>
- (3) A saturated bridge structure (shown below) which is a valence



isomer of the normal form has apparently gained popularity among workers in the field.<sup>1,5,11,34,52</sup> The analogy between the

formation of this bridged species and the dihydrophenanthrene intermediate (shown below) which is formed when cis-stilbene is photocyclized to phenanthrene has been made by various authors.<sup>35,52</sup>



A continuing problem associated with the chromism in general is the lack of knowledge about the exact nature of the colored forms. The PPP method is valuable in calculating pi-excitation energies, and the colors produced are believed to be due to this type of transition in the visible region of the absorption spectrum. Since this is a low energy region, the lowest energy excitations predicted are most important. If a compound absorbs in the visible, it is colored, possessing a color complementary

to that which is absorbed, as follows:

<u>Absorbed Color</u>	<u>Absorbed Wavelength (A)</u>	<u>Absorbed Energy (ev)</u>	<u>Visual Color</u>
Violet	4200	3.0	Yellow
Blue	4900	2.5	Orange
Green	5300	2.3	Red
Yellow	5900	2.1	Violet
Orange	6500	1.9	Blue
Red	7500	1.6	Green

The calculations indicated that the bridged structure was a probable structure for the colored form of a thermochromic ethylene. For example, the bridged isomer of 10,10'-bianthronylidene theoretically possessed a low energy excitation at 1.68 ev.

Some thermochromic compounds are often referred to as overcrowded molecules since, for example, the hydrogen atoms in the hindered positions 4,5,4', and 5' of 10,10'-bianthronylidene are in close proximity.<sup>41</sup> The NMR spectrum of the normal form in CDCl<sub>3</sub> solution indicated that the hydrogen atoms do not interfere with each other since their chemical shift was not in a position downfield relative to the others on the outer rings. This was in contrast to the chemical shift data reported for the hindered protons of bifluorenylidene (Fig. 7-A) which were 0.7 ppm downfield from resonance lines due to protons elsewhere in the molecule.<sup>45</sup> Bifluorenylidene is colored red in the crystalline form and its solutions are the same color.<sup>40</sup> In the red

crystalline state the angle between the middle rings is only  $10^\circ$  and it has been suggested that it naturally exists in the solid state and in solution in a "thermochromic form."<sup>23,25</sup> The above results from NMR data invited us to pursue similar investigations of other over-crowded ethylenes. Magnetic resonance studies (NMR, ESR) of some significance are reported. These included:

(1) NMR spectra of 10,10'-bianthronylidene, 10,10'-bixanthenylidene and diphenylmethylenanthrone at ambient temperature in  $\text{CDCl}_3$  were interpreted.

(2) The ESR spectrum of the hydrobianthrone radical (Fig. 11-B) was obtained when a pyridine solution of 10,10'-bianthranyl (Fig. 10-A) was refluxed, producing 10,10'-bianthronylidene in the process.

(3) The formation of the bridge bond on the valence isomer of the ground state of 10,10'-bianthronylidene was predicted to occur in the process of quenching a highly colored conc. sulfuric acid solution on ice.

## VII. THEORETICAL METHOD

The thermochromic compounds which are of principal interest in this study belong to a much larger class of organic substances whose classical formulas are written entirely or largely in terms of alternating single and double C-C bonds. Such molecules are referred to collectively as conjugated molecules. The valence electrons of these molecules have been classified into two distinct sets, the sigma-electrons and the pi-electrons. The pi-electrons are viewed as being highly delocalized over the carbon skeleton which defines a nodal "surface" for the molecular orbitals describing these electrons. The pi-electron systems are believed to pertain closely to the properties of conjugated molecules.<sup>47</sup>

A semiempirical method of computing molecular electronic wave functions which has proven to be quite helpful in interpreting experimental data such as that obtained from NMR and ESR spectroscopy and electronic absorption spectra is the Pariser-Parr-Pople (PPP) method. An outline of the theory is found below. A thorough discussion can be found in the original papers dealing with the subject and elsewhere.<sup>43,44,47,53</sup>

### A. The Electronic Energy

Neglecting spin-orbit, spin-spin, and relativistic effects, the electronic Hamiltonian  $H$ , for  $n$  electrons in a molecule containing  $N$  nuclei is defined in the Born-Oppenheimer

approximation as

$$H = h_i + V \quad (1)$$

where  $h_i$  is a sum of mono-electronic operators:

$$h_i = -1/2 \sum_i^n \nabla_i^2 - \sum_i^n \sum_k^N Z_k (r_{ik})^{-1} \quad (1a)$$

and  $V$  is the potential-energy operator for nuclear repulsions and electronic repulsions:

$$V = \sum_{k < t}^N Z_k Z_t (r_{kt})^{-1} + \sum_{i < j}^n (r_{ij})^{-1} \quad (1b)$$

The above equations are given in atomic units. Since the nuclear repulsion term is a constant, it can be disregarded in the calculation of electronic spectra.

The electronic energy of the system is obtained from the solution to the relevant eigenvalue equation:

$$H(R_{ki}, r_{ij}) \psi_n(R, r) = E_n(R) \psi_n(R, r) \quad (2)$$

When the nuclear coordinates,  $R$ , are fixed,  $E_n(R)$  is the

energy of the electrons moving in the field of the nuclei.

The wave function is taken as a finite linear combination of antisymmetrized product functions,  $\Phi$ , consisting of molecular spinorbitals,  $\phi$ :

$$\Psi_n = \sum_m^K A_m \phi_m \quad (3)$$

with

$$\phi_m = \det |\phi_{m1} \phi_{m2} \dots \phi_{mn}| \quad (3a)$$

Application of the variation principle to the total energy expression yields a set of linear equations for determining the coefficients  $A_m$ :

$$\sum_m^K A_m (H_{mn} - S_{mn}E) = 0 \quad n = 1, \dots, K \quad (4)$$

and a secular equation for E:

$$\det |H_{mn} - S_{mn}E| = 0 \quad (5)$$

where

$$S_{mn} = \int \phi_m^* \phi_n d\tau \quad (5a)$$

and

$$H_{mn} = \int \phi_m^* H \phi_n d\tau \quad (5b)$$

The number  $K$ , in equation (4) is the number of configurations,  $\phi_m$ , employed in the configuration interaction treatment.

In many molecules with an even number ( $2n$ ) of electrons the most important contribution to the ground state wave function arises from one determinant in which the electrons are grouped in pairs. The number of spinorbitals,  $\phi$ , in equation (3a) will be an even number. The two spinorbitals (e.g.,  $\phi_1$  and  $\phi_2$ ) describing a given pair of electrons have the same spatial function,  $\psi$ , and different spin functions,  $\alpha$  or  $\beta$ :

$$\begin{array}{ll} \phi_1 = \psi_1\alpha, & \phi_2 = \psi_1\beta \\ \\ \phi_3 = \psi_2\alpha, & \phi_4 = \psi_2\beta \\ | & | \\ | & | \\ | & | \\ \phi_{2n-1} = \psi_n\alpha, & \phi_{2n} = \psi_n\beta \end{array}$$

The  $2n$  electrons doubly-occupy the  $n$  lowest energy levels. This is called the "closed shell" case. With the spatial orbitals doubly occupied, the determinantal wavefunction becomes:

$$\Phi = [(2n!)]^{-1} |\bar{\psi}_1 \psi_1 \bar{\psi}_2 \psi_2 \dots \bar{\psi}_{n-1} \psi_{n-1} \bar{\psi}_n \psi_n|$$

which represents the singlet ground state. The bar over a molecular orbital refers to  $\beta$  spin, unbarred refers to  $\alpha$  spin. The ground configuration is given zero energy in the configuration interaction calculation.

The concept of molecular orbitals, referred to as the independent particle picture, is used to gain information about the  $\phi$ 's contributing to the  $\Phi$ 's. It is assumed that each electron moves independently of the other electrons and in an effective field arising from the nuclei and the other electrons. When electron repulsions are neglected, the Hamiltonian is given by:

$$H_0 = \sum_i^{2n} H_{\text{eff}}(i)$$

where  $H_{\text{eff}}$  has the same form for all electrons. In this case there is only one representative eigenvalue problem to solve, the eigenfunctions of which are obtained as an orthogonal set:

$$H_{\text{eff}} \psi_i = \epsilon_i \psi_i \quad (6)$$

To account for electron repulsions,  $H_{\text{eff}}$  is replaced by the Hartree-Fock self-consistent-field operator:<sup>43</sup>

$$F = H_{\text{core}}(i) + G(i) \quad (7)$$

where the  $G(i)$  operator represents an average electronic repulsion field. Once the  $\phi_i$  are known the integrals  $S_{mn}$  and  $H_{mn}$  are expressible in terms of the following integrals:

$$S_{ij} = \int \phi_i^* \phi_j d\tau, \quad (7a)$$

$$I_{ij} = \int \phi_i^* H_{\text{core}} \phi_j d\tau, \quad (7b)$$

and

$$J_{ijkl} = \int \phi_i^*(1) \phi_k^*(2) (r_{12})^{-1} \phi_j(1) \phi_l(2) d\tau_1 d\tau_2 \quad (7c)$$

The determinants are constructed from the Hartree-Fock orbitals. Virtual orbitals (not occupied in the ground state) are used in representing excited states. Singly excited configurations differ from the ground state by one spinorbital, doubly excited configurations by two spinorbitals, and so on, For example, if one electron is promoted from the occupied

orbital  $\psi_j$ , to the virtual orbital  $\psi_k$ , the singlet state

$$1_{\phi_j}^k = 2^{-1/2} (|\psi_1\psi_1\cdots\psi_j\psi_k\cdots\psi_n\psi_n| - |\psi_1\psi_1\cdots\psi_j\psi_k\cdots\psi_n\psi_n|)$$

and the triplet state

$$3_{\phi_j}^k = 2^{-1/2} (|\psi_1\psi_1\cdots\psi_j\psi_k\cdots\psi_n\psi_n| + |\psi_1\psi_1\cdots\psi_j\psi_k\cdots\psi_n\psi_n|)$$

arise for this singly excited configuration. The ground determinant will not mix with singly excited states when the two determinants are constructed from Hartree-Fock orbitals. This restriction arises from Brillouin's theorem.<sup>44</sup> Five different singlet state wavefunctions arise from exciting two electrons simultaneously. These are:

$$1_{\phi_{ss}}^{kk}, 1_{\phi_{st}}^{kk}, 1_{\phi_{ss}}^{km}, 1_{\phi_{st}}^{km(1)}, \text{ and } 1_{\phi_{st}}^{km(2)}.$$

Determinantal wavefunctions for these configurations can be written for each of three classes:<sup>38</sup> (a) no orbitals containing one electron:

$$1_{\phi_{ss}}^{kk} = |\psi_1\psi_1\cdots\psi_k\psi_k\cdots\psi_n\psi_n|,$$

(b) two orbitals containing one electron:

$$I_{\phi st}^{kk} = 2^{-1/2} (|\psi_1 \psi_1 \dots \psi_t \psi_s \psi_k \psi_k \dots \psi_n \psi_n| + |\psi_1 \psi_1 \dots \psi_s \psi_t \psi_k \psi_k \dots \psi_n \psi_n|),$$

and

$$I_{\phi ss}^{km} = 2^{-1/2} (|\psi_1 \psi_1 \dots \psi_k \psi_m \dots \psi_n \psi_n| + |\psi_1 \psi_1 \dots \psi_m \psi_k \dots \psi_n \psi_n|),$$

and (c) four orbitals containing one electron:

$$I_{\phi st}^{km}(1) = 1/2 [|\psi_1 \psi_1 \dots \psi_s \psi_t \psi_k \psi_m \dots \psi_n \psi_n| + |\psi_1 \psi_1 \dots \psi_s \psi_t \psi_k \psi_m \dots \psi_n \psi_n| \\ - |\psi_1 \psi_1 \dots \psi_s \psi_t \psi_k \psi_m \dots \psi_n \psi_n| - |\psi_1 \psi_1 \dots \psi_s \psi_t \psi_k \psi_m \dots \psi_n \psi_n|],$$

and

$$I_{\phi st}^{km}(2) = \frac{1}{2(3)^{-1/2}} \{2 [|\psi_1 \psi_1 \dots \psi_s \psi_t \psi_k \psi_m \dots \psi_n \psi_n| \\ + |\psi_1 \psi_1 \dots \psi_s \psi_t \psi_k \psi_m \dots \psi_n \psi_n|] \\ - [|\psi_1 \psi_1 \dots \psi_s \psi_t \psi_k \psi_m \dots \psi_n \psi_n| + |\psi_1 \psi_1 \dots \psi_s \psi_t \psi_k \psi_m \dots \psi_n \psi_n| \\ + |\psi_1 \psi_1 \dots \psi_s \psi_t \psi_k \psi_m \dots \psi_n \psi_n| + |\psi_1 \psi_1 \dots \psi_s \psi_t \psi_k \psi_m \dots \psi_n \psi_n|]\}.$$

There is interaction between these configurations (doubly excited-doubly excited CI), and also between them and the mono-excited configurations (singly excited-doubly excited CI) and the ground configuration (doubly excited-ground CI). These considerations extend the configuration interaction considerably. General formulas for the appropriate matrix elements have been given by Cizek.<sup>9</sup>

Molecular calculations are often made for a single value of the geometric parameters taken from experimental information. However, it is incorrect to assume that identical arrangements of the atoms persist when considering both the ground states of molecules and the excited states.<sup>20</sup> In fact the excited states of a single compound corresponding to different transitions may have a different geometry. At room temperature, molecules are predominantly in the lowest vibrational level. Thus, the spacings of vibrational energy levels of the ground state do not appear very prominently in the spectra. Since electronic excitation can end in many vibrational levels of the excited state, the vibrations of the excited state appear prominently in the spectra. The operation of the Franck-Condon principle is of prime importance since it specifies the particular vibrational energy levels accessible from the ground state by vertical excitation. Even when the gross geometry of a molecule remains unchanged upon excitation, minor changes in bond distances may generally be expected.<sup>20</sup> These

considerations were not included in the method used in this study.

### B. The LCAO Approximation

The molecular orbitals are made up of a linear combination of atomic orbitals ( $\chi_\nu$ ):

$$\psi_i = \sum_{\nu} C_{i\nu} \chi_{\nu} \quad (8)$$

Applying the variation principle to determine the coefficients  $C_{i\nu}$  leads to equations similar to (4) and (5):

$$\sum_{\mu} C_{i\mu} (H_{\mu\nu}^{\text{eff}} - S_{\mu\nu} e_i) = 0 \quad (9)$$

and

$$\det | H_{\mu\nu}^{\text{eff}} - S_{\mu\nu} e_i | = 0 \quad (10)$$

where  $H_{\mu\nu}^{\text{eff}}$  and  $S_{\mu\nu}$  are defined as integrals over atomic orbitals:

$$S_{\mu\nu} = \int \chi_{\mu}^* \chi_{\nu} d\tau; \quad (10a)$$

$$H_{\mu\nu}^{\text{eff}} = \int \chi_{\mu}^* H^{\text{eff}} \chi_{\nu} d\tau \quad (10b)$$

The effective Hamiltonian,  $H^{\text{eff}}$ , corresponds to the Hartree-Fock

operator ,F. The solutions to these equations are unique if the atomic basis set is complete. In practice one must utilize a rather limited number of atomic functions referred to as a truncated basis set and then attempt to find those particular functions which lead to the minimum energy.

For the closed shell case:

$$F = H_{\text{core}} + \sum_i^n (2J_i - K_i) \quad (11)$$

where

$$J_i(1) \chi_\mu(1) = \int \psi_i^*(2) \psi_i(2) (r_{12})^{-1} d\tau_2 \chi_\mu(1) \quad (11a)$$

and

$$K_i(1) \chi_\mu(1) = \int \psi_i^*(2) \chi_\mu(2) (r_{12})^{-1} d\tau_2 \psi_i(1) \quad (11b)$$

the total energy of one configuration can be written as:

$$E = 1/2 \sum_{\mu, \nu}^n P_{\mu\nu} (H_{\mu\nu}^{\text{core}} + F_{\mu\nu}). \quad (12)$$

The density matrix , $P_{\mu\nu}$ , the core matrix , $H_{\mu\nu}^{\text{core}}$ , and the self-

consistent-field matrix,  $F_{\mu\nu}$ , have the following meaning:

$$P_{\mu\nu} = 2 \sum_i^{\text{occ}} C_i^* \mu C_{i\nu}, \quad (12a)$$

$$H_{\mu\nu}^{\text{core}} = \int \chi_\mu^* H^{\text{core}} \chi_\nu d\tau, \quad (12b)$$

and

$$F_{\mu\nu} = H_{\mu\nu}^{\text{core}} + \sum_{q,\sigma} P_{q\sigma} [(\mu\nu|q\sigma) - 1/2(\mu\sigma|q\nu)] \quad (12c)$$

with

$$(\mu\nu|q\sigma) = \int \chi_\mu^*(1) \chi_q^*(2) (\tau_{12})^{-1} \chi_\nu(1) \chi_\sigma(2) d\tau_1 d\tau_2. \quad (12d)$$

### C. The Pi-Electron Approximation

The wave functions of the molecule are assumed to meet the conditions of sigma-pi separability and consequently only the pi-electrons of carbon (or hetero) atoms are explicitly taken into consideration. The sigma-system is treated as a non-polarizable core and its effect is included in  $H_{\text{core}}$ . Further basic assumptions of the Pariser-Parr-Pople method are:

(1) The overlap integral is neglected for orbitals on different centers,  $S_{\mu\nu} = \delta_{\mu\nu}$ .

(2) The potential due to the core of an atom which contributes pi-electrons is replaced by the potential of the corresponding neutral atom plus that due to the appropriate number of pi-holes.

The potential of the neutral atom is neglected.

(3) The atomic orbitals are assumed to be eigenfunctions of an appropriate one-electron Hamiltonian,  $(T + U_\mu)\chi_\mu = W_\mu\chi_\mu$ , where  $W_\mu$  is an atomic valence state energy.

(4) The resonance integral,  $\beta_{\mu\nu} = H_{\mu\nu}^{\text{core}}$ ,  $\mu \neq \nu$ , is zero for the case where  $\mu$  and  $\nu$  are non-nearest neighbors.

(5) Total zero-differential overlap is assumed for electronic repulsion integrals,  $(\mu\nu|q\sigma) = (\mu\mu|qq)\delta_{\mu\nu}\delta_{q\sigma}$ .

This reduces considerably the number of integrals of this type that are evaluated.

In addition to the above, one of Pople's basic assumptions is invoked, namely, that the potential of a neutral atom without pi-electrons, e.g., a H-atom, is not considered.

With these assumptions the diagonal core element becomes

$$H_{\mu\mu}^{\text{core}} = W_\mu - \sum_{\nu \neq \mu} Z_\nu (\mu\mu|v\nu), \quad (13)$$

where  $Z$  is an effective core charge. The elements of the Hartree-Fock operator may be rewritten as:

$$F_{\mu\mu} = W_\mu + 1/2P_{\mu\mu}(\mu\mu|\mu\mu) + \sum_{\nu \neq \mu} (P_{\nu\nu} - Z_\nu)(\mu\mu|v\nu) \quad (14)$$

and

$$F_{\mu\nu} = \beta_{\mu\nu} - 1/2P_{\mu\nu}(\mu\mu|\nu\nu), (\mu \neq \nu) \quad (15)$$

The total electronic energy can then be formulated as:

$$E = \sum_{\mu} P_{\mu\mu} [W_{\mu} + 1/4P_{\mu\mu}(\mu\mu|\mu\mu)] + \sum_{\substack{\mu, \nu \\ \mu \neq \nu}} P_{\mu\nu} \beta_{\mu\nu} \quad (16)$$

$$+ 1/2 \sum_{\substack{\mu, \nu \\ \mu \neq \nu}} [(P_{\mu\mu} - Z_{\mu})(P_{\nu\nu} - Z_{\nu}) - 1/2P_{\mu\nu} - Z_{\mu}Z_{\nu}] (\mu\mu|\nu\nu)$$

#### D. The Basic Parameters

The remaining quantities to be determined are listed below along with a method for obtaining them.

- (1) The resonance integrals ( $\beta_{\mu\nu}$ ) were chosen empirically (one for each unique bond). They were adjusted for atomic distances by assuming that they are proportional to the overlap of Slater  $2p_{\pi}$  orbitals.<sup>53</sup>
- (2) Values for the atomic valence state ionization potentials of the  $\mu^{\text{th}}$  atom ( $-W_{\mu}$ ) were usually taken from the report by Hinze and Jaffe.<sup>16</sup>
- (3) Values for  $\gamma_{\mu\mu} = (\mu\mu|\mu\mu)$  were taken as an atomic property set equal to the difference of ionization potential and electron

affinity found again in the report by Hinze and Jaffe.<sup>16</sup>

(4) Values for  $\gamma_{\mu\nu} = (\mu\mu|\nu\nu)$  were evaluated by using the following approximation of Mataga and Nishimoto:<sup>36</sup>

$$\gamma_{\mu\nu} = e^2 [r_{\mu\nu} + 2e^2(\gamma_{\mu\mu} + \gamma_{\nu\nu})^{-1}]^{-1}$$

In this expression  $r_{\mu\nu}$  is the distance between the  $\mu^{\text{th}}$  and  $\nu^{\text{th}}$  atoms.

### VIII. THEORETICAL CALCULATIONS: HYDROCARBONS, QUINONES

Compounds containing pi-electrons which are delocalized over a carbon skeleton (hydrocarbons) were treated extensively. Adjustments in the carbon-carbon bond resonance integral ( $\beta_{CC}$ ) and the one-center repulsion integral ( $\gamma_{CC}$ ) were made in order to find agreement between the predicted electronic spectra and the experimentally observed spectra. In some cases it was necessary to use different sets of parameters. It was possible to obtain good results (average deviation was 0.17 ev for 12 transitions) for four structures by employing an unusually low value for  $\gamma_{CC}$  (7.90 ev or 7.40 ev). The four compounds were benzene, naphthalene, anthracene, and trans-stilbene (Fig. 3-A).

The quinones and anthrone are carbonyl compounds. The oxygen atom was treated theoretically by introducing the parameter ( $\delta W_O$ ) which is the difference between the valence state ionization potential of the oxygen atom and that for carbon.<sup>16</sup> The one-center repulsion integral ( $\gamma_{OO}$ ) was also used to characterize the oxygen atom. The magnitude of the carbonyl bond resonance integral ( $\beta_{CO}$ ) can be different from that of  $\beta_{CC}$  for equal bond distances.<sup>53</sup> Parameters were again adjusted to find agreement with observed spectra.

In carrying out the calculations, special attention was devoted to the effect of the extent of configuration interaction on the calculated excitation energies. Comparisons were made between results obtained using mono-excited configuration interaction (MCI) with those including doubly excited configurations (DCI) as well as

results where the relative amounts of each type of configuration were varied.

Oscillator strengths were also calculated. In the tables containing these data, cited values were not given when they agreed very closely with those already reported in the previous column of data. Since a large number of excitation energies is predicted, only those transitions (except the lowest) which have a non-zero oscillator strength and fall in the range of the observed spectral values were listed. Therefore, for each calculated excitation energy, the energy level to which the transition is being made from the singlet ground state (reference level) was indicated. A zero oscillator strength does not necessarily mean that the transition is not going to be observed.<sup>6</sup> Molecules possess, in addition to electronic energy, vibrational and rotational energy. Changes in these energies accompany the changes in electronic energy and give rise to the familiar band spectra. Forbidden bands are frequently observed because of vibrational interaction. Molecules are constantly undergoing vibrations. The symmetry of a molecule will be distorted by vibrational modes which are not symmetric. Since electronic phenomena are vastly more rapid than the motions of nuclei, the sample behaves with respect to light absorption as if it were a mixture of different molecules. Depending on the vibrational states, some molecules have symmetry, but others are vibrationally distorted. The electronically forbidden transitions remain relatively low in intensity, however.

### A. Hydrocarbons

Benzene, naphthalene, anthracene, trans-stilbene (Fig. 3-A), cis-stilbene (Fig. 3-B), and dihydrophenanthrene intermediate (Fig. 3-C) were studied. With the exception of cis-stilbene<sup>4</sup> and probably dihydrophenanthrene intermediate, all of these molecules are planar. The structure of cis-stilbene and dihydrophenanthrene intermediate is not known. The electronic absorption spectra of all of these compounds are known. The geometry of the molecule, the repulsion integral ( $\gamma_{CC}$ ) and the resonance integral ( $\beta_{CC}$ ) were parameters to be specified in each case.

The configuration interaction (CI) matrix was set to hold eighty elements, however, when doubly excited configurations (DCI) were included along with mono-excited configurations (MCI), the total number of configurations possible exceeded eighty. Benzene was an exception.

#### 1. Benzene

Numerous calculations of the singlet spectrum of benzene were compared with the observed spectrum to determine the set(s) of parameters that would give satisfactory agreement. All bond lengths were assumed to be 1.395A and bond angles, 120°. The resonance integral ( $\beta_{CC}$ ) and the repulsion integral ( $\gamma_{CC}$ ) were the remaining parameters to be adjusted.

The observed spectral energies,<sup>44</sup> along with the results of three calculations which involved only the nine singly excited states in the configuration interaction (MCI), are given in Table I.

The choice of parameters was suggested by the references cited in the table. It is noteworthy that all of these results were in close agreement with the experimental spectrum. The average deviation was 0.12 ev ( $968 \text{ cm}^{-1}$ ). The excitation observed at 6.14 ev was predicted to be due to the  $A_{1g} \longrightarrow B_{1u}$  transition.

The character of the calculated spectrum changed on including the 45 doubly excited states in the configuration interaction (DCI). The results shown in Table II, column 1, indicate that not only did the excitation energies change by as much as 1.8 ev but the order of the states  $E_{1u}$  and  $E_{2g}$  was reversed. A comparison of the data given in columns 2 and 3 of Table II show that lowering the value of the resonance integral will tend to bring the  $E_{2g}$  state closer to the  $E_{1u}$  state when the repulsion integral is 10.60 ev. Column 4 of Table II (where the repulsion integral has been lowered to 9.00 ev) gives results which are qualitatively the same as those reported in Table I for the singly excited configuration interaction calculations. The effects of  $\gamma_{cc}$  and  $\beta_{cc}$  on the calculated energy levels of benzene are shown graphically in Figs. 1 and 2, respectively. Numbers shown in the figures do not correlate with those given in Table II since the energy levels are not referred to the ground state ( $A_{1g}$ ) as the zero of energy. Over the large range of values of  $\gamma_{cc}$  used (7.40 ev-11.13 ev) the  $E_{1u}$  state was affected the least (0.28 ev); the  $B_{2u}$  and  $E_{2g}$  states were changed the most (-1.25 ev and -1.26 ev, respectively). The depression of the ground state was the least and was affected the least by  $\gamma_{cc}$

when the smaller values of  $\gamma_{cc}$  were employed. Changing the resonance integral ( $\beta_{cc}$ ) affected the  $E_{2g}$  state the most and the ground state the least. All of the states were increased in energy on lowering  $\beta_{cc}$ ; the  $E_{1u}$ ,  $B_{1u}$ , and  $B_{2u}$  states were affected to about the same extent.

The effect of the choice of parameters on the order of the calculated energy levels for benzene when changing the type of states used in the configuration interaction has been the subject of two papers by Koutecky and coauthors.<sup>29,30</sup> Changes in the character of the calculated spectrum similar to those described above were found, however, no attempt was made to find a set of parameters which would give numerical agreement with experiment.<sup>29,30</sup> The sets of parameters given in columns 4, 5, and 6 of Table II result in spectra that show at least some agreement with the observed spectrum and will be used for larger molecules. If one accepts the excitation observed at 6.14 eV to represent  $A_{1g} \longrightarrow B_{1u}$ , then the values for  $\gamma_{cc} = 7.40$  eV and  $\beta_{cc} = -2.60$  eV (column 6, Table II) give an excellent calculated spectrum.

It will become apparent that in comparison with the other hydrocarbons treated theoretically, benzene (the smallest member of the homologous series) was the most difficult in that the spectrum was most sensitive to the parameters and the extent of configuration interaction used.

## 2. Naphthalene and Anthracene

The bond lengths and bond angles used were all assumed to be 1.395A and 120°, respectively.

Naphthalene has ten pi-electrons and there were ten calculated molecular orbitals; five orbitals were doubly occupied in the ground configuration and five were virtual orbitals. This led to a total of 25 singly excited configurations which could be included in the configuration interaction. The results of two calculations with all singly excited states included are presented in Table III along with the observed energies. Oscillator strengths ( $f$ ) which have been determined both experimentally<sup>19</sup> and theoretically are also shown. The results of the third calculation shown in Table III indicated that one can reduce the amount of configuration interaction to 15 states without affecting most of the calculated spectrum. The corresponding results for anthracene are given in Table IV.

With  $\gamma_{CC} = 11.08$  ev, the predicted excitation energies for naphthalene and anthracene shown in Tables III and IV, respectively, deviated on the average from the observed values by 0.17 ev. Ito and I'Haya have concluded that for naphthalene it would be sufficient to take into account only singly excited configurations when calculating the low-lying energy levels.<sup>19</sup> However, it is interesting to see how the sets of parameters used for benzene transfer to these compounds when including some doubly excited states in the calculations. The results are given in Tables V and VI with a total of 54 excited states mixed in. It was found that lowering the value

of the repulsion integral was necessary to obtain results comparable to those when all of the singly excited states were used. The best results for naphthalene were obtained using  $\gamma_{cc} = 7.90$  ev.

Tables V and VI also show results of calculations where the total number of excited states included has been increased to 79 and the relative amounts of each type varied. In general, the predicted spectra were insensitive to the relative amounts of singly and doubly excited states when the total number of states was large.

It was apparent from the changes in the oscillator strengths for the first and second transitions that a reversal in symmetry may occur when including doubly excited configurations. This was seen in the case of naphthalene when  $\gamma_{cc}$  was low (7.40 ev). Also, with  $\gamma_{cc} = 11.13$  ev, a new low-lying state appeared in the anthracene spectrum which was forbidden.

### 3. Trans-Stilbene and Cis-Stilbene

The relative orientation of the two phenyl rings was the only geometric difference between cis- and trans-stilbene since both were taken to be planar molecules (Figs. 3-A and 3-B, respectively). All bond angles in each molecule were assumed to be  $120^\circ$ . The appropriated bond lengths are indicated in Fig. 3-B. Table XXII can be consulted for the values of the resonance integrals used. When the C-C bond distance used in the calculations was different from 1.395A, the  $\beta_{cc}$  value was determined by making it proportional to the pi-bond overlap integrals.<sup>53</sup>

Table VII shows the results of a number of calculations for trans-stilbene and cis-stilbene. All of the results were not rewarding in that for a given set of parameters they did not reproduce the experimental fact that the lowest singlet transition of trans-stilbene (3.9-4.2 ev)<sup>6,33</sup> lies lower than the corresponding one for cis-stilbene (4.4 ev).<sup>33</sup> The lowest singlet transition of trans-stilbene was consistently predicted to be about 0.2 ev higher than the lowest singlet transition for cis-stilbene. A low value of  $\gamma_{cc}$  was preferred in the case of trans-stilbene. Cis-stilbene was represented correctly by simply introducing the doubly excited states into the CI procedure with  $\gamma_{cc} = 11.13$  ev.

In contrast to the data shown for benzene, the calculated excitation energies did not vary appreciably for different sets of parameters when a combination of singly and doubly excited configurations in the CI matrix was used. This was due partly to the fact that in the case of the stilbene the depression of the ground state was relatively insensitive to the choice of parameters; whereas, with benzene the values ranged over 0.9 ev. A check on whether configurations of sufficiently high energy were being included in the CI calculation to obtain consistent results was done by comparing the calculation containing 58 doubly excited configurations (starting with those of lowest energy) to the calculation obtained using the same total number of configurations but containing none greater than 12.0 ev. This changed 16 of the first 58 configurations found in the former calculation. The

resulting transition energies were not changed by more than 0.04 ev. A similar type of result has been reported for  $C_{14}$  amines.<sup>37</sup>

The ground state of cis-stilbene lies 5.7 kcal/mole above the ground state of trans-stilbene.<sup>35</sup> A calculation of the pi-binding energies using SCF orbitals showed cis-stilbene to be more stable (larger value) by 0.02 ev which is a negligible difference. (lev = 23 kcal/mole). Cis-stilbene raises the main question as to what extent the approximations characteristic of the PPP method are valid in a non-planar system. The long wavelength band of cis-stilbene is a structureless, broad band of lower intensity than that of its isomer. Moderate crowding within a molecule can result in both a hypochromic effect (decrease in intensity) and a hypsochromic shift (higher energy) relative to the spectrum of a planar model.<sup>20</sup> Thus steric crowding which is not considered in the calculation of the pi-binding energy can account for the higher ground state energy of cis-stilbene. Reported results showed that the effect of introducing a correction for non-planarity by varying bond angles was negligible for computing transition energies.<sup>4,33</sup>

#### 4. Dihydrophenanthrene Intermediate

The structural formula for dihydrophenanthrene is shown in Fig. 3-C. It is the proposed intermediate in the photocyclization of cis-stilbene to phenanthrene in the presence of a suitable oxidant such oxygen, and it presumably caused the yellow-orange color due to a very broad absorption band which extended to 2.2 ev (maximum near 2.7 ev).<sup>35</sup> This was also produced on the irradiation of a

degassed solution of pure cis-stilbene.<sup>35</sup> A review of the photocyclization of stilbene has been presented by Stermitz.<sup>52</sup> He concluded that the identification of the yellow color with this dihydrophenanthrene intermediate was most convincing since it explained and correlated all of the observed data from spectral and kinetic studies and did not conflict with any of the data.<sup>52</sup> Thus the absorption band near 2.7 eV for this species was used as a test of the configuration interaction method for obtaining molecular energy levels within the framework of the PPP method.

Dihydrophenanthrene intermediate was treated theoretically by omitting the two carbon atoms which now appear saturated along with the corresponding resonance integrals with their nearest neighbors from the calculation of the cis-stilbene spectrum. The system now contained 12 pi-electrons instead of 14. The results are given in Table VIII.

In both calculations where all of the singly excited states (36) were used, the predicted absorption band was too low in energy. Evidently when a combination of singly and doubly excited configurations were used, the lowest lying excitations which were forbidden did not have to be considered when predicting the spectrum of this type of saturated bridge species. A CI matrix using both types of configurations was preferred. For example, using a value higher than 9.00 eV for  $\gamma_{cc}$  would give a value close to 2.7 eV for a non-forbidden excitation energy. The calculations supported the postulate that the dihydrophenanthrene intermediate is yellow-orange

and were very satisfying in this respect. In comparing the predicted absorption spectra of dihydrophenanthrene with that of cis-stilbene, the former was predicted to have a non-forbidden excitation energy about 1.6 ev below that of the latter. Experimentally the difference was about 1.6 ev.<sup>35</sup>

A calculation of the pi-binding energy indicated that this model, as a reasonably stable intermediate in the cyclization, was poor since with respect to cis-stilbene it was unstable by 225 kcal/mole. Calculations based on an extended Hess's law summation resulted in a ground state energy for the intermediate of 33.3 10 kcal/mole above cis-stilbene.<sup>35</sup>

#### B. p-Quinones and Anthrone

The compounds p-benzoquinone (Fig. 4-A), p-naphthaquinone (Fig. 4-B), 9,10-anthraquinone (Fig. 4-D), and anthrone (Fig. 4-C) were treated. The oxygen atom of each carbonyl group was considered to contribute one pi-electron as well as the carbon atom to which it is bonded. The one-center repulsion integral ( $\gamma_{OO}$ ) was assigned a value of 15.23 ev.<sup>16</sup> These compounds which contain hetero-atoms require that the difference between the valence state ionization potential of the hetero-atom and that of carbon be specified. The value for this quantity ( $\delta W_O$ ) was most frequently taken as -6.54 ev.<sup>16</sup> The carbonyl bond resonance integral ( $\beta_{CO}$ ) was varied.

The fact that calculated energies for the p-quinones are uniformly too high when one employs only singly excited configurations in the CI matrix will be illustrated. This problem

has been pointed out previously.<sup>12,31,32,39</sup> The parameters used by Klessinger<sup>21</sup> to fit the p-benzoquinone spectrum were found to give the same result. It is the main reason the CI matrix was extended to include the doubly excited states. Thus the results for calculations including the doubly excited configurations are of general interest.

#### 1. p-Benzoquinone

The bond lengths used are shown in Fig. 4-A. All bond angles were taken to be 120°. The observed spectrum consists of a very strong band at 5.07 eV and a strong band at 4.28 eV.<sup>12</sup>

Values of  $\gamma_{CC}$  were varied and the  $\beta_{CC}$  values used can be ascertained from Table XXII. The value used for  $\gamma_{OO}$  was always 15.23 eV but  $\beta_{CO}$  was varied. All calculations resulted in one non-forbidden transition out of the first three which agreed with the polarization direction determined for the experimentally observed transition at 5.07 eV, namely, along the axis parallel to the carbonyl bonds. The results of twelve calculations are given in Table IX (two pages). The first six calculations were all done with  $\gamma_{CC} = 11.13$  eV. The carbonyl bond resonance integral was first adjusted to a value of -3.145 eV using only singly excited CI to obtain agreement with the observed spectral energies. After including doubly excited states,  $\beta_{CO}$  had to be increased to -2.60 eV in order to obtain reasonable agreement. Note that the results for six calculations (nos. 3,5,7,8,11, and 12) with  $\beta_{CO} = -2.60$  eV agreed within 0.16 eV with the more intense band observed at 5.07 eV. It

was interesting to compare the three calculations (nos. 3, 4, and 5) with  $\gamma_{cc} = 11.13$  ev and  $\beta_{co} = -2.60$  ev (there were no variations in  $\beta_{cc}$ ). Good results were obtained with DCI = 38 which became poor on increasing DCI to 63. This was caused by a further depression of the ground state (reference level) by 0.42 ev, a consequence of the added doubly excited configurations interacting with it. The third energy level ( $f = 0.43$ ) resulting from a total of 79 excited configurations was actually calculated to be 0.30 ev lower than the corresponding level calculated with a total of 54 excited states included. This was corrected by omitting those configurations whose diagonal CI matrix elements had excitation energies of 15.0 ev or more relative to the ground configuration. This reduced the total to 59 excited configurations (DCI = 43). Now the predicted spectrum is the best of all (no.5). Similar effects were found for benzene.

The calculations attest to the notion that including doubly excited states in the CI calculation makes the PPP method more versatile.

## 2. 9,10-Anthraquinone

The structural formula and bond lengths used for this compound are given in Fig. 4-D. All bond angles were taken to be  $120^\circ$ . The observed electronic spectrum<sup>12</sup> consists of two band regions: (1) a moderately strong band which has a well defined maximum at 3.80 ev polarized in the x-direction, and (2) at least three strong peaks from about 4.50 ev to 5.10 ev. Transitions at 4.53 ev

(y-polarized), 4.70 ev (x-polarized), and 4.98 ev have been identified within the second band region.<sup>11</sup> In analyzing the features of the calculated spectrum, it was noted that the separation of the two regions is about 1.0 ev and the observed spectrum exhibits a "valley" near 5.5 ev.

The results of eight calculations are shown in Table X (two pages). Parameter values were:  $\gamma_{OO} = 15.23$  ev,  $\gamma_{CC} = 11.13$  ev (one exception),  $\delta W_O = -6.54$  ev (two exceptions). Values for  $\beta_{CC}$  can be ascertained from Table XXII. Values used for  $\beta_{CO}$  are given in Table X. In attempting to fit the observed spectrum it was noted that generally by decreasing the value for  $\beta_{CO}$  or  $\delta W_O$  the calculated excitation energies were improved. It is curious that the lowest lying transition was non-forbidden when doubly excited states were included only when the value used for  $\delta W_O$  had been decreased to -7.00 ev. The best calculated results were obtained when values for  $\beta_{CO} = -2.20$  ev and  $\delta W_O = -7.00$  ev were employed ( $\gamma_{CC} = 11.13$  ev). The two lower lying transitions were calculated correctly. This result was of major importance since the extended CI procedure was applied to some thermochromic ethylenes (section IX). The colors associated with these compounds are due to low energy transitions. Returning to the anthraquinone calculation, allowed transitions are predicted at 4.50 ev and 5.24 ev representing the second observed band region. The separation of the two regions was predicted to be about 1.2 ev. Of the 43 doubly excited configurations included in this calculation, eight were of an energy greater than 12.0 ev.

Replacing these with configurations of energies less than 12.0 ev did not change the character of the spectrum and in general transition energies changed only by 0.06 ev. Unfortunately a reasonable spectrum was not obtained by employing a value of  $\beta_{CO} = -2.60$  which gave such good results in the case of p-benzoquinone.

Calculations which used various values of  $\gamma_{OO}$  along with the lower value of  $\beta_{CO}$  were not significantly changed. Transition energies resulting from a calculation employing  $\gamma_{CC} = 9.00$  ev and  $\beta_{CO} = -2.30$  ev with a total of 79 excited configurations did not show any improvement.

### 3. p-Naphthaquinone and Anthrone

A limited number of calculations were done on these compounds. Bond lengths and angles were assumed to be the same as those used for anthraquinone except the C-C bond distance of 1.39A was shortened to 1.38A for p-naphthaquinone (Fig. 4-B). Anthrone (Fig. 4-C) was treated theoretically as a 14 pi-electron system by omitting one carbonyl group and the corresponding resonance integrals with its nearest neighbor C-atoms from the calculation of the anthraquinone spectrum. Values for  $\beta_{CC}$  that were used can be found in Table XXII.

The observed electronic absorption spectra of these compounds are similar to that of anthraquinone in that they show two strong band regions.<sup>12</sup> The p-naphthaquinone spectrum is characterized by a strong peak at 3.71 ev and a very strong band from 4.80 ev to 5.00 ev.

The higher energy band consists of three peak maxima and is predominantly polarized in the y-direction.<sup>12</sup> The anthrone spectrum consists of a strong peak at 4.00 ev and a very strong band near 5.00 ev which is polarized in the y-direction.<sup>49</sup>

The results of the p-naphthaquinone calculations with  $\gamma_{cc} = 11.13$  ev,  $\gamma_{oo} = 15.23$  ev, and  $\delta W_o = -6.54$  ev (one exception) are given in Table XI. The lowest four excitation energies are shown and in each case the one with the largest calculated oscillator strength was polarized in the y-direction. Thus its value was compared with the observed peak maxima near 4.90 ev.

The best results shown in Table XI are those from calculations which employed a value of -2.30 ev for  $\beta_{co}$ . These could be improved by decreasing  $\beta_{co}$  perhaps to -2.45 ev. Of the 53 doubly excited configurations included in this calculation, 19 were of an energy greater than 12.0 ev. Replacing these with configurations of energies less than 12.0 ev did not change the character of the spectrum and in general transition energies changed by only 0.07 ev.

The results of the anthrone calculations with  $\gamma_{cc} = 11.13$  ev,  $\gamma_{oo} = 15.23$  ev, and  $\delta W_o = -6.54$  ev (one exception) are given in Table XII. The lowest four excitation energies are shown. None of the results were satisfactory. The last two columns in Table XII show results with some improvement over the others but the first excitation energies were about 0.50 ev too high. In comparing the predicted absorption spectrum of anthrone with that of anthraquinone, the former was predicted to have a non-forbidden excitation energy

about 0.8 eV above that of the latter. Experimentally the difference was about 0.2 eV. As with anthraquinone, changing  $\delta W_0$  to -7.00 eV increased the oscillator strength for the first transition. The higher energy band region appears to be predicted correctly.

### C. Discussion

Six hydrocarbon structures and four carbonyl-containing compounds were treated theoretically with the PPP method including doubly excited configuration interaction. In order to evaluate the reliability of this method and, it was hoped, establish some guidelines for its use a number of different types of comparisons were made. In the following paragraphs conclusions are drawn from these comparisons.

The results of calculations which included all singly excited configurations were given. Reasonable agreement for benzene, naphthalene, anthracene, and p-benzoquinone was obtained. The predicted transition energies deviated on the average from the observed values by 0.15 eV. In order to obtain comparable results with doubly excited configurations included, the basic parameters had to be readjusted. For the three hydrocarbons agreement was restored principally by lowering the one-center repulsion integral on carbon ( $\gamma_{CC}$ ). This had the effect of changing all two center integrals ( $\gamma_{\mu\nu}$ ) since Mataga's expression was employed throughout (p. 27). Basically a low value for  $\gamma_{CC}$  suppresses the tendency of the theory to over-emphasize ionic structures, results in a more covalent molecule and apparently reduces the need for, or the

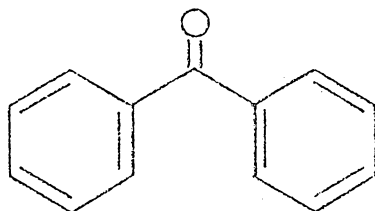
influence of, CI.<sup>43</sup> With one set of parameters ( $\gamma_{CC} = 7.90$  ev,  $\beta_{CC} = -2.55$  ev) reasonable agreement was obtained for benzene, naphthalene, anthracene, and trans-stilbene. The predicted transition energies deviated on the average from the observed values by 0.17 ev. Three-fourths of these energies agreed within 0.09 ev. In order to obtain agreement for the transition of symmetry  $B_{1u}$  in the case of benzene, 23 states out of the original 45 represented in the CI matrix had to be omitted. The remaining states were those with excitation energies less than 15.0 ev.

The calculated results for cis-stilbene were improved by including doubly excited configurations ( $\gamma_{CC} = 11.13$  ev). A value for  $\gamma_{CC}$  larger than 9.00 ev was preferred because it predicted correctly the 2.7 ev spectral band of dihydrophenanthrene intermediate. It is interesting that the spectra of these two hydrocarbons were more readily reproduced by using the extended CI procedure and a more conventional value for the one-center repulsion integral ( $\gamma_{CC}$ ). Although it has been pointed out that these molecules are probably non-planar (p. 30), they were treated as planar systems. This seems to indicate that the inclusion of doubly excited states is important when treating non-planar systems with a planar model. This conclusion is perhaps premature, however.

The results obtained for the p-quinones were much better when the extended CI procedure was employed. This was particularly true for the lowest transition energy. Agreement was obtained by readjusting only the carbonyl bond resonance integral ( $\beta_{CO}$ ). The

transition energies of p-benzoquinone (the smallest member of the homologous series) were found to be the most sensitive to the parameters used and the extent of CI employed. Similar conclusions were made for benzene. The best results were obtained for p-benzoquinone by including all configurations less than 15.0 eV partly because the rest of the doubly excited configurations stabilized the ground state (reference level) too extensively. Benzene and p-benzoquinone were the only two molecules whose CI matrix contained elements with an energy of at least 15.0 eV. Overall, the predicted transition energies for the p-quinones deviated on the average from the observed values by 0.16 eV. Minor adjustments in  $\beta_{CO}$  had to be made in order to accomplish this.

The results for anthrone were unsatisfactory. The very strong band at 5.00 eV was predicted correctly, however. The geometry used in the calculations for anthrone also represent a planar model of benzophenone (shown below). The pi-electron systems of these two



molecules are identical. The experimental absorption spectra of anthrone and benzophenone are quite similar.<sup>49</sup> The higher energy band region in each case is near 5.00 ev. The lower energy band region for benzophenone occurs at a higher energy (4.34 ev) than that for anthrone (4.00 ev).<sup>49</sup> Employing the set of parameters which gave the best results for anthraquinone produced calculated results which were better for benzophenone than anthrone (Table XII, column 4). Anthrone (Fig. 4-C) is constrained by the CH<sub>2</sub> bridge, and hence the rings certainly must approach coplanarity more closely than in benzophenone.

Generally, the calculated transition energies were less sensitive to the choice of parameters when the extended CI treatment was used. Consistent results were obtained particularly when the total number of configurations was increased to 80. It was shown that the relative amounts of each type of excited configuration did not appreciably affect the calculated spectra for a given set of parameters with MCI + DCI = 79. The reason for this can be seen if the maximum energies appearing in the CI matrices for the complete MCI calculation and the (MCI + DCI = 79) calculation are compared. In the latter case the maxima appears among the doubly excited states. For the compounds except benzene and p-benzoquinone the maxima which ranged from 11.4 - 14.7 ev differed by 1.4 ev at the most. For that compound, anthracene, the DCI matrix contained 3 states with energies from 5.0 - 7.0 ev, 35 states with energies from 8.0 - 11.0 ev, and 13 states with energies from 11.0 - 13.0 ev. The complete

MCI matrix contained 12 states with energies from 3.0 - 7.0 ev, 29 states with energies from 7.0 - 11.0 ev, and 8 states with energies from 11.0 - 14.0 ev. Since only one of these 8 states with energies from 11.0 - 14.0 ev preceded a state of energy outside this range, one could obtain a total of 78 states with energies up to 11.0 ev by using a CI matrix of 92 elements. This was typical of the CI matrices that were used. For example, the CI matrix in the anthraquinone spectrum which gave the best results contained 71 out of 79 states with energies up to 11.0 ev; 36 were singly excited and 35 were doubly excited. Evidently a large number of states with energies up to 11.0 ev with one half of them in the CI matrix from each type represented a desirable combination. This was further substantiated by results reported for trans-stilbene, anthraquinone, and p-naphthaquinone which showed that spectral energies were not noticeably changed when CI matrix elements above 12.0 ev were omitted.

It is felt that the method employed should be used when molecules contain hetero-atoms. The results for the p-quinones and those reported earlier by Hirota and Nagakura<sup>17</sup> for pyridine, phenol, aniline, pyrrole, and furan point out the importance of including DCI.

For the compounds which have a seemingly more direct relationship to the thermochromic ethylenes, reasonable agreement was achieved with the larger value for  $\gamma_{CC}$ . These compounds were cis-stilbene, dihydrophenanthrene intermediate, and the p-quinones (particularly anthraquinone). Therefore, a value of 11.13 ev for  $\gamma_{CC}$  was used for the thermochromic ethylenes (section IX).

## IX. THEORETICAL CALCULATIONS: THERMOCHROMIC ETHYLENES

The Pariser-Parr-Pople method including configuration interaction was used to calculate pi-electronic transition energies of a number of large molecules. Organic compounds, each with an "ethylenic" linkage between carbon atoms bonding the two halves of the molecule together, were treated extensively. For example, 10,10'-bianthronylidene (Fig. 5-A) was studied by employing the CI procedure including only singly excited states (MCI), and by using a CI matrix containing a combination of singly and doubly excited states (DCI) for comparison. The results obtained from each type of calculation differed by only 0.11 ev for the lowest lying transition energy. This difference of 0.11 ev for the lowest transition energy was indicative of the results obtained for all six compounds containing the "ethylenic" linkage. These compounds were: 10,10'-bianthronylidene (Fig. 5-A), 10,10'-bixanthylenylidene (Fig. 6-A), diphenylmethylenanthrone (Fig. 7-A), bifluorenylidene (Fig. 8-A), helianthrone (Fig. 9-A), and mesonaphthobianthrone (Fig. 8-C). The first three compounds are thermochromic ethylenes. The calculations reported for each compound refer to the appropriate planar model of the ground form. Only in the case of bifluorenylidene is this form expected to be highly colored since the solid is red.<sup>40</sup>

Calculations were also done on bridged structures (Figs. 5-B, 6-B, 7-B, 8-B, and 9-B) and betaine-like structures (Figs. 5-C, and 6-C). For the thermochromic ethylenes, these structures have been proposed for the colored form produced, e.g., on heating solutions of

the appropriate compound. The MCI and DCI procedures were used. On the average, the results from the two calculations for each structure differed by 0.32 eV when the lowest lying transition energies were compared. This did not change the final conclusion that the bridged structure was the more probable structure for the colored form of a thermochromic ethylene.

Which of the two configuration interaction procedures (MCI or DCI) was the better method for studying these large molecules was not established. When the results obtained by the two methods were further compared, two general features became apparent. The theoretical oscillator strengths were smaller when DCI was employed. This is typical of the DCI treatment.<sup>2,17</sup> This has been attributed mainly to the fact that the CI matrix included many doubly excited configurations having zero transition moments from the ground configuration.<sup>17</sup> Also, with the addition of excited states to the CI procedure, more states with predicted transition energies in the ultraviolet-visible spectrum range appeared.

The following general points refer to all calculations in this section:

- (1) Results were obtained for MCI, and for a combination of MCI and DCI.
- (2) The  $\beta_{cc}$  values can be found in Table XXII.
- (3) All bond angles except in bifluorenylidene were 120°.
- (4) When oxygen contributes one pi-electron,  $\gamma_{oo} = 15.23$  eV;  $\delta W_o = -6.54$  eV for MCI,  $\delta W_o = -7.00$  eV for MCI - DCI.

- (5) When oxygen contributes two pi-electrons,  $\gamma_{OO} = 18.78$  ev and  $\delta W_O = -22.92$  ev.
- (6)  $\gamma_{CC} = 11.13$  ev.
- (7)  $\beta_{CO} = -2.793$  ev for MCI,  $\beta_{CO} = -2.06$  ev for MCI - DCI.

#### A. Compounds and Bridged Structures

The thermochromic compounds treated theoretically were 10,10'-bianthronylidene (Fig. 5-A), 10,10'-bixanthylenylidene (Fig. 6-A), and diphenylmethylenanthrone (Fig. 7-A). Bifluorenylidene (Fig. 8-A) was also investigated since its structure does contain an "ethylenic" linkage between the two halves of the molecule although it is not considered to be thermochromic.<sup>25</sup> The structure for all four of these compounds which contain a single saturated bridge bond between two carbon atoms in close proximity analogous to the dihydrophenanthrene saturated bond were also considered. The bridged structure has not been unequivocally identified but is a proposed intermediate leading to cyclization in this type of compound and presumably is the colored species produced in solution.<sup>52</sup> It was treated theoretically by omitting the two carbon atoms which now appear saturated and the corresponding resonance integrals to their nearest neighbors from the calculation of the spectrum for the compound itself. This reduced the number of pi-electrons by two.

##### 1. 10,10'-Bianthronylidene

The structural formulas and bond distances chosen for the compound 10,10'-bianthronylidene and its bridged structure are shown in Figs. 5-A and 5-B, respectively. Table XIII shows the results of

the calculations and three predominant absorption maxima in the observed spectrum of the compound. Predicted transitions with very small oscillator strengths ( $<0.001$ ) were omitted. Neither calculation for the compound predicted a transition near 3.7 eV where the observed spectrum exhibits a "valley". The colored species absorbs strongly near 1.80 eV and thus appears blue-green.<sup>11,26</sup> Both calculations predicted the bridged structure to be colored. The calculation employing 66 singly excited states predicted absorption at 2.42 eV where none is observed.

Calculated oscillator strengths for the bridged structure were decidedly lower than those calculated for the compound itself. This was particularly true for the DCI results. A direct comparison can be made using the first transition. The reason for this can be seen if the energies appearing in the CI matrices are compared. Although the energies were quite similar for the singly excited states in each matrix, for the compound only 8 doubly excited states had energies from 5.0 - 8.0 eV. The remaining doubly excited states (43) had larger excitation energies. However, the bridged structure had 45 doubly excited states with energies ranging from 2.0 - 8.0 eV. These lower matrix elements lowered the predicted oscillator strengths.

When the MCI treatment was used, the triplet spectra were also calculated. The bridged structure was predicted to have a triplet ground state by 0.019 eV. Therefore, the triplet state of the bridged structure could be contributing to the observed color

phenomena.

## 2. 10,10'-Bixanthenylidene

The structural formulas and bond distances chosen for the compound 10,10'-bixanthenylidene and its bridged structure are shown in Figs. 6-A and 6-B, respectively. The oxygen atom now contributes two pi-electrons to the system. Table XIV shows the results of the calculations and two predominant absorption maxima in the observed spectrum of the "colorless" compound. Predicted transitions with very small oscillator strengths ( $<0.01$ ) were omitted. Both calculations for the compound were very good. The colored species absorbs strongly near 1.95 eV and also near 3.9 eV.<sup>24</sup> These two bands are the distinguishing features of the spectrum of the colored form. Both calculations (MCI and MCI - DCI) predicted the bridged structure will absorb in the visible.

## 3. Diphenylmethylenanthrone

The structural formulas and bond distances for the compound diphenylmethylenanthrone and its bridged structure are shown in Figs. 7-A and 7-B, respectively. Table XV shows the results of the calculations and three observed absorption band maxima for the compound. The lowest energy excitation for the compound was not predicted correctly. The calculated values were 0.45 eV too low. This might be a consequence of the fact that the compound is non-planar with the phenyl groups out of the plane of the anthrone moiety. Although the other related compounds are non-planar, this is the only compound with six-membered rings which do not belong to

a fused ring system.

Considering the planar structures, this compound bears the same relationship to 10,10'-bianthrnylidene as anthrone does to anthraquinone from the standpoint of the pi-electrons. If the lowest lying excitation had shown an increase over the value of that calculated for 10,10'-bianthrnylidene, then the agreement would be better. It did in the case of anthrone vs. anthraquinone but by too much.

The colored form of this compound has been described as being red-orange.<sup>14</sup> This means that it could be absorbing near 2.4 ev, 1.0 ev lower than the longest wavelength band of the compound itself. The calculations for the bridged structure predicted an absorption band 0.8 - 1.2 ev lower than the longest wavelength band predicted by the corresponding calculation on the compound. Consequently the transition energies were too low.

No additional band in the visible part of the spectrum was observed on heating this compound in decalin to 153°C.<sup>14</sup> Since the area under the extinction curve did not change with temperature, Grubb and Kistiakowsky concluded that the thermochromism was due to the broadening of a near-ultraviolet absorption region by the changing distribution of molecules among vibrational states.<sup>14</sup> Their data show the hot solution absorbing down to only 2.94 ev. It is curious that the heated samples of this compound appear so red.

#### 4. Bifluorenylidene

The structural formulas and bond distances chosen for the

compound bifluorenylidene and its bridged structure are shown in Figs. 8-A and 8-B, respectively. Geometrically the five and six-membered rings were regular. The crystalline solid and solutions are reported to be red.<sup>40,45</sup> The results of the calculations are shown in Table XVI. The unbridged compound was predicted to be yellow and the bridged structure was predicted to be red.

### B. Other Structures

A number of other structures were treated: (1) helianthrone (Fig. 9-A), which is produced irreversibly in the photochemistry of 10,10'-bianthrnylidene,<sup>7</sup> (2) dihydrobianthrone (Fig. 11-A), which is probably involved in the mechanism leading to paramagnetic species,<sup>1</sup> (3) a doubly bridged structure, and (4) protonated structures related in the intensely colored acid solutions which have been observed. The acid solutions were of particular interest since they present a chemical method of preparing the thermochromic form,<sup>22</sup> and some interesting results were obtained experimentally (section X).

#### 1. Helianthrone and Mesonaphthobianthrone

The structural formulas for the compound helianthrone and its bridged structure, and mesonaphthobianthrone are shown in Figs. 9-A, 9-B, and 9-C, respectively. All of the types of parameters used in the calculations were identical to those chosen for 10,10'-bianthrnylidene. The observed spectra of helianthrone and mesonaphthobianthrone show the longest wavelength absorption maxima are near 2.79 eV and 3.04 eV, respectively.<sup>26</sup> Calculations for these

two compounds are given in Tables XVII and XVIII. Including doubly excited states in the configuration interaction improved the results but the lowest lying excitation was 0.3 ev too high in each case.

Becker and Earhart have suggested that the bridged structure of helianthrone is the photochromic form of this compound.<sup>5</sup> It was first proposed as an intermediate in the irreversible photochemistry of helianthrone to mesonaphthobianthrone.<sup>7</sup> No experimental absorption bands were assigned to it. Both calculations in Table XVII predicted the structure to be colored.

## 2. Dihydrobianthrone and Dihydrohelianthrone

For these compounds each oxygen atom contributes two pi-electrons. The carbon to oxygen bond length was taken to be 1.36A with  $\beta_{CO} = -2.013$  ev for the MCI calculations and  $\beta_{CO} = -1.53$  ev for the calculations including DCI. In all other aspects of the calculations these compounds were taken to be identical to 10,10'-bianthrnylidene and helianthrone, respectively. The calculated spectra given in Table XVIII showed very little difference between the two structures. Dihydrohelianthrone is known to cause a deep blue color in solution.<sup>7</sup> An absorption band at 605 nm (2.04 ev) has been assigned to the 2,7'-dimethyl derivative of this compound which could cause a blue coloration. Becker and Earhart refer to a green coloration which can be trapped on cooling the solution to 77°K.<sup>5</sup> The calculated spectrum of dihydrohelianthrone was in agreement with the experimental evidence. Dihydrobianthrone was also predicted to have an absorption band near 2.0 ev. Experimentally this compound

is not highly colored.<sup>7</sup> Becker and Earhart have assigned an absorption band at 425 nm (2.9 eV) to the 2,7'-dimethyl derivative of this compound.<sup>5</sup>

### 3. 10,10'-Bianthronylidene Double Bridge Structure

This structure consisted of 26 pi-electrons and is theoretically handled by ignoring the pi-centers at the 4,4',5, and 5' positions of 10,10'-bianthronylidene. The results are indicated in Table XIX. The calculated singlet spectrum showed very long wavelength transitions and thus does not agree with anything that has been observed. Similar calculated results were obtained elsewhere.<sup>34</sup>

### 4. Protonated Structures

These structures were studied because acid solutions of 10,10'-bianthronylidene and diphenylmethylenanthrone are highly colored. The acid solutions yield solid samples of the colored form when quenched on ice. Sulfuric acid solutions of 10,10'-bianthronylidene are violet-red due to absorption at 2.23 eV.<sup>28</sup> Bands at 2.79 eV, 3.29 eV, and 4.28 eV are also observed.<sup>28</sup> The dark green sulfuric acid solution of diphenylmethylenanthrone showed absorption at 1.82 eV and 2.76 eV. The results of the calculations shown in Tables XX and XXI indicated that the protonated species in solution is probably not bridged. The monoprotonated species can be used to represent the colored form in each solution of these compounds.

### 5. Betaines

Ionic structures (both positive and negative) were treated

with the PPP method including CI (both MCI and MCI - DCI) for 10,10'-bianthronylidene and 10,10'-bixanthenylidene. Each negative ion was a 16 pi-electron system and each positive ion was a 14 pi-electron system. The lowest lying energy transitions were allowed and appeared at longer wavelengths than those of the respective compounds. For 10,10'-bianthronylidene the values were: (1) MCI; negative ion (2.66 ev), positive ion (2.44 ev), and (2) MCI - DCI; negative ion (2.30 ev), positive ion (2.20 ev). For 10,10'-bixanthenylidene the values were: (1) MCI; negative ion (2.47 ev), positive ion (2.71 ev), and (2) MCI - DCI; negative ion (2.22 ev), positive ion (2.21 ev). Although these structures were predicted to be colored, the colors cannot account for the observed chromism. It is quite possible that the betaines represent contributing resonance structures for describing the chemistry of these compounds particularly in polar solvents such as sulfuric acid.

### C. Discussion

The PPP method including CI of types MCI and MCI - DCI was applied to the calculation of electronic spectrum of some thermochromic ethylenes and structures known to pertain to such systems. The interest in these compounds is as vivid as the colors they produce upon treatment by a variety of methods. For six of the structures treated the longest wavelength absorptions are experimentally known. This absorption band for 10,10'-bianthronylidene, 10,10'-bixanthenylidene, and dihydrohelianthrone was predicted correctly. Helianthrone and mesonaphthobianthrone

results were fair. The results for diphenylmethylenanthrone were poor.

Five of the compounds treated were written structurally as a valence isomer of the ground form by forming a single saturated C-C bond between atoms in hindered positions. The bridged structure in all cases appeared to have a long wavelength transition close to the observed absorption band causing the color. Therefore it is believed that the bridged structure is a probable form for the colored species. Ionic structures (betaines) could not account for the observed colors. The double bridged structure of 10,10'-bianthronylidene was ruled out.

The intense colors of sulfuric acid solutions were explained theoretically with a simple monoprotonated structure and the protonated bridge structure did not give reasonable agreement. The colored form of 10,10'-bianthronylidene and diphenylmethylenanthrone can be formed by quenching the acid solution in ice water. Although the hindered C-atom positions of protonated 10,10'-bianthronylidene were calculated to have identical slightly positive electronic charge, the positions for protonated diphenylmethylenanthrone were oppositely charged (+ 0.043, -0.007). The latter type of charge distribution indicates some tendency for bond formation between these atoms.

The pi-binding energies of 10,10'-bianthronylidene and its bridged structure were calculated to be 53.7 eV and 45.6 eV, respectively. This is a difference of 186.3 kcal/mole suggesting

that the bridged structure as a reasonably stable species is a poor model. This was similar to the results obtained for dihydrophenanthrene (p. 38). and no explanation for this is offered.

## X. EXPERIMENTAL

Magnetic resonance techniques (NMR and ESR) were used to study 10,10'-bianthrnylidene (Fig. 5-A), 2,7'-dimethyl-10,10'-bianthrnylidene, 10,10'-bixanthenylidene (Fig. 6-A), and diphenylmethyleneanthrone (Fig. 7-A). These compounds are thermochromic ethylenes and when heated in solution produced brilliant colors. Sulfuric acid solutions of three of these compounds, 10,10'-bianthrnylidene<sup>22,28</sup> and its dimethyl derivative, and diphenylmethyleneanthrone, were highly colored and produced a colored precipitate when quenched on ice. The colored precipitate from the sulfuric acid solution of 10,10'-bianthrnylidene has been shown to be identical to the thermochromic form produced in heated solutions of this compound by comparing electronic spectra data.<sup>22</sup> In each case (colored precipitate or heated solution) the normal form of 10,10'-bianthrnylidene was regenerated by letting the sample stand at room temperature.

Nuclear magnetic resonance (NMR) was used to study heated samples of each compound and the results were compared with NMR spectra obtained at room temperature of the corresponding "colorless" modification. Electron spin resonance (ESR) and NMR were used to study sulfuric acid-d<sub>2</sub> solutions and samples obtained by quenching the acid in cold D<sub>2</sub>O. Similar investigations were pursued for the related compounds anthrone (Fig. 4-C), anthraquinone (Fig. 4-D), and 10,10'-bianthranyl (Fig. 10-A).

The research given in this section includes the results of each

experiment performed under the subsection headed by the name of the compound of principle interest. All chemical shift data are given in parts per million (ppm) downfield from the proton magnetic resonance line of internal tetramethylsilane.

#### A. Spectra Simulator Programs

Proton magnetic resonance spectra were simulated with the NMR spectrum calculator and plotter program described in reference 51 (appendix C). The chemical shift parameter,  $\nu$ , for each magnetically inequivalent proton and the proton-proton coupling constants,  $J_{ab}$ , are given whenever simulation of a particular spectrum was possible.

Electron spin resonance spectra were simulated with the SESR plotter program kindly provided by Dr. Raymond E. Dessy of the chemistry department of Virginia Polytechnic Institute and State University. All simulations used 100% Lorentzian line shape and are characterized by electron-proton splitting constants with the number of protons assigned to each constant given.

#### B. Instrumentation

Proton magnetic resonance spectra were recorded on a Japan Electron Optics Laboratory Co. Ltd., C-60H NMR spectrometer equipped with a proton JNM-C-60H variable temperature probe. The temperature was adjusted with a JEOLCO JES-VT-3 temperature controller (max. 300°C).

Electron spin resonance spectra were recorded on a Varian Associates E-12 spectrometer equipped with a VFR 2503 magnet power supply, E-101 microwave bridge, and E-231 cavity. Low temperature

was accomplished by boiling liquid nitrogen through a standard Dewar sleeve which fits into the cavity and holds the sample tube.

### C. Materials and Purification

10,10'-Bianthrnylidene, diphenylmethylenanthrone, and hexabromobenzene were purchased from the Aldrich Chemical Company, Inc., Cedar Knolls, New Jersey. These compounds were recrystallized from nitrobenzene. The 10,10'-bianthrnylidene was further purified by recrystallization from chloroform. It decomposed on heating to about 320°C showing no thermochromism in the solid. Diphenylmethylenanthrone was further purified by recrystallization from carbon tetrachloride. It was then dissolved in chloroform and passed over a neutral alumina column (10 cm); the first fraction of eluent was collected and evaporated to dryness. This compound melted reversibly red at 207-209°C. The hexabromobenzene was washed with chloroform. Its melting point was 324-325°C.

10,10'-Bixanthenylidene and 2,7'-dimethyl-10,10'-bianthrnylidene were purchased from Chemicals Procurement Laboratories, Inc., College Point, New York. Both compounds were recrystallized from nitrobenzene. 10,10'-Bixanthenylidene was further purified by recrystallization from chloroform. The white solid turned yellow on heating, blue-green at about 300°C and melted to a purple liquid at 312°C which froze on cooling to give a yellow solid. 2,7'-Dimethyl-10,10'-bianthrnylidene was further purified by recrystallization from carbon tetrachloride. It

decomposed on heating to about 223°C and showed no thermochromism in the solid.

Anthraquinone and p-xylene were purchased from East Kodak-Eastman Organic Chemicals, Rochester, New York. The anthraquinone was purified by dissolving in chloroform and passing over a neutral alumina column (30 cm); the first fraction of eluent was collected and evaporated to dryness.

Anthrone, nitrobenzene, and neutral alumina (Brockman Activity I) were purchased from Fisher Scientific Company, Fair Lawn, New Jersey. The anthrone was purified in the same manner as the anthraquinone. The nitrobenzene was redistilled.

Chloranil (tetrachloro-p-benzoquinone) was purchased from Matheson Coleman and Bell, East Rutherford, New Jersey and recrystallized from nitrobenzene.

Chloroform-d<sub>1</sub> (99.8% isotopic purity), sulfuric acid-d<sub>2</sub> (99.5% isotopic purity) and water-d<sub>2</sub> were purchased from Diaprep, Inc., Atlanta, Georgia.

10,10'-Bianthranyl was synthesized from anthrone as described in subsection D.

#### D. Anthrone

The structural formula for anthrone is shown in Fig. 4-C and the NMR spectrum is discussed in reference 51, page 16.

Neither a solution of anthrone in chloroform nor a 0.72M solution in conc. sulfuric acid gave an ESR signal. Irradiation of these solutions at room temperature with an ultra-violet lamp did

not produce a signal.

When this compound was dissolved in sulfuric acid-d<sub>2</sub>, deuterium exchange occurred with the methylene hydrogens. The NMR spectrum of a 0.64M solution is given in Fig. 12. The aromatic protons show intense resonance lines; the methylene protons (-4.31 ppm) show only a weak signal. A 0.51M solution was prepared and after three minutes quenched on cold D<sub>2</sub>O. The precipitate was filtered and dried. The NMR spectrum in chloroform-d<sub>1</sub> showed by its integration curve of the methylene protons relative to the aromatic protons that 54% exchange had occurred. This partially deuteriated anthrone was redissolved in sulfuric acid-d<sub>2</sub> to form a 0.28M solution and after 30 minutes quenched on cold D<sub>2</sub>O. NMR showed that 70% exchange of the methylene hydrogens was accomplished. This indicates that in anthrone the hydrogens bonded to the saturated carbon atom are relatively labile.

10,10'-Bianthranyl was prepared from anthrone following the procedure of Cohen, Millar, and Richards.<sup>10</sup> A solution of 3.79g ( $1.54 \times 10^{-2}$  moles) of chloranil in 80 ml of p-xylene was prepared. While warming the solution, 3.00g ( $1.54 \times 10^{-2}$  moles) of anthrone were added in small portions and then the orange solution was refluxed for one hour. On cooling, the desired product precipitated and was washed with ether. The white solid decomposed on heating to about 263°C. Experiments with this compound are described in subsection G.

### E. Anthraquinone

The structural formula for this compound is given in Fig. 4-D. The proton magnetic resonance spectrum of a saturated solution of anthraquinone in chloroform- $d_1$  is shown in Fig. 13. Simulation of this spectrum was possible using the following set of parameters:

$$\nu_1 = -8.36 \text{ ppm}$$

$$\nu_2 = -7.84 \text{ ppm} \quad J_{12} = 7.45 \text{ Hertz}$$

$$\nu_3 = -7.84 \text{ ppm} \quad J_{13} = 1.88 \text{ Hertz} \quad J_{23} = 7.96 \text{ Hertz}$$

$$\nu_4 = -8.36 \text{ ppm} \quad J_{14} = 0.20 \text{ Hertz} \quad J_{24} = 1.88 \text{ Hertz} \quad J_{34} = 7.45 \text{ Hertz}$$

where protons 1-4 are bonded to the corresponding carbon atoms numbered 1-4 on the structural formula (Fig. 13). This is identical to the spectrum reported as bianthrnylidene-B in reference 51, page 22. Anthraquinone melt at  $290^\circ\text{C}$  gave the same resolved NMR spectrum.

Anthraquinone did not give an ESR signal when dissolved in conc. sulfuric acid. A 0.26M sulfuric acid- $d_2$  solution was prepared and after two hours quenched on  $\text{D}_2\text{O}$ . The precipitate was collected and dried in a vacuum dessicator. No proton-deuterium exchange occurred as shown by the NMR spectrum of a saturated solution of this precipitate in chloroform- $d_1$ . If exchange had occurred, the over-all intensity of the resonance lines would have diminished in comparison with the original spectrum and probably the relative intensity of the lines for  $\nu_1$  ( $\nu_4$ ) and  $\nu_2$  ( $\nu_3$ ) would have changed. These effects were not observed.

F. 10,10'-Bianthronylidene and  
2,7'-Dimethyl-10,10'-Bianthronylidene

The structural formula for 10,10'-bianthronylidene is shown in Fig. 5-A. Its proton magnetic resonance spectrum in chloroform- $d_1$  is given in Fig. 14. Simulation of this spectrum was possible using the following set of parameters:

$$\nu_1 = -8.09 \text{ ppm}$$

$$\nu_2 = -7.41 \text{ ppm} \quad J_{12} = 7.90 \text{ Hertz}$$

$$\nu_3 = -7.16 \text{ ppm} \quad J_{13} = 1.80 \text{ Hertz} \quad J_{23} = 6.30 \text{ Hertz}$$

$$\nu_4 = -7.09 \text{ ppm} \quad J_{14} = 0.30 \text{ Hertz} \quad J_{24} = 1.80 \text{ Hertz} \quad J_{34} = 6.30 \text{ Hertz}$$

where protons 1-4 are bonded to the corresponding carbon atoms numbered 1-4 on the structural formula. This is the spectrum reported as bianthronylidene-A in reference 51, page 24, and the simulated spectrum is shown in Fig. 12 page 23 of that same reference.

Solutions of these compounds exhibited reversible thermochromism. The NMR spectrum of 10,10'-bianthronylidene in chloroform- $d_1$  at 70°C showed some line broadening. This effect was so drastic in the case of the dimethyl compound that the spectrum at 135°C barely showed any absorption lines for the methyl protons. Cooling the sample to room temperature reversed this phenomenon. The broadening of the proton magnetic resonance lines may be caused by the presence of paramagnetic species whereby the larger interaction of the nuclear moment with the electronic moment compared to nuclear magnetic moment interactions

will shorten the relaxation time.<sup>8</sup> It is known that when these compounds in solution are exposed to light an ESR signal develops which increases on heating.<sup>1,5,23</sup> The ESR spectrum has been resolved and assigned to the hydrobianthrone radical in which the odd electron shows splittings from only one half of the molecule.<sup>1,50</sup> The structural formula is shown in Fig. 11-B. In all instances care was taken not to expose the samples to direct room light by working with red light bulbs. Nevertheless it was not possible to obtain a sample free from at least a weak unresolvable ESR signal of 20 gauss total width.

2,7'-Dimethyl-10,10'-bianthrnylidene was further purified with a neutral alumina column. It decomposed to a red solid at 233°C. The NMR spectrum of this red solid dissolved in chloroform-d<sub>1</sub> is shown in Fig. 15. The material was not very soluble but the two methyl peaks indicate that the sample may contain primarily the 2,7'-dimethyl derivative of helianthrone (Fig. 9-A) in which the methyl groups are magnetically inequivalent. There is a noticeable shift of the aromatic proton region downfield. The signal at -1.6 ppm was not identified but was due to an impurity in the solvent.

10,10'-Bianthrnylidene was also passed over a neutral alumina column. The solid material collected melted reversibly green at 265°C. The NMR spectrum showed that it had partially reacted on the column to form an appreciable amount of anthraquinone. Theilacker, et. al., indicate that on exposing a hot solution of

10,10'-bianthrnylidene to air the green color disappears rapidly and anthraquinone is isolated as a product from the reaction with molecular oxygen.<sup>54</sup> It has been reported that the active sites in alumina involve molecular oxygen.<sup>13</sup> The original material melted reversibly green when mixed with anthraquinone, anthrone, or hexabromobenzene. Apparently the depression of the melting point to 300°C by an impurity caused the green droplets described by Padova when this compound was first synthesized.<sup>42</sup> NMR samples of these melts turned black and the broad resonance lines were unresolvable. No additional resonances were observed outside of the aromatic region.

A sample of 10,10'-bianthrnylidene in cold chloroform-d<sub>1</sub> was irradiated with an ultra-violet lamp which caused the solution to turn crimson red, then brown. The NMR spectrum of the relatively insoluble material showed the same downfield shift in the aromatic region as that previously noted for the dimethyl derivative after melting (red solid, Fig. 15). An additional peak at -1.23 ppm appeared which was not identified.

It is also known that when these compounds are dissolved in conc. sulfuric acid or a solution of hydrogen fluoride in sulfur dioxide, the acid solutions are highly colored (blood red or purplish red). When the acid solution is quenched in cold water or on ice a green precipitate forms which reverts to a yellowish substance on standing at room temperature or when dissolved into solution at room temperature. The acid solution can be quenched

in a cold organic solvent such as ethanol or the green precipitate collected quickly and dissolved in the cold; in either case, a green solution presumably containing just the thermochromic form in high yield results.<sup>22,51</sup> An attempt was made to obtain an NMR spectrum of such solution in chloroform- $d_1$  formed from 10,10'-bianthrnylidene,<sup>51</sup> and also from the dimethyl derivative but either the solutions were not concentrated enough due to the low temperature ( $-50^{\circ}\text{C}$  and  $-70^{\circ}\text{C}$ , respectively) for a characteristic spectrum or possibly the samples contained enough paramagnetic species to cause severe line broadening.

Solutions of 10,10'-bianthrnylidene and its dimethyl derivative in a liquid hydrogen fluoride-sulfur dioxide mixture were prepared using Kel-F test tubes and dry ice-acetone slush baths. The characteristic green solid was formed by quenching each acid solution on ice; the precipitates were collected and dried. These samples turned yellow in the process. The first sample gave an NMR spectrum at room temperature of only regenerated 10,10'-bianthrnylidene but the dimethyl compound gave an intense signal at  $-1.23$  ppm in addition to regenerated 2,7'-dimethyl-10,10'-bianthrnylidene (Fig. 16). This signal was not identified. The dimethyl derivative still melted to give, on cooling, a red solid. The NMR spectrum of the red solid at room temperature in chloroform- $d_1$  showed the same characteristics as before (Fig. 15) and an intense signal at  $-1.23$  ppm.

A major quintet of lines was obtained for the ESR signal

observed by dissolving the green solid formed from 10,10'-bianthrnylidene and HF:SO<sub>2</sub> in chloroform to which a small amount of carbon disulfide had been added so that the solution would not freeze in a dry ice-acetone bath (Fig. 17). Simulation of this spectrum was possible using four splitting constants (3.297 gauss, 2.951 gauss, 0.853 gauss, 0.665 gauss) and assigning each constant to two protons; the line width was 0.635 gauss. These parameters are identical to those found for the hydrobianthrone radical.<sup>1</sup> However, a solution of 10,10'-bianthrnylidene in chloroform gave an unresolved ESR signal of comparable intensity. The hydrobianthrone radical exists in the 10,10'-bianthrnylidene and the analogous radical in the 2,7'-dimethyl-10,10'-bianthrnylidene used in these studies.

After ten minutes, a 0.096M solution of 10,10'-bianthrnylidene in sulfuric acid-d<sub>2</sub> was quenched on cold D<sub>2</sub>O. The precipitate was dried and dissolved in CDCl<sub>3</sub>. The NMR spectrum showed that no hydrogen-deuterium exchange had occurred on any of the protons around the rings. If at least partial exchange had occurred for the protons in the hindered positions (4,5,4',5'), then this would be evidence for a more labile type of hydrogen analogous to the exchange of the methylene protons of anthrone and lend support to the bridged structure (Fig. 5-B).

#### G. 10,10'-Bianthranyl

This compound was prepared from anthrone and differs in its structural formula from 10,10'-bianthrnylidene in that the

"ethylenic" linkage is saturated with two hydrogen atoms (Fig. 10-A). It does not exhibit an ESR signal when dissolved in chloroform or pyridine at room temperature. The infra-red spectrum and the NMR spectrum (the bridge protons have a chemical shift of  $-4.75$  ppm) agreed with those reported elsewhere.<sup>10</sup> The resonance peak of the bridge protons ( $-4.63$  ppm) was quite narrow when 10,10'-bianthranyl was dissolved in  $D_2SO_4$  indicating that they did not exchange in acid. Further evidence of this was obtained by quenching the acid solution on cold  $D_2O$  and observing no difference in the NMR spectrum of the precipitate as compared to that of the original material.

It has been suggested that by boiling a solution of 10,10'-bianthranyl in pyridine that enolization would occur forming dihydrobianthrone (Fig. 11-A).<sup>3</sup> It would be interesting to observe the NMR spectrum of this form because the "enolic" protons may have a chemical shift near the  $-1.23$  ppm signal observed with various other samples (pgs. 69, 70, 70) which has not been identified. After two hours of refluxing a solution of 10,10'-bianthranyl in pyridine the solvent was vacuum distilled and a brown solid remained. Part of this sample was washed with ether giving a yellow solid which by its "melting" point and NMR spectrum was identified as 10,10'-bianthranylidene. When the brown solid was redissolved in pyridine the solution exhibited a well resolved ESR spectrum of the hydrobianthrone radical (Fig. 18); this was simulated using a line width of 0.190 gauss (Fig. 19).

The splitting constants for this radical have been given on page 71. An infra-red spectrum of the brown material showed no absorption bands characteristic of an alcohol. It is possible that the ESR signal assigned to the hydrobianthrone radical (Fig. 11-B) is due to the bianthranyl radical (Fig. 10-B) since the odd electron could be showing splittings from the part of the molecule which is identical in each structure.

#### H. 10,10'-Bixanthenylidene

The structural formula of this compound is given in Fig. 6-A. The proton magnetic resonance spectrum of a 0.024M solution in  $\text{CDCl}_3$  is shown in Fig. 20. Simulation of this spectrum was possible using the following set of parameters:

$$\nu_1 = -7.29 \text{ ppm}$$

$$\nu_2 = -7.24 \text{ ppm} \quad J_{12} = 8.20 \text{ Hertz}$$

$$\nu_3 = -6.88 \text{ ppm} \quad J_{13} = 1.45 \text{ Hertz} \quad J_{23} = 7.80 \text{ Hertz}$$

$$\nu_4 = -7.16 \text{ ppm} \quad J_{14} = 0.86 \text{ Hertz} \quad J_{24} = 1.75 \text{ Hertz} \quad J_{34} = 8.70 \text{ Hertz}$$

where hydrogen atoms 1-4 are bonded to the carbon atoms numbered 1-4 on the structural formula. The spectrum simulation is shown in Fig. 21. Heating this sample to  $120^\circ\text{C}$  and then cooling back down to room temperature caused no change in the NMR spectrum.

In order to obtain complete solubility for a 0.056M solution of 10,10'-bixanthenylidene in decalin, the temperature must be relatively high. A well resolved NMR spectrum was obtained at  $176^\circ\text{C}$  and is shown in Fig. 22. In comparison with the room temperature spectrum in  $\text{CDCl}_3$ , if one assumes no shift in the total

spectrum, simulation can be obtained simply by changing  $\nu_4$ , from -7.16 ppm to -7.23 ppm. This simulation is shown in Fig. 23. It is not known whether this change is due to a concentration effect, a temperature effect, or a solvent effect ( $\text{CDCl}_3$  vs. decalin). It could be that the difference is connected with the formation of the blue-green color because a more planar configuration would cause a downfield shift of the protons in the hindered position (still magnetically equivalent). This would be analagous to the downfield peak position of the hindered protons in bifluorenylidene (Fig. 8-A) but these are shifted ten times as far.<sup>45</sup> This is consistent with the more planar geometry which bifluorenylidene exhibits in the crystalline state where the angle between the middle rings is only  $10^\circ$  whereas in 10,10'-bixanthenylidene the corresponding angle is much larger ( $40^\circ$ ).<sup>15,40,41</sup> Since the bifluorenylidene is red it has been suggested that it exists in a "thermochromic form" as a solid and in solution and in fact it exhibits no thermochromic or photochromic properties.<sup>25,27</sup> It would be interesting to see whether the NMR spectrum of bifluorenylidene in solution is noticeably temperature dependent. Heating the decalin sample of 10,10'-bixanthenylidene to a higher temperature caused less resolved NMR lines due to broadening.

10,10'-Bixanthenylidene forms an orange solution in sulfuric acid and in  $\text{HF}:\text{SO}_2$  solution. Quenching either of these acid solutions on ice does not produce a colored form.

A mixture of hexabromobenzene and 10,10'-bixanthenylidene

which melted reversibly purple at 277-278°C did not give a resolved NMR spectrum at 285°C but a single broad line.

Solid 10,10'-bixanthenylidene did not exhibit an ESR signal. After melting, the fused solid was crushed. The material gave a single line ESR signal of 20 gauss total width and an NMR spectrum in  $\text{CDCl}_3$  identical to that of the original compound.

#### I. Diphenylmethylenanthrone

The structural formula for this compound is shown in Fig. 7-A. The NMR spectrum in  $\text{CDCl}_3$  is given in Fig. 24 and Fig. 25 (two sweep widths). This spectrum is readily interpreted by assigning the downfield multiplet to the protons bonded on the positions alpha to the carbonyl group. The remainder of the protons on the three-fused ring system produce the upfield lines with the exception of the most intense line which is due to the phenyl ring protons. The phenyl ring protons show some splitting in Fig. 25 but they are comparatively equivalent. This solution gave the same NMR spectrum at 113°C. No ESR signal was observed either before or after heating the sample or after exposing it to room light for eight hours.

The NMR spectrum of diphenylmethylenanthrone melt (red) at 230°C is shown in Fig. 26. No additional resonance peaks were observed and the line width compared well with the room temperature spectrum in  $\text{CDCl}_3$  of the same sweep width.

In decalin solution the NMR spectrum changed as shown in Figs. 27 and 28 at 100°C and 180°C, respectively. The downfield

multiplet for the alpha protons was observed in the same relative position but is not shown. The obvious difference in these spectra is the increase in splitting of the phenyl ring protons as the temperature was increased; this phenomenon was reversible.

Diphenylmethylenanthrone formed a green solution in sulfuric acid due to an electronic absorption band at 6800A (1.82 ev). An orange-red precipitate formed when the acid solution was quenched in ice-water. Drying the sample in a vacuum dessicator caused it to turn to a green-black color which reverted to the orange color on exposing it to moist air for a few minutes. This process could be repeated. The infra-red spectrum of this solid which could be a colored acid-salt ( $+ >C-OH \cdot HSO_4^-$ ) did show a band at  $1460 \text{ cm}^{-1}$  characteristic of a saturated  $\Rightarrow C-H$  bond. Further investigations with this material should be pursued to determine whether a saturated bridge structure has indeed formed.

#### J. Summary

This summary is a list of the important results obtained. The text can be consulted for the details of the experimental studies.

(1) NMR spectra of anthrone,  $^{51}$  anthraquinone, 10,10'-bianthrnylidene, 10,10'-bixanthenylidene, diphenylmethylenanthrone, and 10,10'-bianthranyl $^{10}$  at ambient temperature in  $CDCl_3$  were interpreted.

(2) NMR line broadening was observed for the spectra obtained by heating  $CDCl_3$  solutions of 10,10'-bianthrnylidene and its dimethyl

derivative, and by heating a decalin solution of 10,10'-bixanthyrylidene above 176°C. Broad NMR lines were also observed for the spectra obtained by melting mixtures of (a) 10,10'-bianthronylidene and anthraquinone, and (b) 10,10'-bixanthyrylidene and hexabromobenzene.

(3) Melted diphenylmethylenanthrone gave no additional NMR signals and although the spectrum was not well resolved, the line width was comparable to that observed in the spectrum obtained at ambient temperature in  $\text{CDCl}_3$ . The phenyl protons of diphenylmethylenanthrone showed increased splitting of NMR lines in a heated decalin solution. The NMR spectra of 10,10'-bixanthyrylidene obtained in  $\text{CDCl}_3$  at ambient temperature and in decalin at 176°C showed a slight difference.

(4) Sulfuric acid solutions of 10,10'-bianthronylidene, 2,7'-dimethyl-10,10'-bianthronylidene, and diphenylmethylenanthrone gave colored precipitates when quenched in ice water whereas the acid solution of 10,10'-bixanthyrylidene did not. 10,10'-Bianthronylidene and its dimethyl derivative were regenerated from the corresponding colored precipitate by simply dissolving in chloroform at ambient temperature. It is not known whether any diphenylmethylenanthrone can be regenerated from its colored precipitate; an infra-red spectrum of the precipitate indicates that saturated  $\text{>C-H}$  bonds are present. This red-orange precipitate in an evacuated desiccator changed to a dark green color (the color of the acid solution) presumably because the sample

was dried. Exposing it to air reproduced the red-orange color as the material absorbed moisture.

(5) It was not possible to obtain an NMR spectrum in cold  $\text{CDCl}_3$  of the colored precipitates formed on quenching the corresponding acid solutions of 10,10'-bianthrnylidene<sup>51</sup> and its dimethyl derivative.

(6) Proton-deuterium exchange in  $\text{D}_2\text{SO}_4$  was observed for the methylene protons of anthrone. No exchange for any protons was observed with anthraquinone, 10,10'-bianthrnylidene, or 10,10'-bianthranyl.

(7) An unidentified signal at -1.23 ppm was observed in the NMR spectra obtained when 10,10'-bianthrnylidene in solution was decomposed by ultra-violet light and when its dimethyl derivative was regenerated after quenching the acid solution in ice water.

(8) Helianthrone was possibly formed when 10,10'-bianthrnylidene in solution was decomposed by ultra-violet light as indicated by the resulting NMR spectrum. This is known to occur as shown by the electronic absorption data.<sup>26</sup> The dimethyl derivative of helianthrone was possibly formed when 2,7'-dimethyl-10,10'-bianthrnylidene was melted and then refrozen (red solid) as indicated by the NMR spectrum of the red solid obtained in  $\text{CDCl}_3$ .

(9) 10,10'-Bianthrnylidene formed some anthraquinone on a neutral alumina column. The mixture melted reversibly green. Dimethyl-10,10'-bianthrnylidene did not decompose on a neutral alumina column but its melting point was increased by  $10^\circ\text{C}$ .

(10) The ESR spectrum of the hydrobianthrone radical was obtained when a pyridine solution of 10,10'-bianthranyl was refluxed producing 10,10'-bianthronylidene in the process. It seems that this radical was always present in the 10,10'-bianthronylidene and the corresponding radical in the 2,7'-dimethyl-10,10'-bianthronylidene. An ESR signal was observed in the solid obtained by first melting 10,10'-bixanthenylidene and then refreezing it. None was observed in a heated solution of 10,10'-bixanthenylidene.<sup>1</sup>

## XI. CONCLUSION

The Pariser-Parr-Pople method with configuration interaction including singly excited and doubly excited states was used to calculate the electronic spectra of a variety of molecules. It was first applied to six hydrocarbons and four carbonyl compounds. It was necessary to reduce the one-center integral on carbon ( $\gamma_{cc}$ ) to obtain good results for benzene, anthracene, naphthalene, and trans-stilbene. Relatively minor adjustments were made in parameters for the other compounds. Good results were consequently obtained for cis-stilbene, dihydrophenanthrene intermediate, anthraquinone, and p-benzoquinone. Improved results over the MCI procedure were also obtained for p-naphthaquinone, however, the results for anthrone were puzzling.

Calculations of electronic spectra of some thermochromic ethylenes and structures found in such systems produced interesting results. A single saturated bridge structure was shown to be a probable form causing the vivid colors which are characteristic of the photochemistry. It is believed that the color formed by other means such as heating solutions is due to the same chemical species.<sup>5</sup>

The bridged structure shown for 10,10'-bianthrnylidene in Fig. 5-B would be expected to have a different electronic charge distribution as a result of the bridge in comparison to the normal form of the molecule (Fig. 5-A). The calculations did show a noticeable change in charge densities for the carbon atoms numbered 1 and 3. The bridged structure was calculated to have 0.048 and

0.021 units of negative charge less in these respective positions than the normal form. The charge densities at positions 8 (8') and 1 (1') were not identical. Neither were those at positions 7 (7') and 2 (2'), or at positions 6 (6') and 3 (3') on the outer rings of the bridged structure. The charge density at position 5 (5') was different from the others. No results were given by the calculation for position 4 or 4', since, when the bridge forms, these carbon atoms are no longer in the pi-system.

The protons bonded to the carbon atoms which have different charge densities would be magnetically inequivalent resulting in a complex NMR spectrum with much hyperfine structure. The splitting of NMR resonance lines as the bridged structure formed from the ground state of the molecule could be at least partially causing the NMR line broadening observed in various samples studied experimentally. Paramagnetism can also contribute to NMR lines being unresolved. Kortum and Koch have shown that the thermochromism and paramagnetism observed in solution are independent of each other.<sup>23</sup>

The intense colors of sulfuric acid solutions were explained theoretically with a simple monoprotonated structure and the protonated bridge structure was ruled out. Since the colored form was produced on quenching the sulfuric acid solution on ice, the bridge must form during this process. If the bridged form were the predominant form causing the color in acid, the bridge protons would have appeared in the NMR spectrum of the deuteriated acid solution

as in the case of 10,10'-bianthranyl. The bridge protons would not have been observed if they exchanged with deuterium as in the case of the methylene protons of anthrone. No deuterium exchange was observed in the 10,10'-bianthranylidene which was regenerated from  $D_2SO_4$  by quenching the solution in cold  $D_2O$ . Resonance lines of the bridge protons could have been severely broadened by paramagnetic molecules, however, paramagnetism did not increase and/or was not produced in acid solution.

TABLE I. BENZENE CALCULATIONS; MONO-EXCITED CI

Exp. <sup>44</sup>		Calculated			
Symmetry	Energy (ev)	Symmetry	Energy (ev); MCI = 9		
B <sub>2u</sub>	4.89	B <sub>2u</sub>	4.92	4.77	4.92
B <sub>1u</sub> or E <sub>2g</sub>	6.14	B <sub>1u</sub>	6.21	6.06	5.88
E <sub>1u</sub>	6.75	E <sub>1u</sub>	7.04	6.88	6.67
		E <sub>2g</sub>	8.53	8.30	8.38
		$\gamma_{cc}$ (ev)	11.13	11.08	9.40
		$-\beta_{cc}$ (ev)	2.395	2.319	2.405
		ref.	43	21	48

TABLE II. BENZENE CALCULATIONS; DOUBLY EXCITED CI

Symmetry	Excitation Energies (ev)								
	MCI = 9; DCI = 45						MCI = 9; DCI = 22		
	1	2	3	4	5	6	7	8	9
B <sub>2u</sub>	4.15	4.18	4.63	4.57	4.78	4.94	4.03	4.57	4.97
B <sub>1u</sub>	7.15	6.91	7.28	6.47	6.20	6.15	6.49	6.16	6.00
E <sub>1u</sub>	7.47	7.26	7.67	6.94	6.71	6.67	7.42	6.96	6.70
E <sub>2g</sub>	6.75	6.77	7.45	7.26	7.54	7.76	6.83	7.38	7.86
$\gamma_{cc}$ (ev)	11.13	10.60	10.60	9.00	7.90	7.40	11.13	9.00	7.40
$-\beta_{cc}$ (ev)	2.395	2.388	2.610	2.50	2.55	2.60	2.395	2.50	2.60
$-G^*$ (ev)	1.145	1.239	1.141	0.74	0.50	0.40	0.71	0.40	0.23

\* denotes ground state (A<sub>1g</sub>) depression

TABLE III. NAPHTHALENE CALCULATIONS; MONO-EXCITED CI

Exp. 19	Calculated Excitation Energies		
	MCI = 25		MCI = 15
(ev) - $f^*$	(ev) - f - transition	(ev) - transition	(ev) - transition
3.97 (0.002)	4.15 (0) 1	4.02 1	4.25 1
4.29 (0.18)	4.49 (0.25) 2	4.38 2	4.51 2
5.63 (1.70)	5.81 (2.05) 3	5.68 3	5.81 3
6.51 (0.20)	6.47 (0.60) 7	6.31 7	6.48 7
7.41 (0.6)	8.08 (0.99) 13	7.87 13	8.09 12
$\gamma_{cc}$ (ev)	11.13	11.08	11.13
$-\beta_{cc}$ (ev)	2.395	2.319	2.395

\* oscillator strength

TABLE IV. ANTHRACENE CALCULATIONS; MONO-EXCITED CI

Exp. <sup>43</sup>	Calculated Excitation Energies		
	MCI = 49		MCI = 15
(ev)	(ev) - f* - transition	(ev) - transition	(ev) - transition
3.49	3.47 (0.30) 1	3.40 1	3.54 1
4.89s	5.09 (2.81) 6	4.97 6	5.15 5
5.64	6.11 (0.002) 8	5.96 8	6.12 8
	6.32 (0.27) 11	6.16 11	6.41 9
$\gamma_{cc}$ (ev)	11.13	11.08	11.13
$-\beta_{cc}$ (ev)	2.395	2.319	2.395

\* oscillator strength

TABLE V. NAPHTHALENE CALCULATIONS; DOUBLY EXCITED CI

	MCI = 15; DCI = 39				MCI=19;DCI=60	MCI=25;DCI=54
	(ev) - f <sup>**</sup> - tr <sup>#</sup>	(ev) - tr	(ev) - f - tr	(ev) - f - tr	(ev) - f - tr	(ev) - tr
	4.01 (0) 1	4.20 1	4.28 (0) 1	4.30 (0.23) 1	4.18 (0) 1	4.19 1
	4.91 (0.15) 2	4.52 2	4.35 (0.21) 2	4.36 (0) 2	4.43 (0.19) 2	4.48 2
	6.10 (1.45) 5	5.78 4	5.62 (1.57) 3	5.59 (1.60) 3	5.78 (1.52) 4	5.79 4
	7.14 (0.31) 10	6.69 8	6.49 (0.40) 7	6.46 (0.41) 7	6.37 (0.37) 7	6.40 7
	8.63 (0.89) 15	8.23 15	8.05 (0.77)15	8.05 (0.76)15	8.20 (0.73)15	8.20 15
$\gamma_{cc}$ (ev)	11.13	9.00	7.90	7.40	9.00	9.00
$-\beta_{cc}$ (ev)	2.395	2.50	2.55	2.60	2.50	2.50
$-G^{**}$ (ev)	0.75	0.43	0.31	0.26	0.44	0.44

\* oscillator strength

\*\* ground state depression

# transition number

TABLE VI. ANTHRACENE CALCULATIONS; DOUBLY EXCITED CI

	MCI = 15; DCI = 39				MCI=28; DCI=51	MCI=21; DCI=58
	(ev) - f* - tr <sup>#</sup>	(ev) - f - tr	(ev) - tr	(ev) - tr	(ev) - f - tr	(ev) - f - tr
	3.68 (0) 1	3.44 (0.24) 1	3.28 1	3.23 1	3.64 (0) 1	3.40 (0.19) 1
	3.78 (0.20) 2	5.08 (2.09) 6	4.96 6	4.95 6	3.73 (0.20) 2	5.07 (1.18) 6
	5.30 (1.98) 5	6.16 (0.02) 10	5.95 9	5.92 9	5.29 (2.02) 6	6.16 (0.01) 11
	6.59 (0.02) 10	6.48 (0.08) 12	6.35 12	6.35 12	6.57 (0.02) 12	6.29 (0.08) 12
$\gamma_{cc}$ (ev)	11.13	9.00	7.90	7.40	11.13	9.00
$-\beta_{cc}$ (ev)	2.395	2.50	2.55	2.60	2.395	2.50
$-G^{**}$ (ev)	0.54	0.33	0.24	0.20	0.54	0.32

\* oscillator strength

\*\* ground state depression

<sup>#</sup> transition number

VII. STILBENE CALCULATIONS

	MCI = 49	MCI=21; DCI=58	MCI = 15; DCI = 39			
	(ev) - f* - tr <sup>#</sup>	(ev) - f - tr	(ev) - f - tr	(ev) - tr	(ev) - tr	(ev) - tr
<u>TRANS</u> <sup>2</sup>	4.29 (1.19) 1	4.28 (1.03) 1	4.28 (1.04) 1	4.55 1	4.16 1	4.13 1
	4.57 (0) 2	4.65 (0) 2	4.78 (0) 2	4.78 2	4.78 2	4.84 2
	4.58 (0) 3	5.71 (0.51) 5	5.75 (0.61) 6	6.02 5	5.61 5	5.60 5
<u>CIS</u> <sup>1</sup>	4.09 (0.43) 1	4.09 (0.36) 1	4.10 (0.37) 1	4.35 1	3.99 1	3.97 1
	4.49 (0) 2	4.57 (0) 2	4.73 (0) 2	4.70 2	4.74 2	4.79 2
	4.55 (0) 3	5.40 (0.55) 4	5.50 (0.56) 5	5.75 5	5.37 4	5.36 4
$\gamma_{cc}$ (ev)	11.13	9.00	9.00	11.13	7.90	7.40
$-G^{**}$ (ev)	-	0.15	0.15	0.26	0.10	0.09

\* oscillator strength

\*\* ground state depression (CIS)

# transition number

1 lowest singlet transition 4.4ev<sup>33</sup>

2 lowest singlet transition 3.9-4.2ev<sup>33,6</sup>

TABLE VIII. DIHYDROPHENANTHRENE CALCULATIONS

Exp. 35	MCI = 36	MCI = 36	MCI=21; DCI=58	MCI=26; DCI=53	MCI=33; DCI=46
(ev)	(ev) - f* - tr <sup>#</sup>	(ev) - f - tr	(ev) - f - tr	(ev) - f - tr	(ev) - tr
2.7	2.23 (0.55) 1	2.01 (0.52) 1	1.95 (0) 1	2.03 (0) 1	2.03 1
	2.96 (0) 2	2.94 (0) 2	2.77 (0) 2	2.41 (0.35) 2	2.43 2
	3.97 (0) 3	3.88 (1.05) 3	2.90 (0.32) 3	2.98 (0) 3	3.04 3
	4.15 (1.08) 4	3.98 (0) 4	3.90 (0) 4	3.72 (0) 4	3.73 4
$\gamma_{cc}$ (ev)	11.13	9.00	11.13	9.00	9.00
$-G^{**}$ (ev)	-	-	1.069	0.67	0.67

\* oscillator strength

\*\* ground state depression

# transition number

TABLE IX. p-BENZOQUINONE CALCULATIONS

Exp. <sup>12</sup>	1	2	3	4	5 <sup>Δ</sup>	6
	MCI = 16	MCI = 16; DCI = 38	MCI=16; DCI=38	MCI = 16; DCI = 63	MCI = 16; DCI = 43	MCI = 16; DCI = 63
(ev)	(ev) - f <sup>*</sup>	(ev) - f	(ev)	(ev) - f	(ev) - f	(ev) - f
4.28s	4.49 (0)	4.79 (0)	4.37	4.62 (0)	4.20 (0)	3.63 (0)
5.07vs	5.16 (0.83)	5.50 (0)	4.43	4.74 (0)	4.30 (0)	4.14 (0)
	7.09 (0)	5.74 (0.60)	5.23	5.35 (0.43)	5.03 (0.76)	4.49 (0.41)
$\gamma_{cc}$ (ev)	11.13	11.13	11.13	11.13	11.13	11.13
$-\beta_{co}$ (ev)	3.145	3.145	2.60	2.60	2.60	2.30
$-G^{**}$ (ev)	-	1.00	1.09	1.51	0.96	1.25

\* oscillator strength

\*\* ground state depression

<sup>Δ</sup> cut off at 15.0 ev

TABLE IX. p-BENZOQUINONE CALCULATIONS (cont.)

	7	8	9	10 <sup>Δ</sup>	11	12
	MCI = 16; DCI = 38	MCI=16; DCI=63	MCI=16; DCI=63	MCI=16; DCI=50	MCI=16; DCI=38	MCI=16; DCI=38
	(ev) - f*	(ev)	(ev)	(ev)	(ev)	(ev)
	3.88 (0)	4.00	3.81	3.68	3.67	3.58
	4.39 (0)	4.60	4.53	4.38	4.43	4.49
	5.13 (0.68)	5.15	5.06	5.05	5.11	5.12
$\gamma_{cc}$ (ev)	9.00	9.00	9.00	9.00	7.90	7.40
$-\beta_{co}$ (ev)	2.60	2.60	2.50	2.50	2.60	2.60
$-G^{**}$ (ev)	1.02	1.26	1.30	1.13	1.00	1.02

\* oscillator strength

\*\* ground state depression

Δ cut off at 15.0 ev

TABLE X. ANTHRAQUINONE CALCULATIONS

Exp. <sup>12</sup>	MCI = 64	MCI=15; DCI=39	MCI=21; DCI=58	MCI=28; DCI=51
(ev)	(ev) - f* - tr <sup>#</sup>	(ev) - f - tr	(ev) - f - tr	(ev) - f - tr
3.80ms	4.29 (0.19x) 1	3.92 (0) 1	3.96 (0) 1	3.90 (0) 1
4.53s	4.38 (0) 2	4.03 (0.25x) 2	4.12 (0.23x) 2	4.10 (0.24x) 2
4.70s	4.42 (0) 3	4.17 (0) 3	4.29 (0) 3	4.21 (0) 3
4.98s	4.94 (0.47y) 4	4.70 (0.54y) 4	4.55 (0.50y) 4	4.53 (0.49y) 4
	5.44 (0.92x) 5	5.57 (0.94x) 5	5.54 (0.68x) 6	5.54 (0.69x) 7
$\gamma_{cc}$ (ev)	11.13	11.13	11.13	11.13
$-\beta_{co}$ (ev)	3.12	2.30	2.30	2.30
$-G^{**}$ (ev)	-	0.29	0.41	0.39

\* oscillator strength

\*\* ground state depression

# transition number

TABLE X. ANTHRAQUINONE CALCULATIONS (cont.)

	MCI=36; DCI=43	MCI=28; DCI=51	MCI=36; DCI=43	MCI=28; DCI=51
	(ev) - f* - tr <sup>#</sup>	(ev) - f - tr	(ev) - f - tr	(ev) - f - tr
	3.81 (0) 1	3.71 (0.20x) 1	3.72 (0.22x) 1	3.75 (0) 1
	4.01 (0.23x) 2	3.93 (0) 2	3.78 (0) 2	4.23 (0.22x) 2
	4.07 (0) 3	4.06 (0) 3	3.98 (0) 3	4.30 (0) 3
	4.68 (0.47y) 4	4.61 (0.50y) 4	4.50 (0.47y) 4	4.44 (0.51y) 4
	5.41 (0.71x) 6	5.34 (0.62x) 5	5.24 (0.67x) 5	5.53 (0.68x) 8
$\gamma_{cc}$ (ev)	11.13	11.13	11.13	9.00
$-\beta_{co}$ (ev)	2.30	2.30 <sup>Δ</sup>	2.20 <sup>Δ</sup>	2.30
$-G^{**}$ (ev)	0.30	0.24	0.19	0.38

\* oscillator strength

\*\* ground state depression

# transition number

$$\Delta\delta W_0 = -7.00 \text{ ev}$$

TABLE XI. p-NAPHTHAQUINONE CALCULATIONS

Exp. <sup>12</sup>	MCI = 36	MCI=15; DCI=39	MCI=15; DCI=39	MCI=15; DCI=39	MCI=26; DCI=53
(ev)	(ev) - f*	(ev) - f	(ev) - f	(ev) - f	(ev) - f
3.71s	4.28 (0.008y)	4.39 (0.057x)	4.20 (0.060x)	3.78 (0.053x)	3.64 (0.063x)
4.80-	4.24 (0.099x)	4.60 (0.020y)	4.41 (0.018y)	4.08 (0.023y)	3.87 (0.001y)
5.00vs	4.95 (0.64y)	5.43 (0.52y)	5.16 (0.54y)	4.59 (0.53y)	4.54 (0.52y)
	5.42 (0.20x)	5.94 (0.16x)	5.80 (0.16x)	5.02 (0.045x)	4.97 (0.049x)
$\gamma_{cc}$ (ev)	11.13	11.13	11.13	11.13	11.13
$-\beta_{co}$ (ev)	3.12	3.12	2.81	2.30	2.30 <sup>Δ</sup>
$-G^{**}$ (ev)	-	0.60	0.59	0.61	0.61

\* oscillator strength

$$\Delta\delta W_0 = -7.00 \text{ ev}$$

\*\* ground state depression

TABLE XII. ANTHRONE CALCULATIONS

Exp. <sup>49</sup>	MCI = 49	MCI=15; DCI=39	MCI=15; DCI=39	MCI=28; DCI=51	MCI=28; DCI=51
(ev)	(ev) - f*	(ev) - f	(ev) - f	(ev) - f	(ev) - f
4.00s	4.67 (0.026x)	4.96 (0.049x)	4.74 (0.082x)	4.57 (0.27x)	4.61 (0.23x)
5.00vs	4.67 (0.011y)	5.14 (0.001y)	4.82 (0y)	4.66 (0.012y)	4.70 (0.012y)
	5.08 (0.47x)	5.35 (0.44x)	4.96 (0.43x)	4.72 (0.18x)	4.77 (0.22x)
	5.40 (0.18y)	5.78 (0.22y)	5.00 (0.25y)	5.17 (0.22y)	5.23 (0.21y)
$\gamma_{cc}$ (ev)	11.13	11.13	11.13	11.13	11.13
$-\beta_{co}$ (ev)	3.12	3.12	2.30	2.20 <sup>Δ</sup>	2.30 <sup>Δ</sup>
$-G^{**}$ (ev)	-	0.33	0.33	0.34	0.34

\* oscillator strength

$$\Delta\delta W_0 = -7.00 \text{ ev}$$

\*\* ground state depression

TABLE XIII. 10,10'-BIANTHRONYLIDENE CALCULATIONS

Exp. <sup>26,28</sup>	Compound			Bridged		
	MCI = 66	MCI = 28; DCI = 51		MCI = 66	MCI = 28; DCI = 51	
(ev)	(ev) - f* - tr#	(ev) - f - tr	(ev) - f - tr	(ev) - f - tr	(ev) - f - tr	(ev) - f - tr
3.24	3.20 (0.80) 1	3.09 (0.72) 1	2.00 (0.29) 1	1.68 (0.03) 1		
	4.24 (0.19) 3	4.12 (0.26) 4	2.42 (0.17) 2	2.13 (0.16) 2		
4.31	4.34 (0.18) 5	4.19 (0.28) 5	3.23 (0.99) 3	3.16 (0.14) 3		
4.84	4.74 (0.35) 9	4.35 (0.15) 7	3.43 (0.21) 4	3.30 (0.37) 4		
	5.12 (0.06) 12	4.64 (0.14) 9	3.82 (0.19) 5	3.37 (0.08) 5		
	5.33 (1.05) 14	5.25 (0.06) 12	3.96 (0.13) 7	3.56 (0.01) 6		
	5.59 (0.02) 15	5.51 (0.32) 16	4.34 (0.23) 10	3.93 (0.32) 7		
	5.70 (1.11) 18	5.51 (0.12) 17	4.36 (0.24) 11	4.07 (0.06) 10		
	5.70 (0.01) 19	5.54 (1.33) 19	4.47 (0.26) 12	4.12 (0.37) 11		

\* oscillator strength

# transition number

TABLE XIV. 10,10'-BIXANTHENYLIDENE CALCULATIONS

Compound				Bridged								
Exp. <sup>24</sup>	MCI = 45			MCI = 28; DCI = 51			MCI = 45			MCI = 28; DCI = 51		
(ev)	(ev)	f*	tr#	(ev)	f	tr	(ev)	f	tr	(ev)	f	tr
3.41	3.31	(0.64)	1	3.46	(0.56)	1	2.09	(0.40)	1	1.89	(0.01)	1
4.45	4.56	(0.04)	2	4.60	(0.02)	3	2.69	(0.08)	2	2.44	(0.27)	2
	4.67	(0.17)	7	4.61	(0.13)	4	3.45	(1.53)	3	3.04	(0.04)	3
	5.13	(0.53)	9	4.69	(0.01)	7	3.79	(0.01)	4	3.69	(0.23)	4
	5.16	(0.46)	10	5.14	(0.63)	9	3.97	(0.09)	5	3.90	(0.51)	5
	5.39	(0.50)	13	5.21	(0.48)	11	4.20	(0.16)	6	4.13	(0.29)	6
							4.31	(0.02)	8	4.25	(0.17)	7
							4.54	(0.14)	10	4.49	(0.03)	8
							4.59	(0.11)	11	4.77	(0.15)	12

\* oscillator strength

# transition number

TABLE XV. DIPHENYLMETHYLENEANTHRONE CALCULATIONS

Exp.	Compound						Bridged					
	MCI = 66			MCI = 28; DCI = 51			MCI = 66			MCI = 28; DCI = 51		
(ev)	(ev)	f*	tr#	(ev)	f	tr	(ev)	f	tr	(ev)	f	tr
3.42	2.96	(0.70)	1	2.98	(0.60)	1	2.15	(0.23)	1	1.81	(0.04)	1
4.43	4.17	(0.06)	3	3.73	(0.10)	2	2.81	(0.11)	2	2.49	(0.13)	2
4.86	4.51	(0.15)	7	4.03	(0.16)	3	3.28	(1.10)	3	3.10	(0.29)	3
	4.54	(0.23)	8	4.33	(0.06)	5	3.89	(0.07)	4	3.56	(0.43)	5
	4.73	(0.12)	9	4.40	(0.14)	6	3.91	(0.43)	5	3.81	(0.09)	6
	4.91	(0.34)	10	4.47	(0.02)	7	4.02	(0.11)	6	4.09	(0.07)	8
	5.11	(0.28)	12	4.78	(0.20)	9	4.12	(0.04)	7	4.28	(0.68)	9
	5.13	(0.74)	13	4.94	(0.03)	10	4.28	(0.36)	9	4.51	(0.07)	10
	5.15	(0.03)	14	5.04	(0.25)	11	4.43	(0.08)	10	4.65	(0.15)	12

\* oscillator strength

# transition number

TABLE XVI. BIFLUORENYLIDENE CALCULATIONS

Compound			Bridged		
Exp. <sup>6</sup>	MCI = 45	MCI = 28; DCI = 51	MCI = 45		
(ev)	(ev) - f* - tr#	(ev) - f - tr	(ev)	f	tr
2.43	2.86 (0.99) 1	2.96 (0.79) 1	2.21 (0.31) 1		
	3.08 (0.07) 3	2.99 (0.03) 3	2.57 (0.12) 2		
	4.01 (0.13) 4	3.90 (0.15) 5	3.12 (0.17) 3		
	4.51 (0.09) 7	4.50 (0.02) 7	3.33 (0.03) 4		
	4.99 (0.33) 9	4.89 (0.03) 10	3.44 (1.11) 5		
	5.14 (0.41) 11	5.20 (0.37) 12	3.86 (0.19) 6		
			4.19 (0.07) 8		
			4.51 (0.05) 10		
			4.52 (0.52) 11		

\* oscillator strength

# transition number

TABLE XVII. HELIANTHRONE CALCULATIONS

Compound**			Bridged			
MCI = 45		MCI = 28; DCI = 51	MCI = 45		MCI = 28; DCI = 51	
(ev) - f* - tr#	(ev) - f - tr	(ev) - f - tr	(ev) - f - tr	(ev) - f - tr	(ev) - f - tr	
3.21 (0.85) 1	3.12 (0.75) 1	2.01 (0.29) 1	1.63 (0.04) 1			
3.66 (0.16) 2	3.46 (0.11) 2	2.44 (0.23) 2	2.11 (0.17) 2			
4.12 (0.19) 3	3.77 (0.21) 3	3.27 (1.07) 3	3.10 (0.15) 3			
4.34 (0.11) 6	4.05 (0.06) 4	3.33 (0.17) 4	3.30 (0.51) 4			
4.46 (0.06) 7	4.10 (0.12) 5	3.64 (0.07) 5	3.72 (0.07) 7			
4.71 (0.08) 8	4.16 (0.02) 6	3.86 (0.05) 7	3.94 (0.56) 9			
4.88 (0.78) 10	4.64 (0.07) 8	4.00 (0.51) 8	4.00 (0.09) 10			
5.13 (0.42) 12	4.73 (0.28) 10	4.32 (0.05) 10	4.27 (0.06) 11			
5.16 (0.18) 13	5.01 (0.38) 11	4.49 (0.24) 12	4.37 (0.12) 12			

\* oscillator strength    \*\* lowest singlet transition 2.79 eV<sup>26</sup>

# transition number

TABLE XVIII. DIHYDROBIANTHRONE, DIHYDROHELIANTHRONE, AND MESONAPHTHOBIANTHRONE CALCULATIONS

Dihydrobianthrone		Dihydrohelianthrone		Mesonaphthobianthrone <sup>1</sup>	
MCI = 45	MCI=28; DCI=51	MCI = 45	MCI=28; DCI=51	MCI = 45	MCI=28; DCI=51
(ev) - f* - tr#	(ev) - f - tr	(ev) - f - tr	(ev) - f - tr	(ev) - f - tr	(ev) - f - tr
1.99 (1.19) 1	2.00(0) 1	2.00(1.16) 1	1.97(0) 1	3.48(0.87) 1	3.34(0.86) 1
3.34 (0.05) 3	2.49(0.66) 2	3.34(0.05) 4	2.46(0.66) 2	3.56(0.26) 2	3.39(0.33) 2
3.74 (0.04) 7	3.56(0.02) 4	3.48(0.02) 6	3.56(0.01) 4	4.68(1.37) 8	4.18(0.02) 6
4.18 (0.23) 11	3.90(0.01) 6	3.57(0.01) 7	4.06(0.01) 8	4.82(0.13) 9	4.68(0.89) 9
4.41 (0.01) 12	4.40(0.27) 12	4.17(0.06) 10	4.46(0.83) 12	5.14(1.02) 12	4.86(0.21) 11
4.42 (1.73) 13	4.54(0.75) 13	4.40(1.92) 11	4.75(0.01) 13	5.30(0.07) 13	5.19(0.19) 13
4.80 (0.02) 16	4.67(0.01) 14	4.58(0.10) 13	5.07(0.44) 17	5.31(0.73) 14	5.19(0.18) 14

\* oscillator strength

1 lowest singlet transition 3.04 eV<sup>26</sup>

# transition number

TABLE XIX. DOUBLE BRIDGE STRUCTURE OF 10,10'-BIANTHRONYLIDENE

MCI = 45			MCI = 28; DCI = 51		
(ev)	- f*	- tr <sup>#</sup>	(ev)	- f	- tr
1.04	(0.49)	1	1.03	(0)	1
1.30	(0)	2	1.25	(0)	2
1.63	(0.19)	3	1.45	(0.07)	3
1.91	(0)	4	2.25	(0.02)	4
2.60	(0.47)	5	2.77	(0.01)	5
2.84	(0.34)	7	3.04	(0.73)	9
2.85	(0.95)	8	3.54	(0.02)	10
3.72	(0.04)	11	3.61	(0.14)	11
4.08	(0.02)	14	3.87	(0.29)	13
4.40	(0.20)	16	3.93	(0.02)	14
4.56	(1.36)	18	4.14	(0.01)	16

\* oscillator strength

<sup>#</sup> transition number

TABLE XX. PROTONATED COMPOUNDS

<u>1.</u>			<u>2.</u>			<u>3.</u>		
MCI = 45			MCI = 45			MCI = 45		
MCI=28; DCI=51			MCI=28; DCI=51			MCI=28; DCI=51		
(ev) - f* - tr <sup>#</sup>	(ev) - f - tr		(ev) - f - tr	(ev) - f - tr		(ev) - f - tr	(ev) - f - tr	
2.18 (0.61) 1	2.07 (0.63) 1		2.07 (0.57) 1	2.13 (0.64) 1		1.98 (0.56) 1		
3.02 (0.01) 2	2.59 (0.03) 2		2.79 (0.01) 3	3.17 (0.02) 2		2.91 (0.15) 2		
3.09 (0.02) 3	2.73 (0.01) 3		2.99 (0.73) 5	3.32 (0.15) 3		3.02 (0.01) 4		
3.17 (0.24) 5	2.80 (0.11) 4		4.11 (0.42) 10	3.33 (0.41) 4		3.14 (0.01) 5		
3.24 (0.39) 6	3.10 (0.12) 5		4.16 (0.44) 11	3.35 (0.05) 5		3.16 (0.17) 6		
3.71 (0.03) 7	3.22 (0.35) 6		4.21 (0.45) 13	3.36 (0.14) 6		3.31 (0.23) 7		
4.05 (0.10) 8	3.46 (0.05) 7		4.27 (0.01) 14	3.84 (0.03) 7		4.06 (0.04) 8		
4.58 (0.22) 9	3.91 (0.06) 8		4.71 (0.01) 15	3.97 (0.01) 8		4.69 (0.02) 11		
4.64 (0.10) 10	4.35 (0.18) 9		5.13 (0.01) 16	4.60 (0.15) 9		4.73 (0.09) 12		
4.76 (0.02) 12	4.66 (0.15) 12		5.22 (0.08) 18	4.74 (0.31) 10		4.75 (0.41) 13		

1. Monoprotonated 10,10'-Bianthrnylidene

2. Diprotonated 10,10'-Bianthrnylidene

3. Monoprotonated Diphenylmethylenanthrone

\* oscillator strength

# transition number

TABLE XXI. PROTONATED BRIDGE STRUCTURES

<u>1.</u>			<u>2.</u>					
MCI = 45			MCI = 28; DCI = 51			MCI = 28; DCI = 51		
(ev)	f*	tr#	(ev)	f	tr	(ev)	f	tr
0.91	(0.06)	1	0.54	(0.04)	1	0.45	(0.04)	1
2.24	(0.26)	2	1.80	(0.07)	2	1.93	(0.03)	2
2.40	(0.41)	3	2.24	(0.02)	3	2.35	(0.41)	3
3.00	(0.20)	4	2.30	(0.43)	4	2.41	(0.12)	4
3.11	(0.08)	6	2.71	(0.09)	6	2.91	(0.06)	6
3.23	(0.21)	7	2.92	(0.08)	7	3.08	(0.02)	7
3.50	(0.28)	8	3.06	(0.05)	8	3.45	(0.25)	9
3.62	(0.35)	9	3.33	(0.28)	9	3.61	(0.06)	10
3.82	(0.13)	11	3.50	(0.03)	10	3.74	(0.07)	11
3.94	(0.39)	12	3.68	(0.16)	12	3.98	(0.02)	12
4.34	(0.48)	13	4.18	(0.54)	16	4.08	(0.49)	13

1. Protonated 10,10<sup>1</sup>-Bianthronylidene Bridge

\* oscillator strength

2. Protonated Diphenylmethyleanthrone Bridge

# transition number

TABLE XXII. BOND RESONANCE INTEGRAL VALUES (ev)

C-C Bond Distance A	$\gamma_{cc}$ values determine the set of $\beta$ 's used			
	11.13 ev	9.00 ev	7.90 ev	7.40 ev
1.478	-2.047	-2.14	-2.18	-2.22
1.477	-2.057	-2.15	-2.19	-2.23
1.45	-2.173	-2.27	-2.31	-2.36
1.40	-2.376	-	-	-
1.395	-2.395*	-2.50*	-2.55*	-2.60*
1.39	-2.405	-2.51	-2.56	-2.61
1.38	-2.463	-2.57	-2.62	-2.67
1.33	-2.675	-2.79	-2.85	-2.90
1.31	-2.801	-2.92	-2.98	-3.04

\* all other values proportional to pi-bond overlap(s)<sup>53</sup>

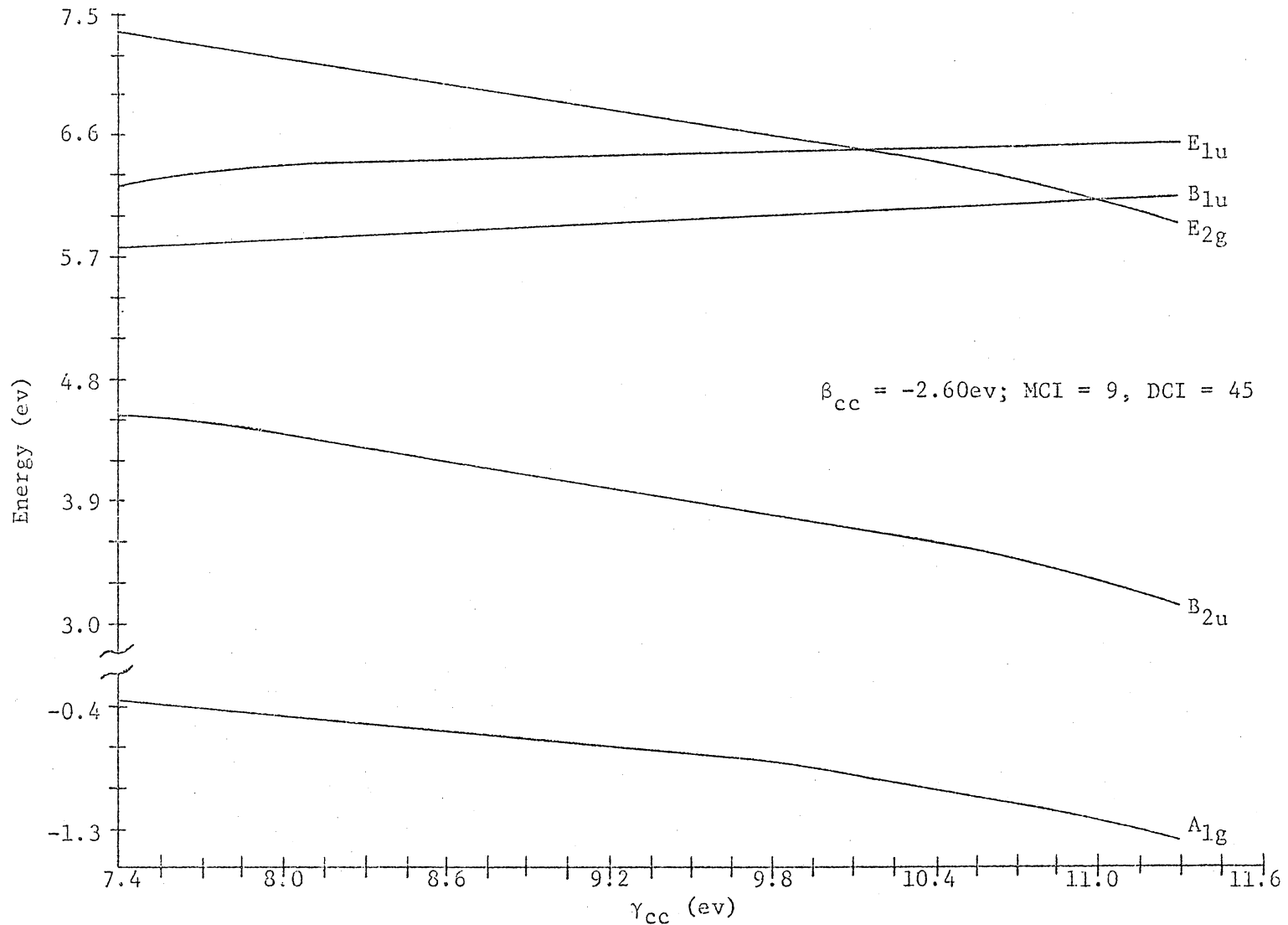


Figure 1. Effect of  $\gamma_{cc}$  on Energy Levels of Benzene.

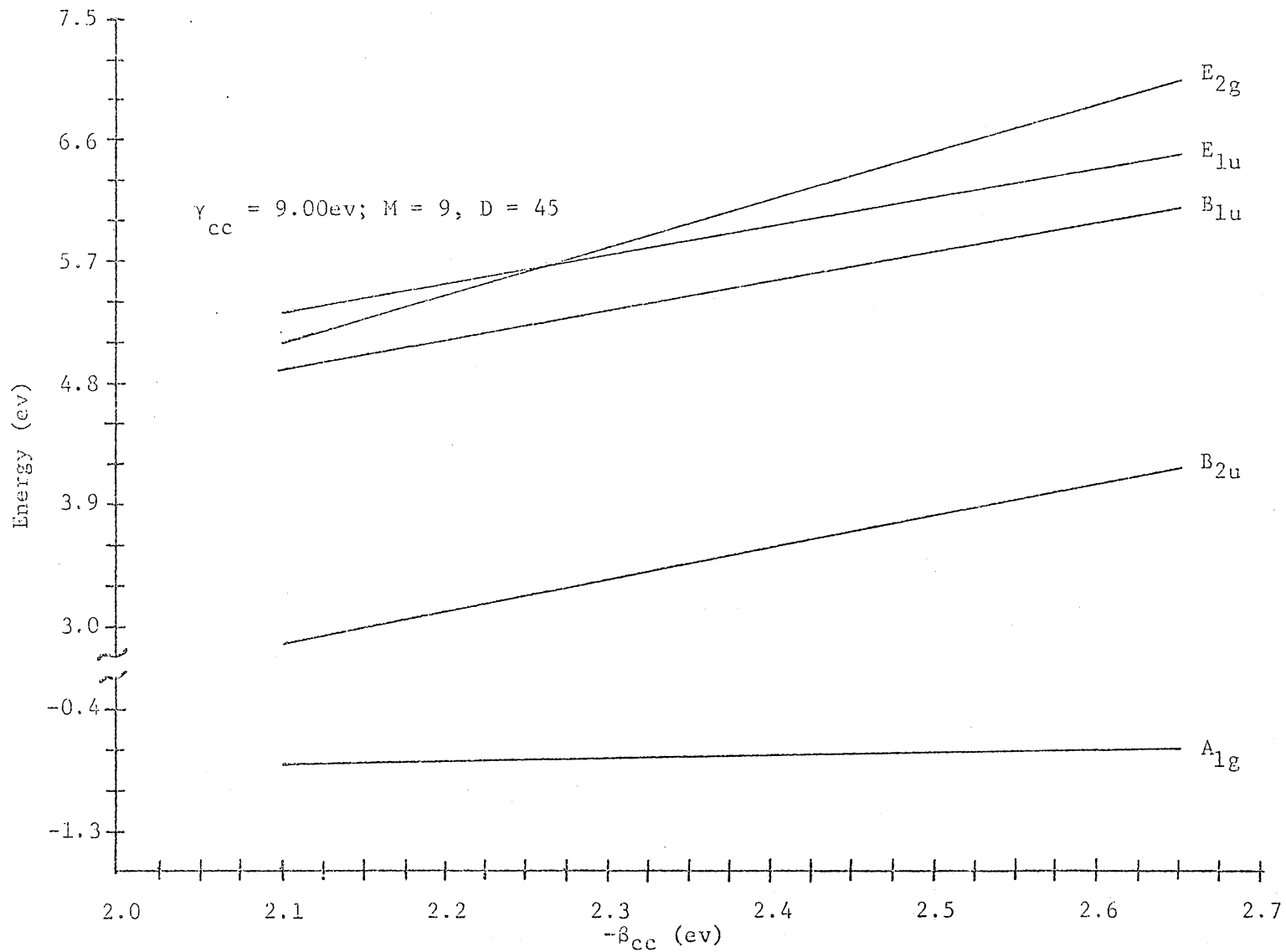


Figure 2. Effect of  $\beta_{cc}$  on Energy Levels of Benzene.

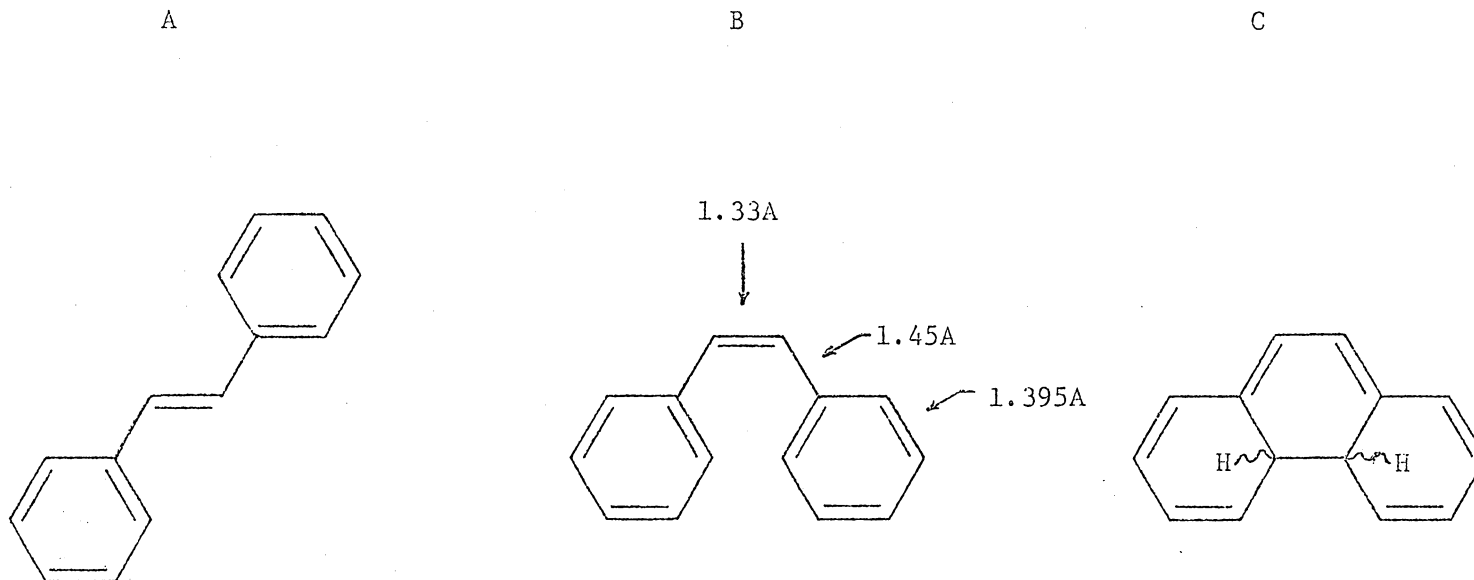


Figure 3. Trans-Stilbene, Cis-Stilbene, and Dihydrophenanthrene Intermediate.

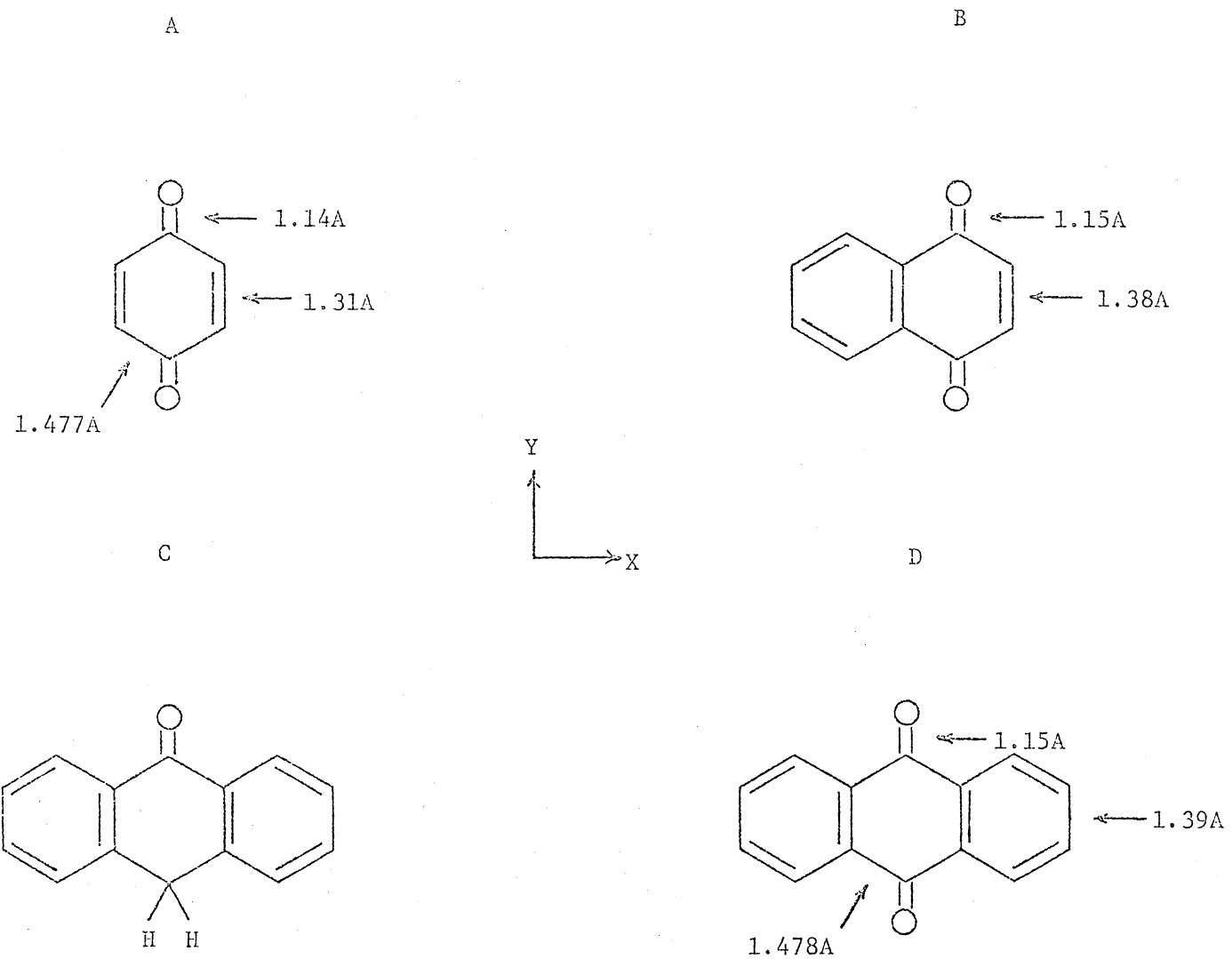


Figure 4. p-Quinones and Anthrone.

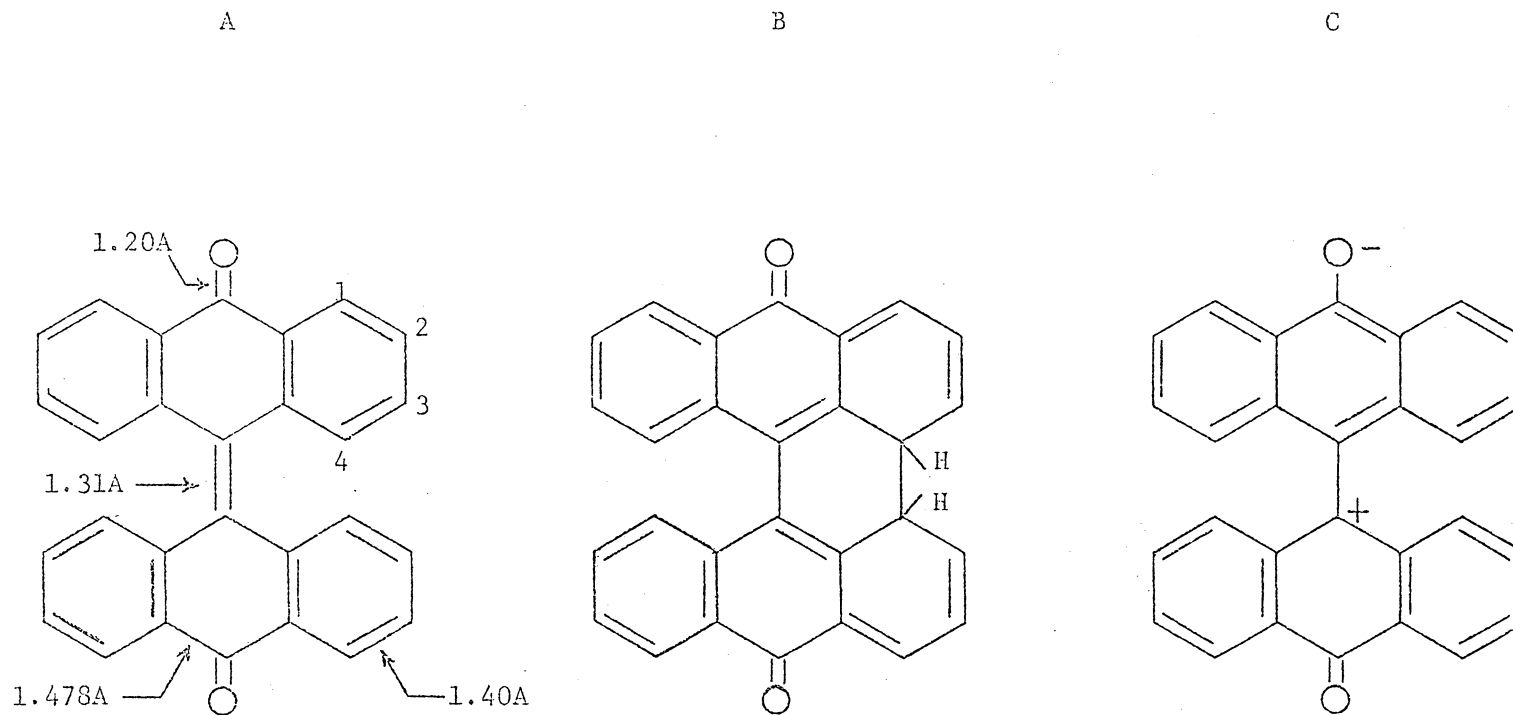
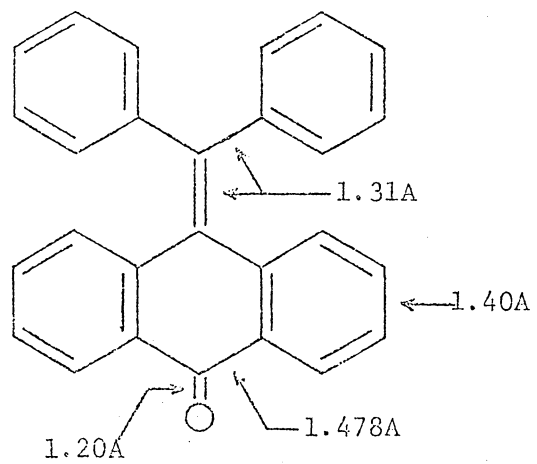


Figure 5. 10,10'-Bianthronylidene Structures.



A



B

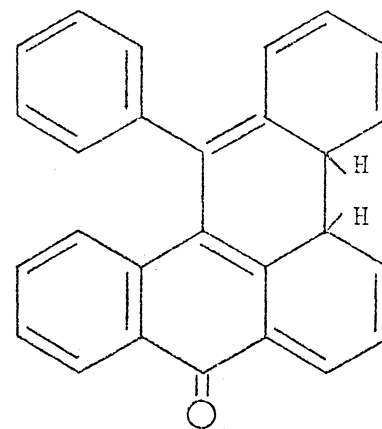
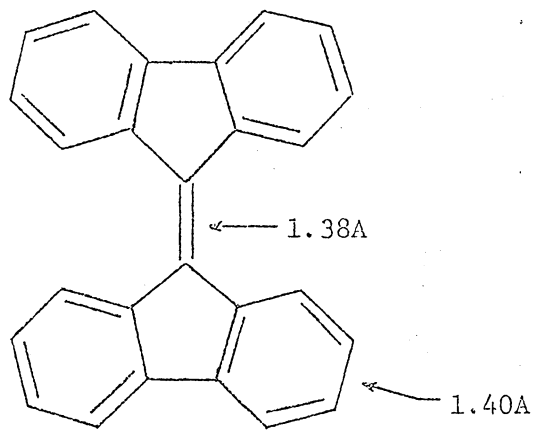


Figure 7. Diphenylmethylenedianthracene Structures.

A



B

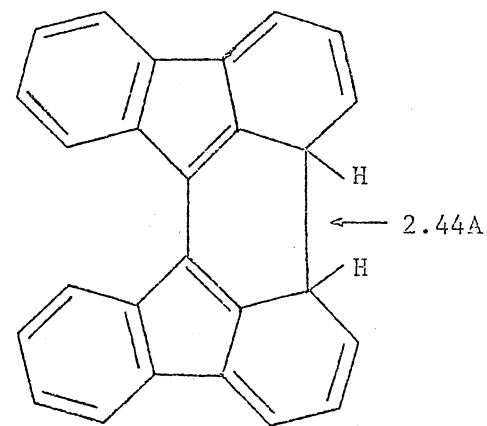
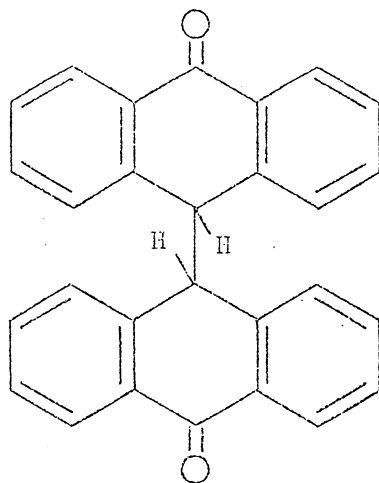


Figure 8. Bifluorenylidene Structures.



A



B

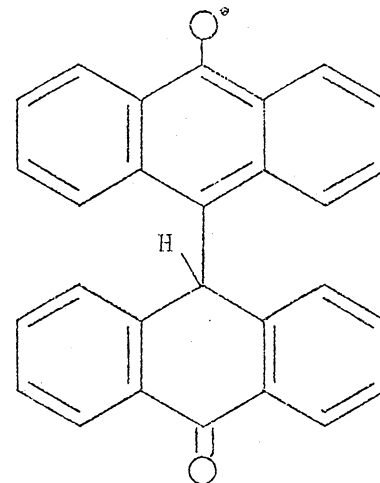
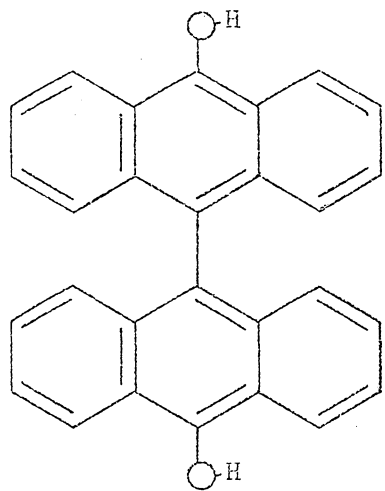


Figure 10. 10,10'-Bianthranyl and 10,10'-Bianthranyl Radical.

A



B

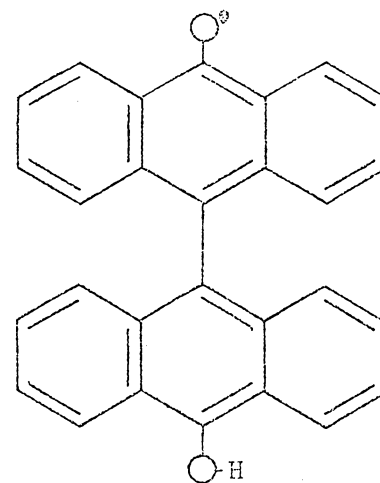


Figure 11. Dihydrobianthrone and Dihydrobianthrone Radical.

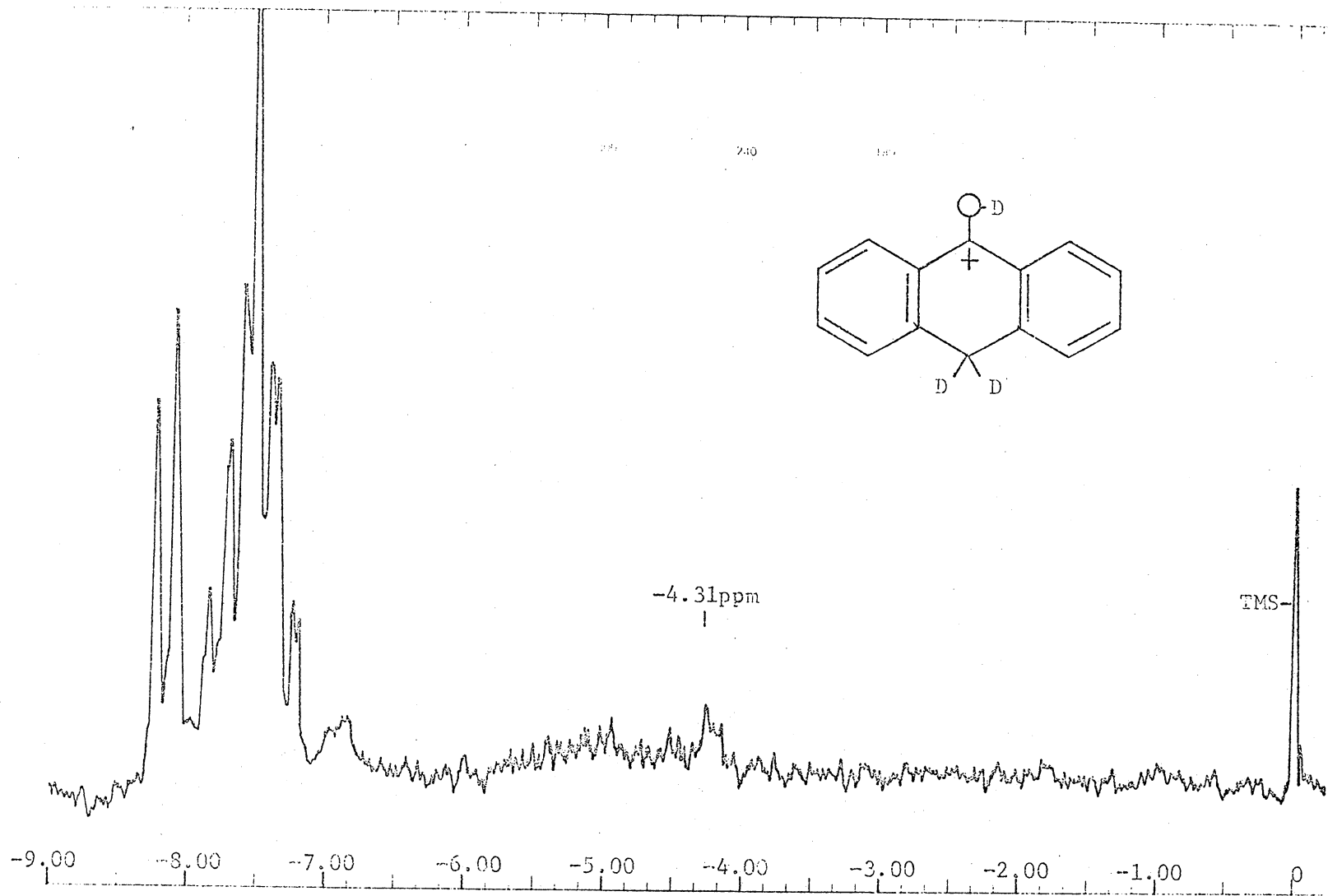


Figure 12. NMR Spectrum of Anthrane in  $D_2SO_4$ ; sweep width 9.00 ppm.

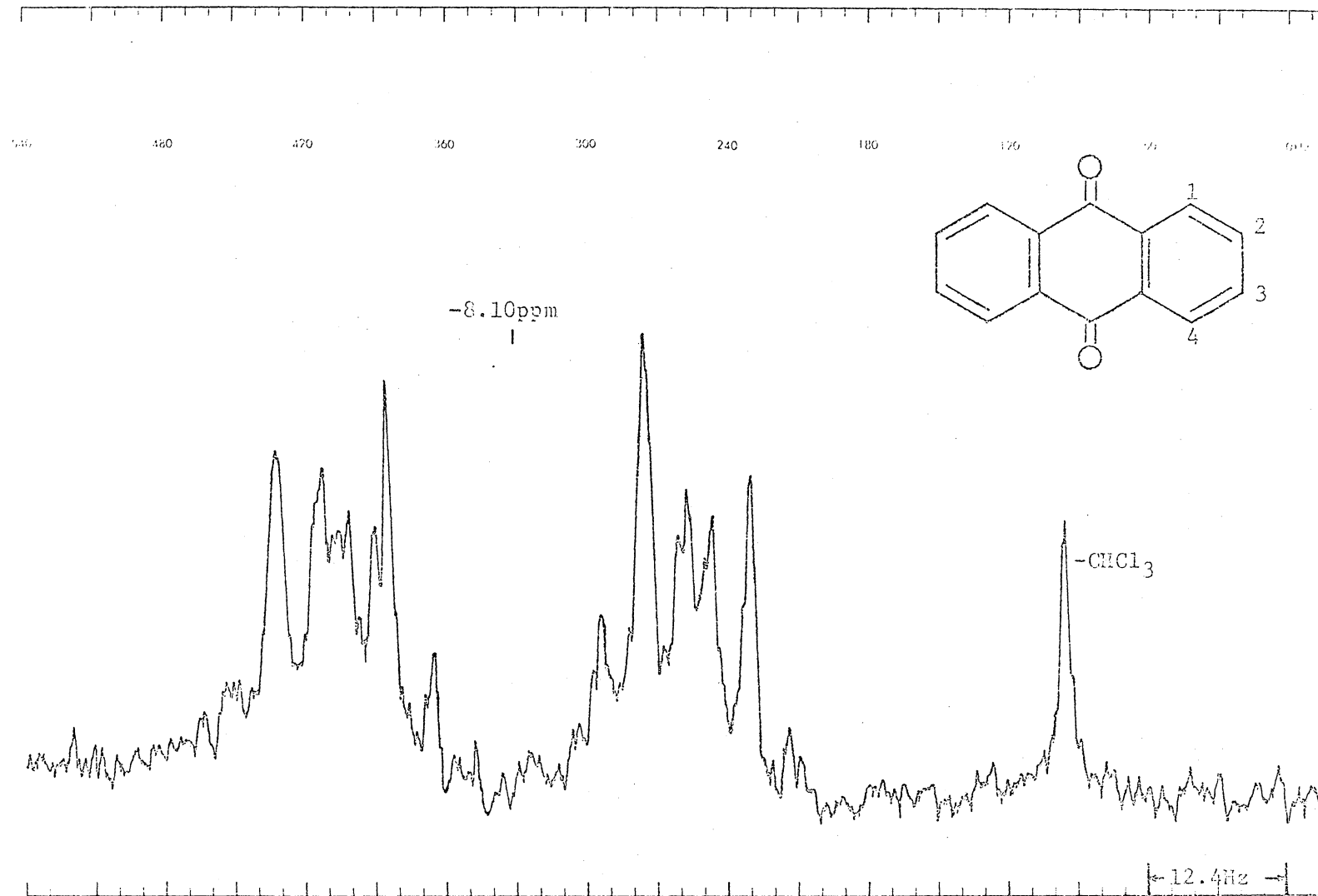


Figure 13. NMR of Anthraquinone in  $\text{CDCl}_3$ ; sweep width 1.85 ppm.

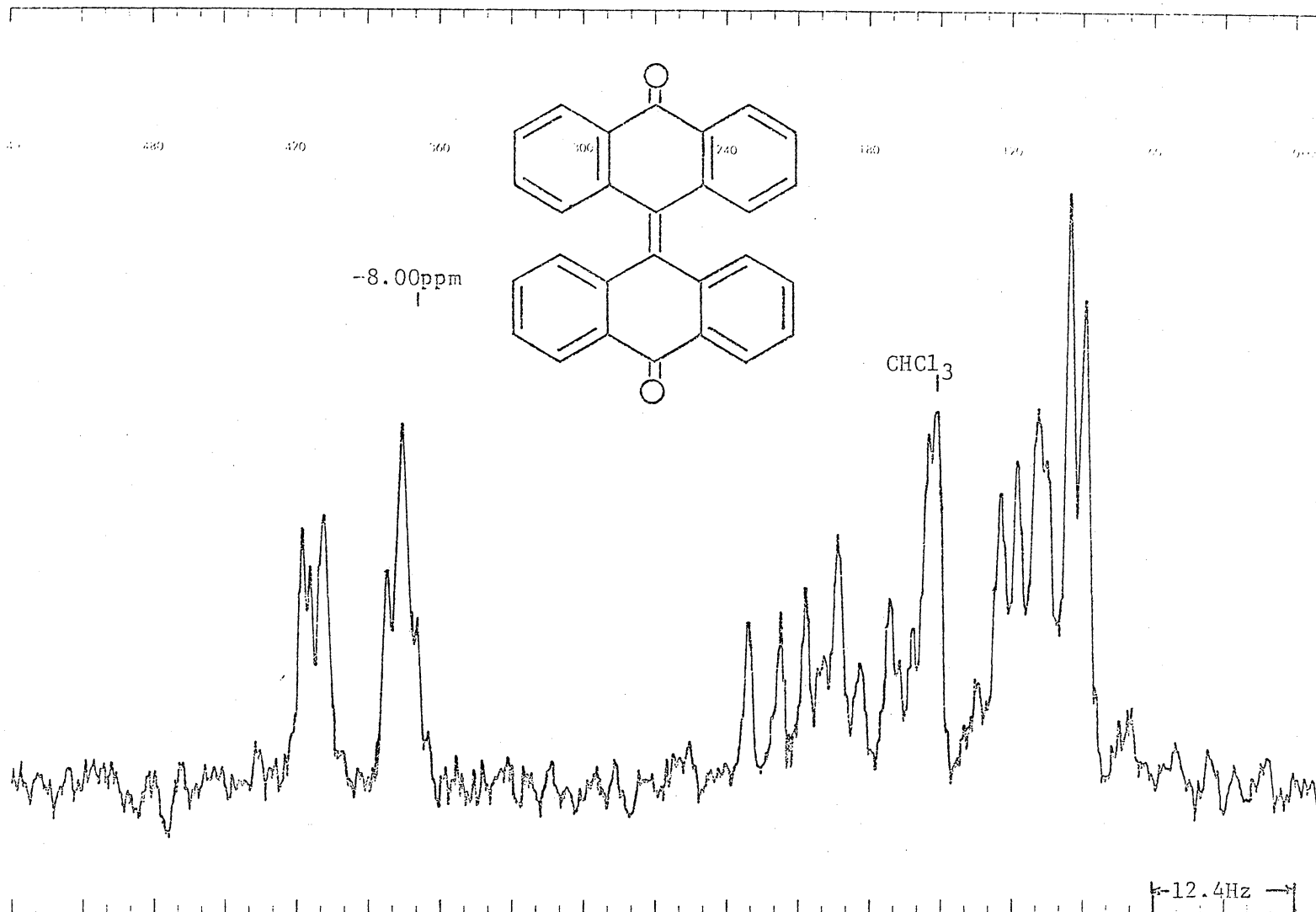


Figure 14. NMR Spectrum of 10,10'-Bianthronylidene in CDCl<sub>3</sub>; sweep width 1.85 ppm.

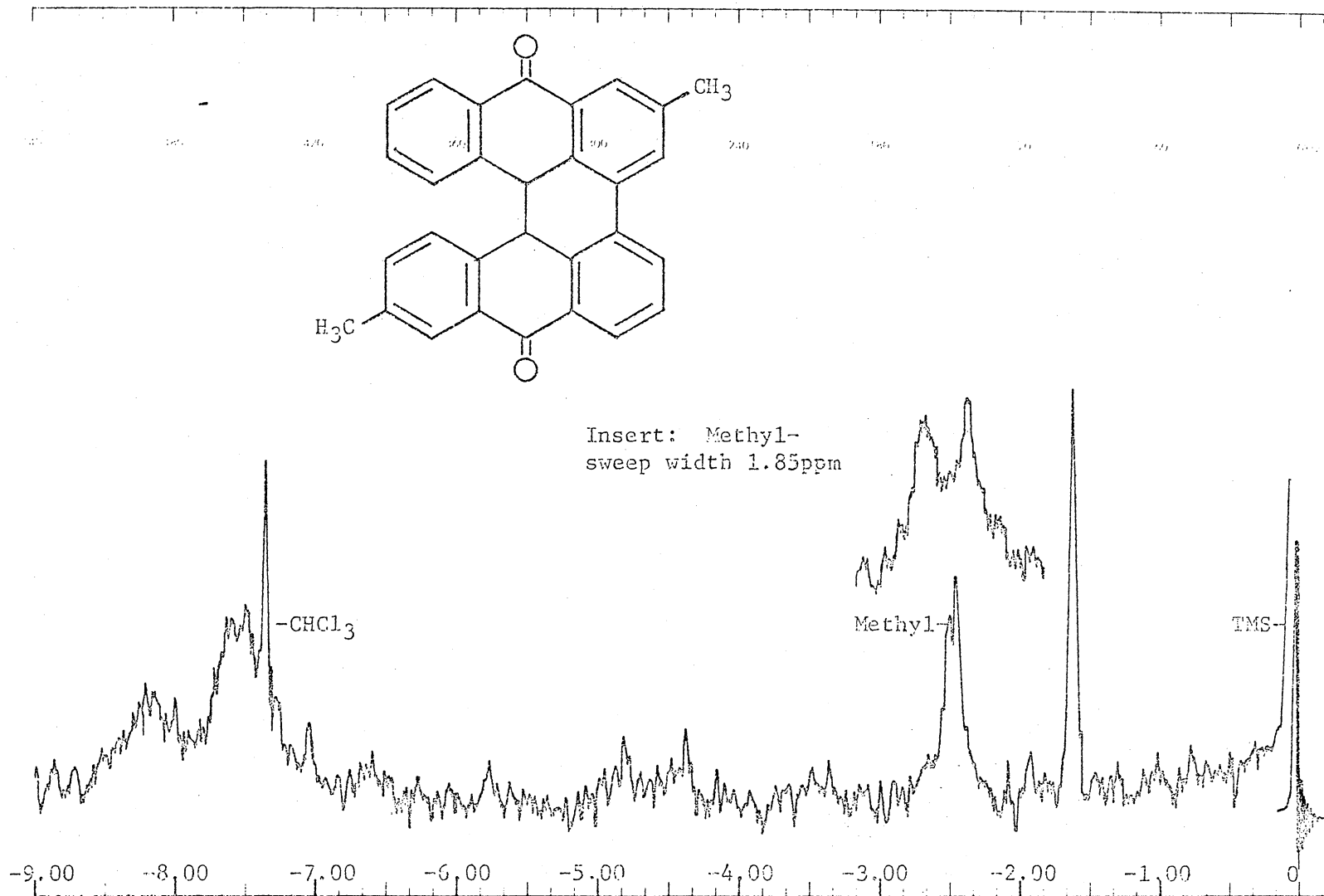


Figure 15. NMR Spectrum of 2,7'-Dimethyl-10,10'-Bianthronylidene Melt in CDCl<sub>3</sub>; sweep width 9.00 ppm.

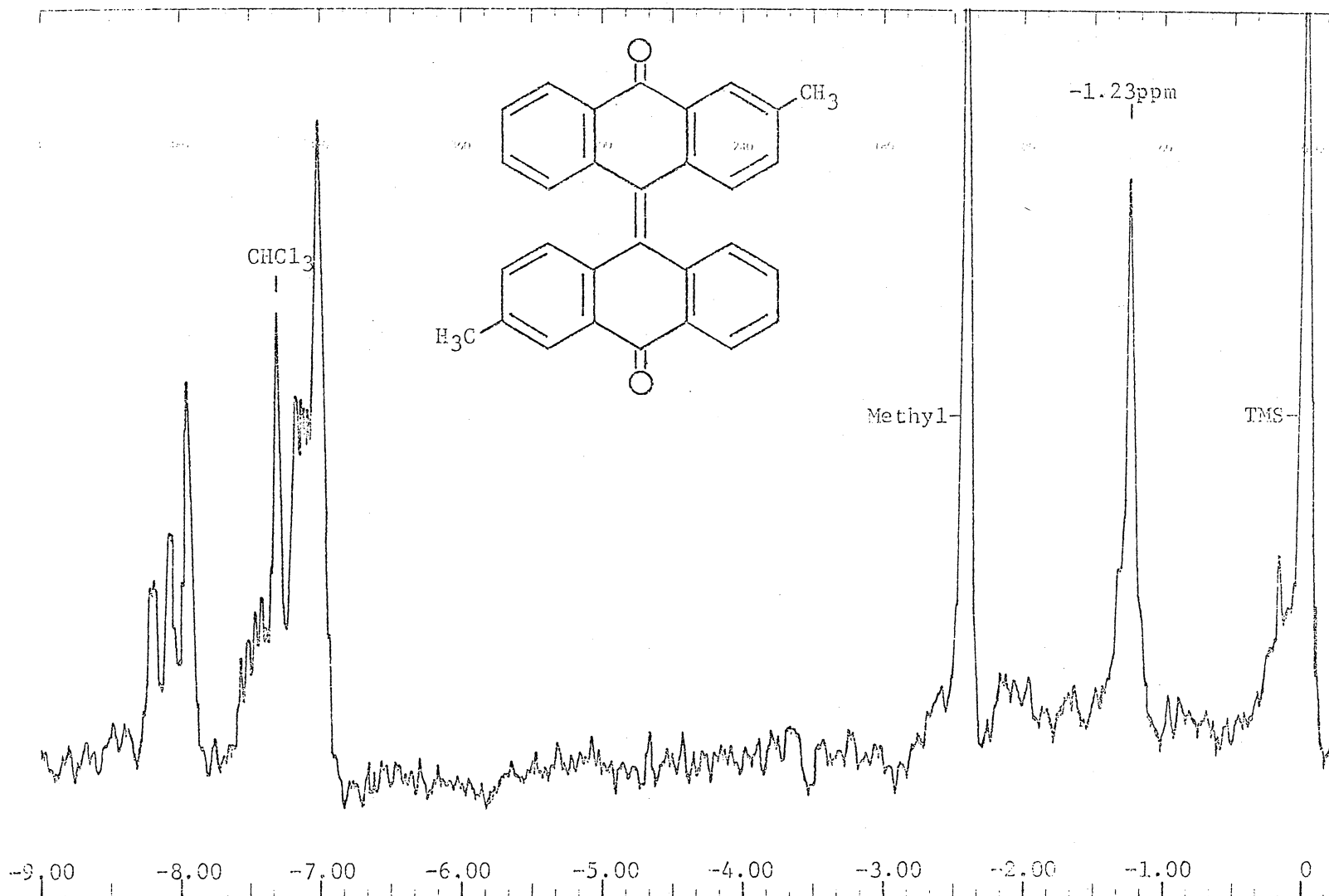


Figure 16. NMR Spectrum of Regenerated 2,7'-Dimethyl-10,10'-Bianthronylidene in  $\text{CDCl}_3$ ; sweep width 9.00 ppm.

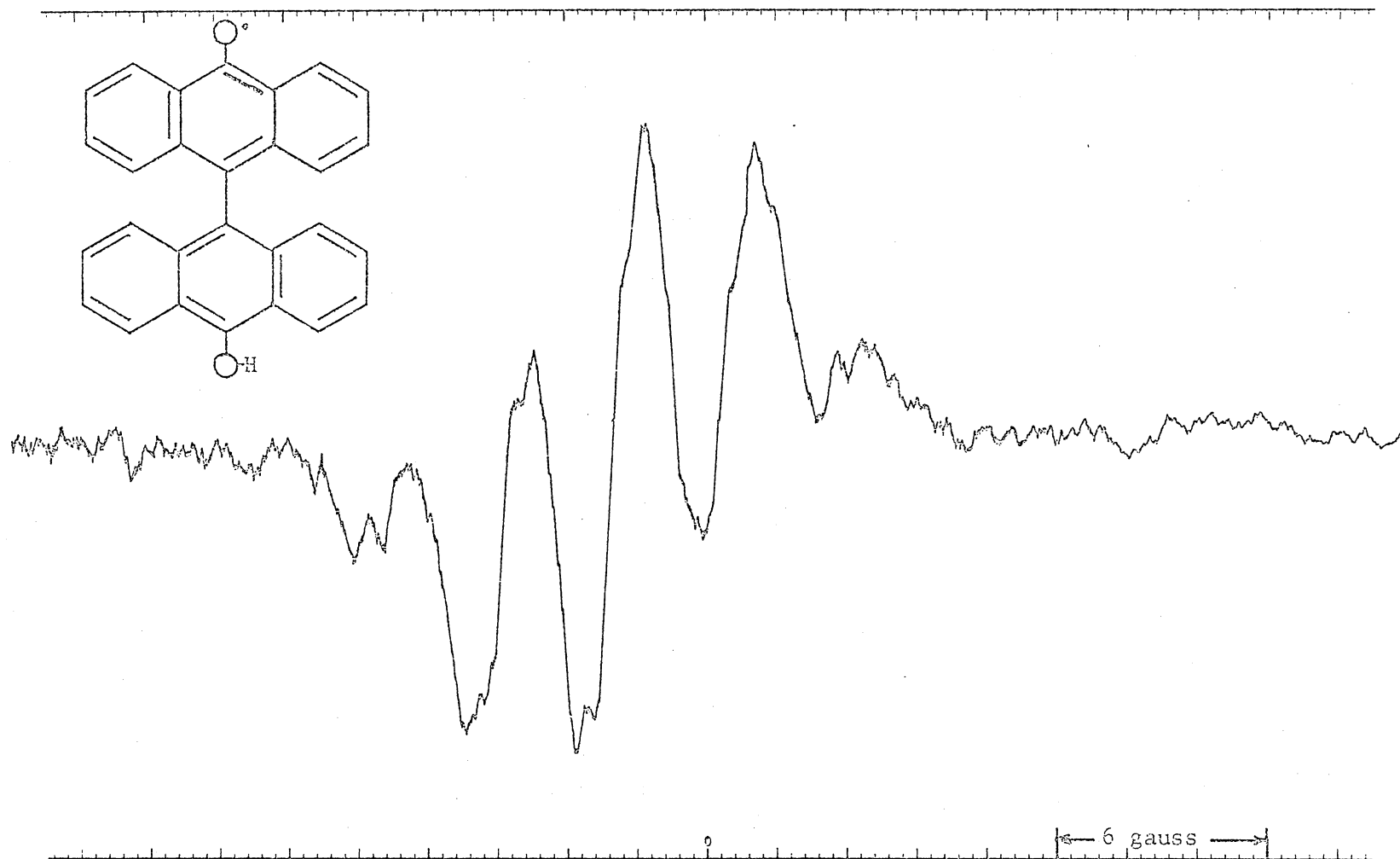


Figure 17. ESR Spectrum of Hydrobianthrone Radical in  $\text{CHCl}_3$  at  $-75^\circ\text{C}$ ; sweep width 40 gauss.

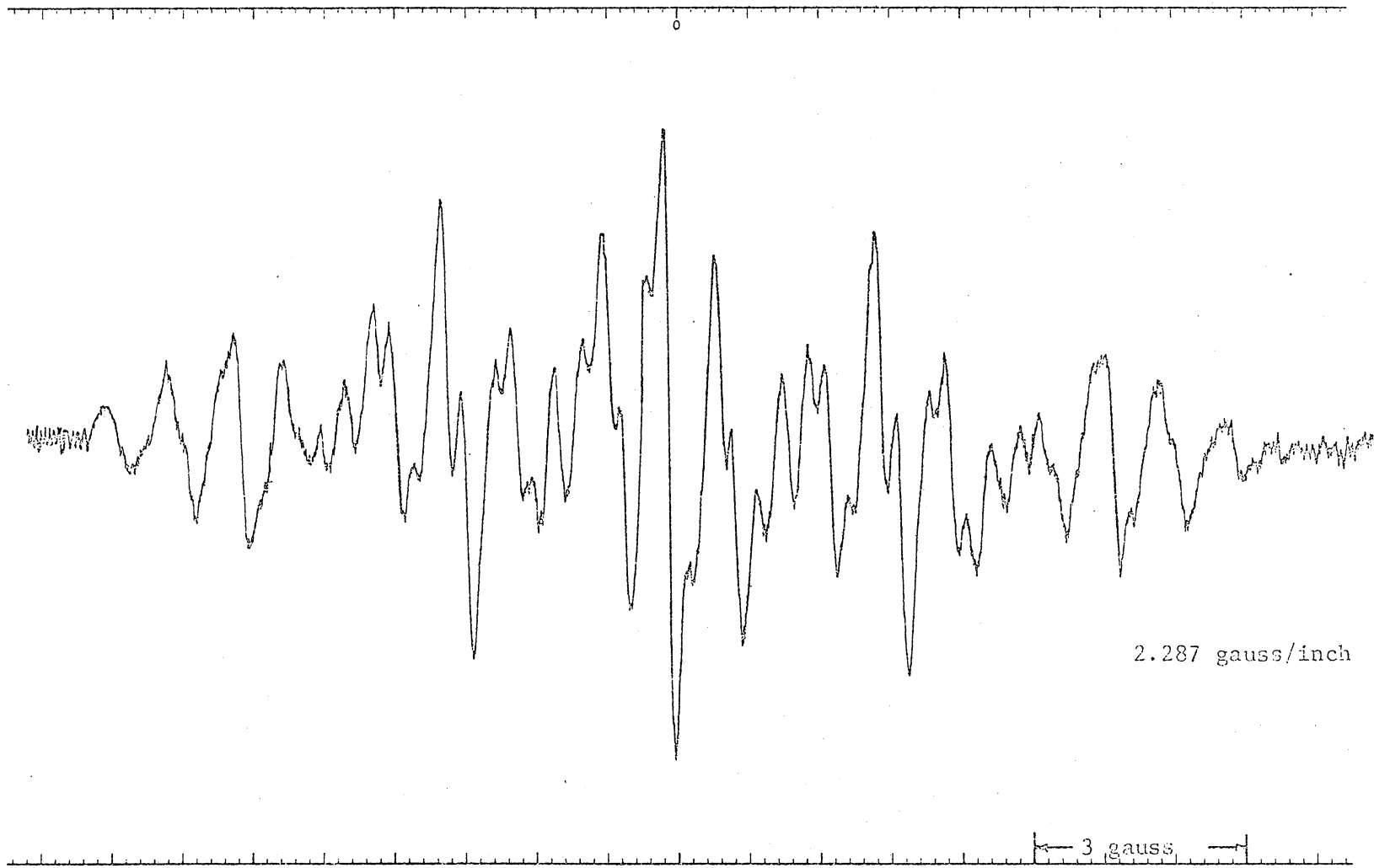


Figure 18. ESR of Hydrobianthrone Radical in Pyridine; sweep width 20 gauss.

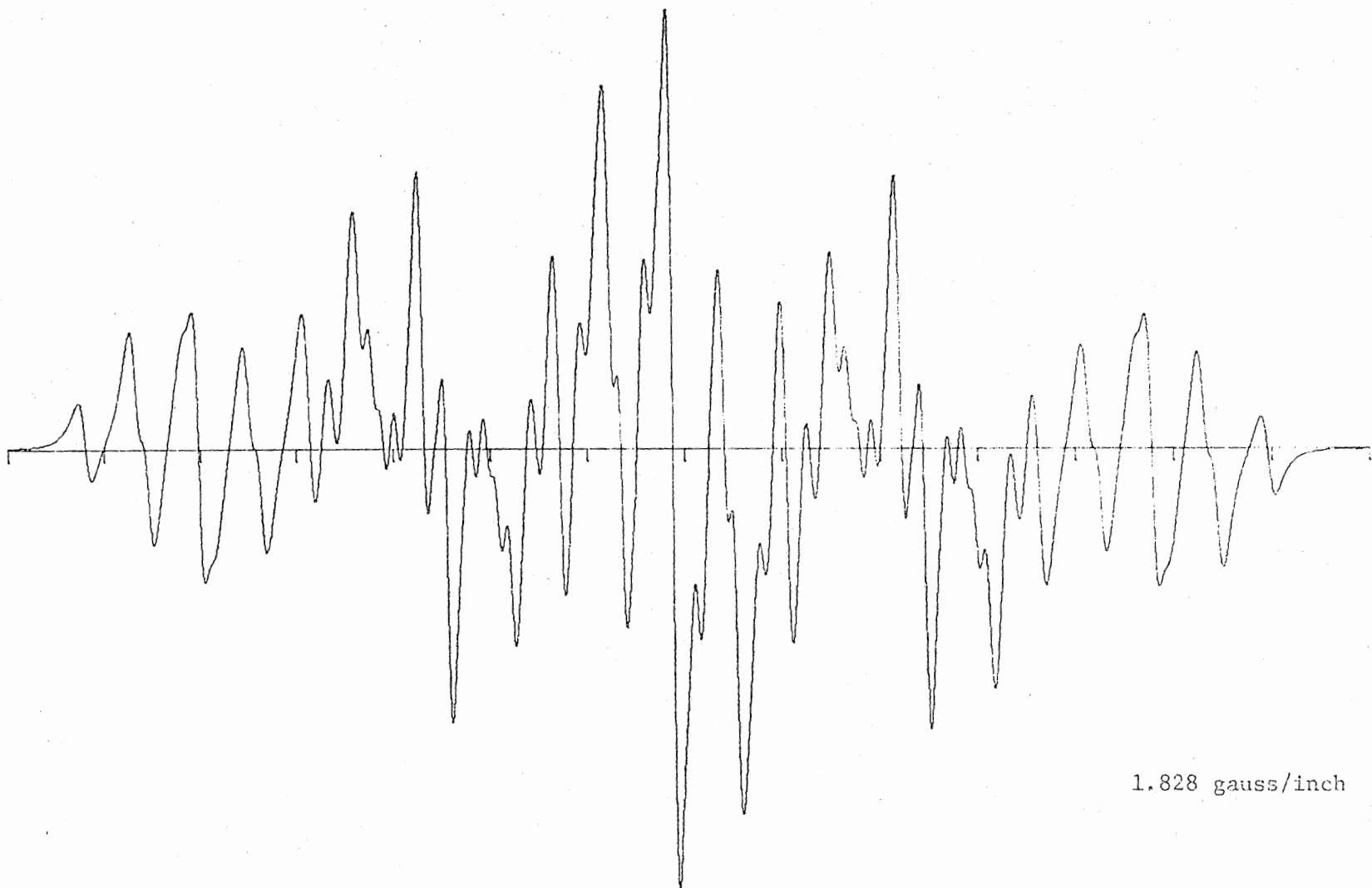


Figure 19. Simulation of ESR of Hydrobianthrone Radical; length 15.535 gauss.

1.828 gauss/inch

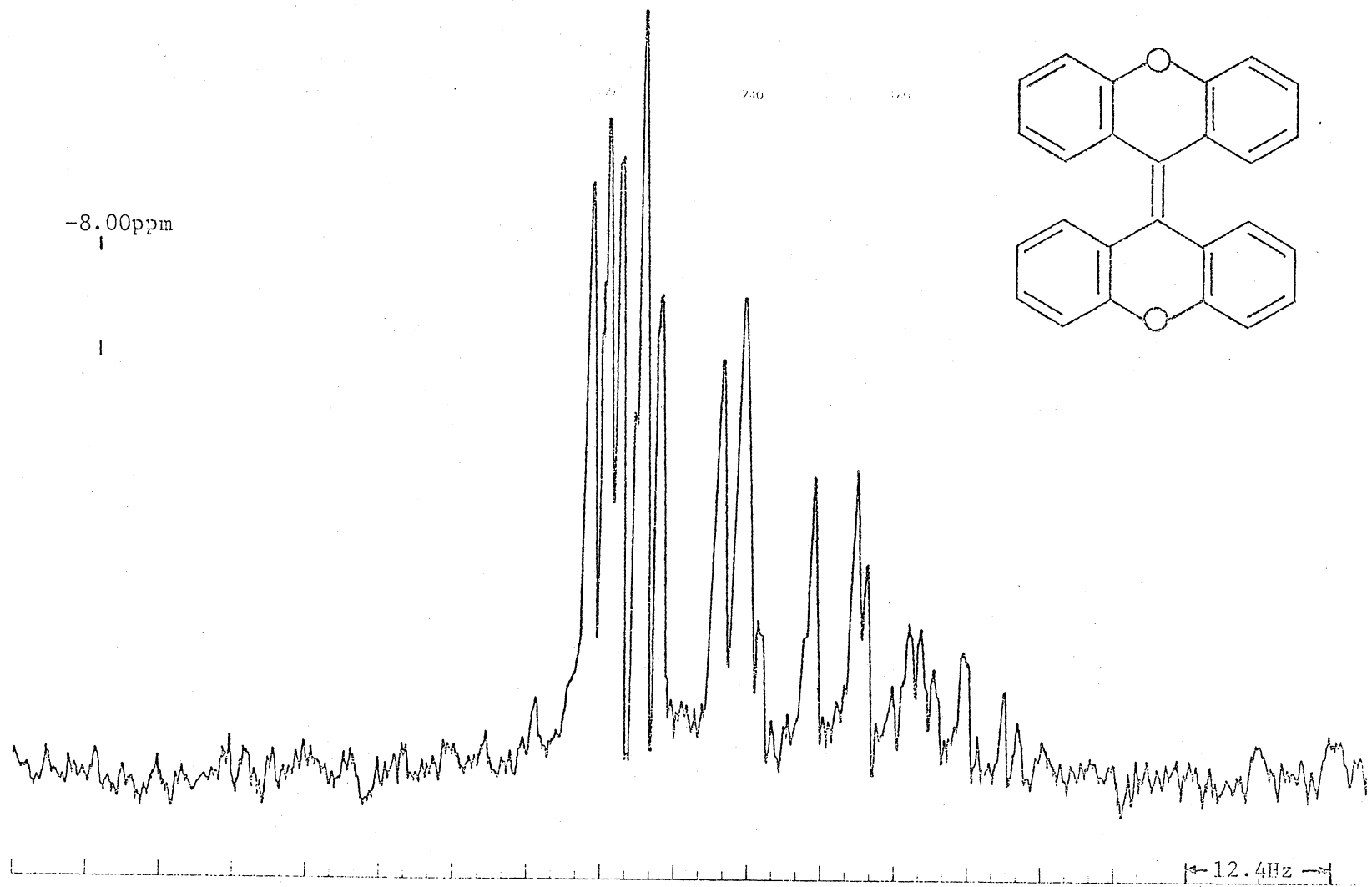


Figure 20. NMR Spectrum of 10,10'-Bixanthenylidene in  $\text{CDCl}_3$ ; sweep width 1.85 ppm.

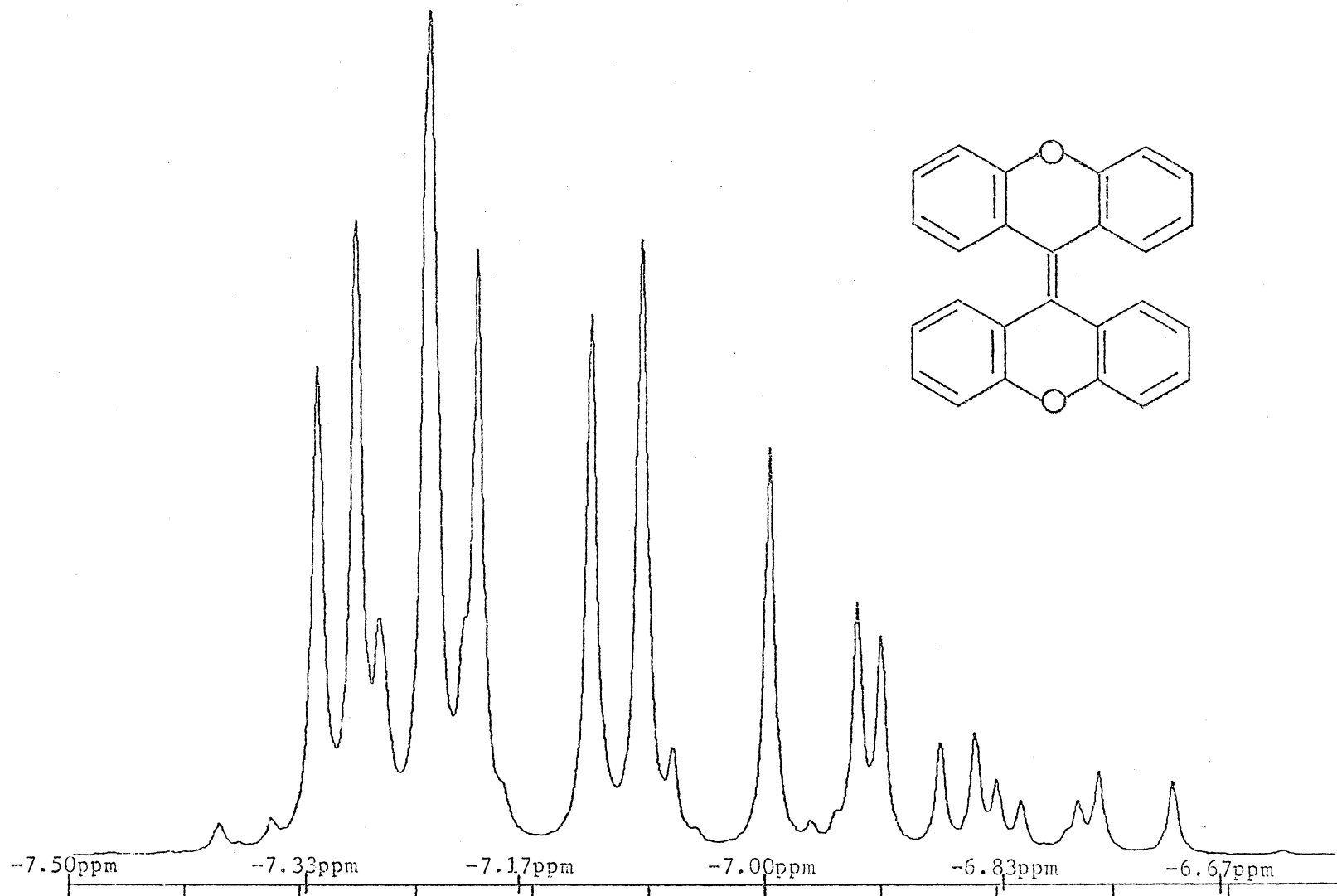
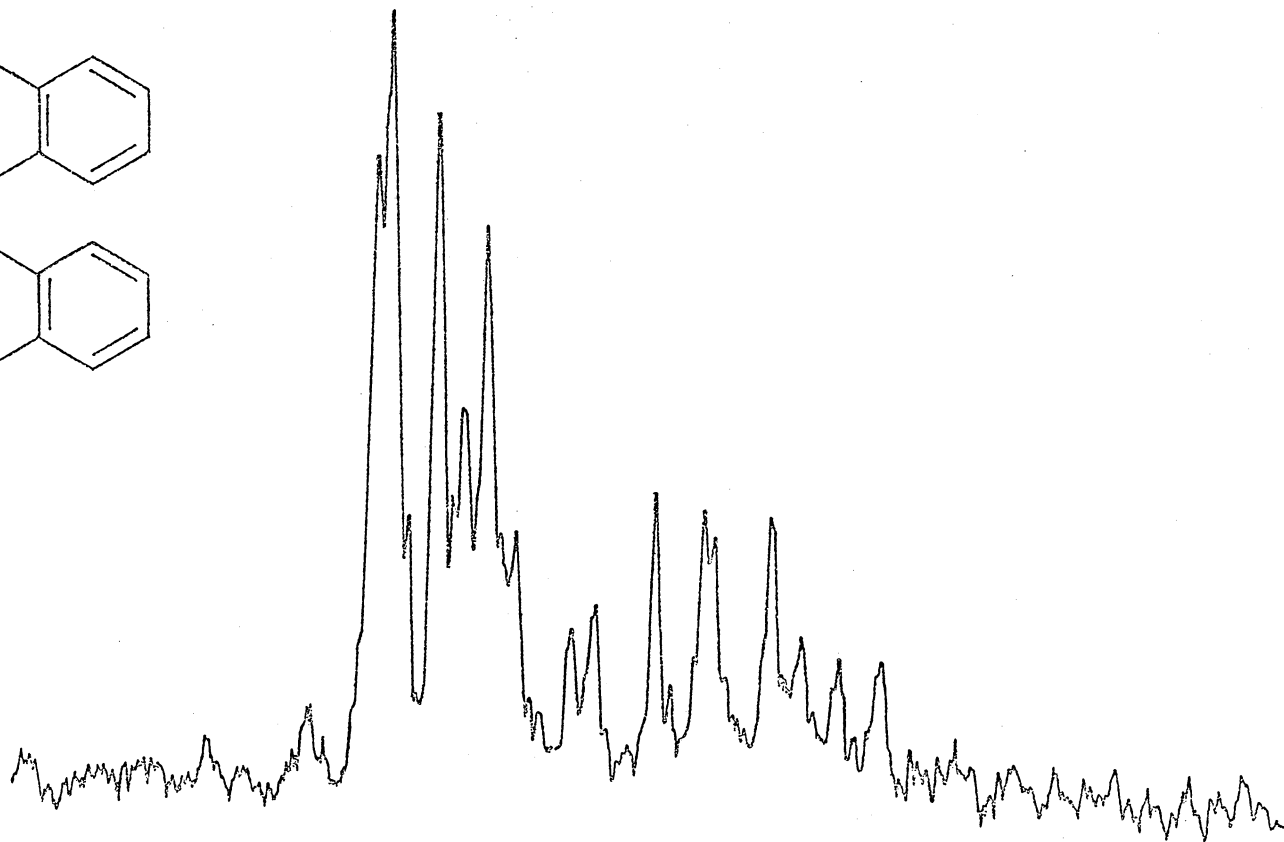
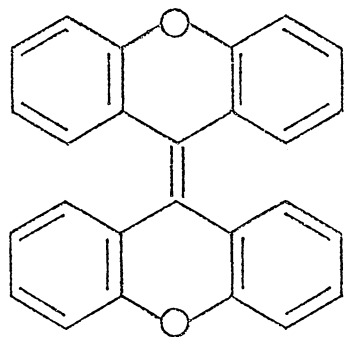


Figure 21. Simulation of NMR Spectrum of 10,10'-Bixanthenylidene in  $\text{CDCl}_3$ , room temperature.



← 12.4 Hz →

Figure 22. NMR Spectrum of 10,10'-Bixanthenylylidene in Decalin at 176°C; sweep width 1.85 ppm.

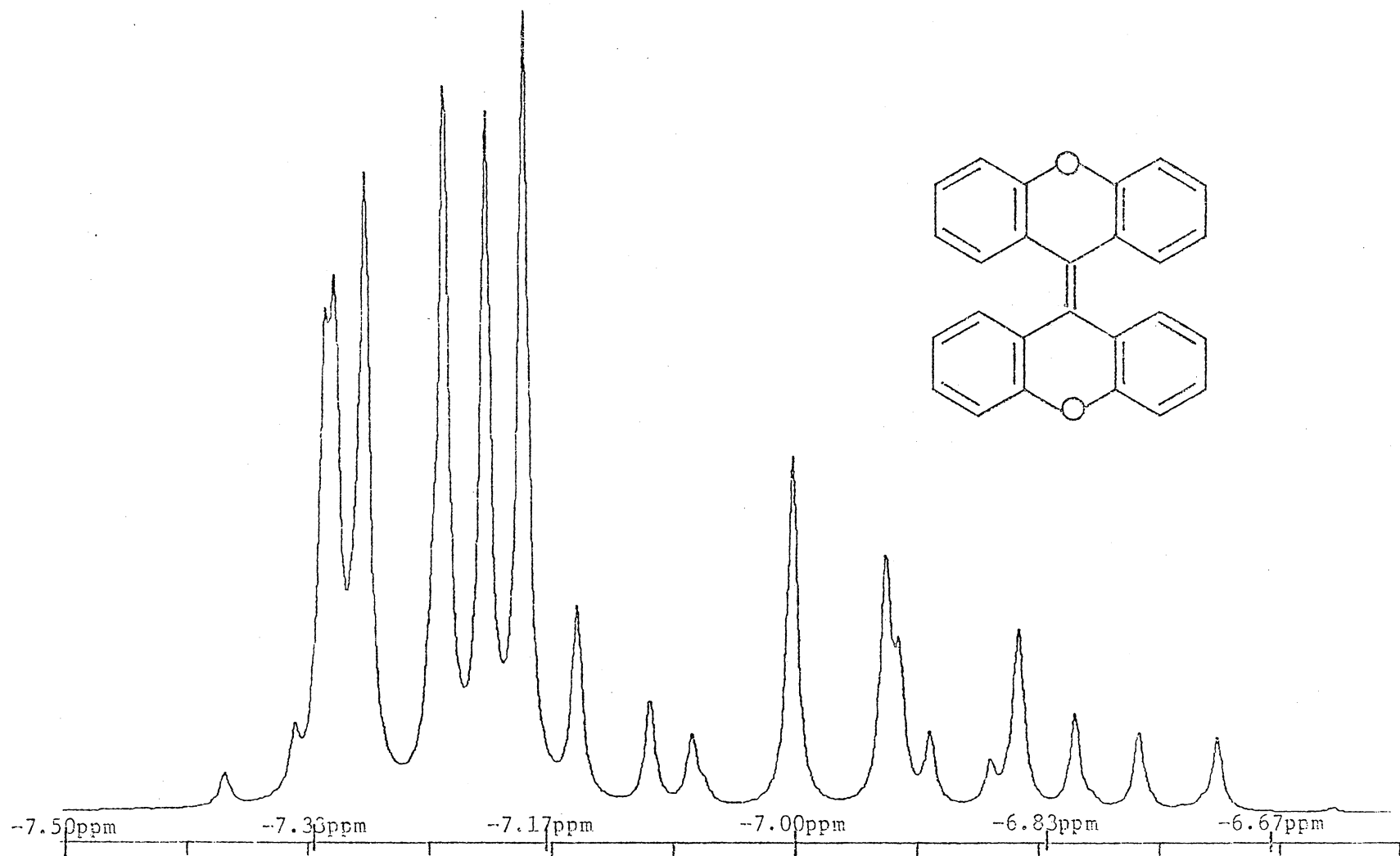


Figure 23. Simulation of NMR Spectrum of 10,10'-Bixanthenylidene in Decalin at 176°C.

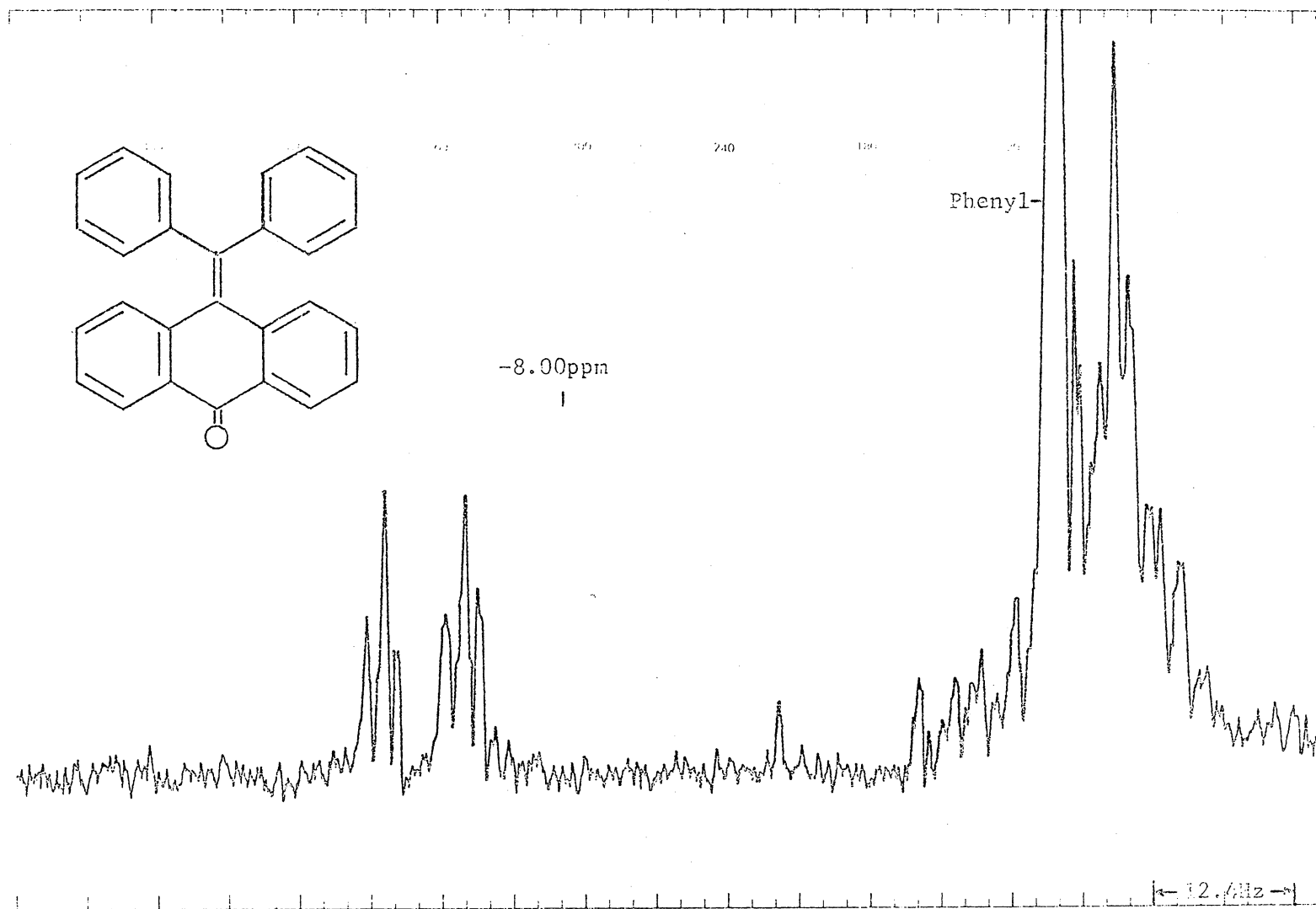


Figure 24. NMR Spectrum of Diphenylmethylenanthrone in CDCl<sub>3</sub>; sweep width 1.85 ppm.

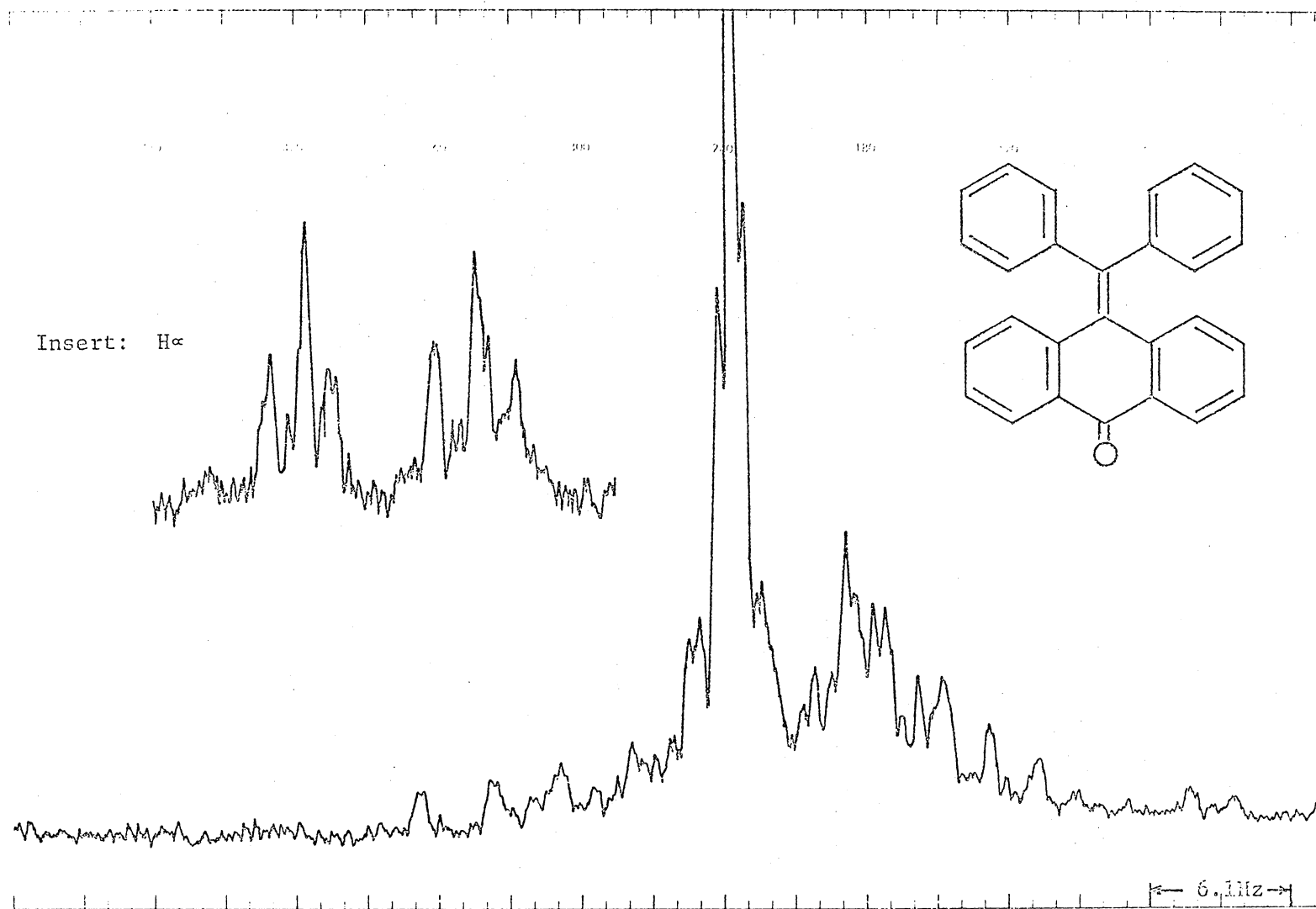


Figure 25. NMR Spectrum of Diphenylmethylenanthrone in  $\text{CDCl}_3$ ; sweep width 0.92 ppm.

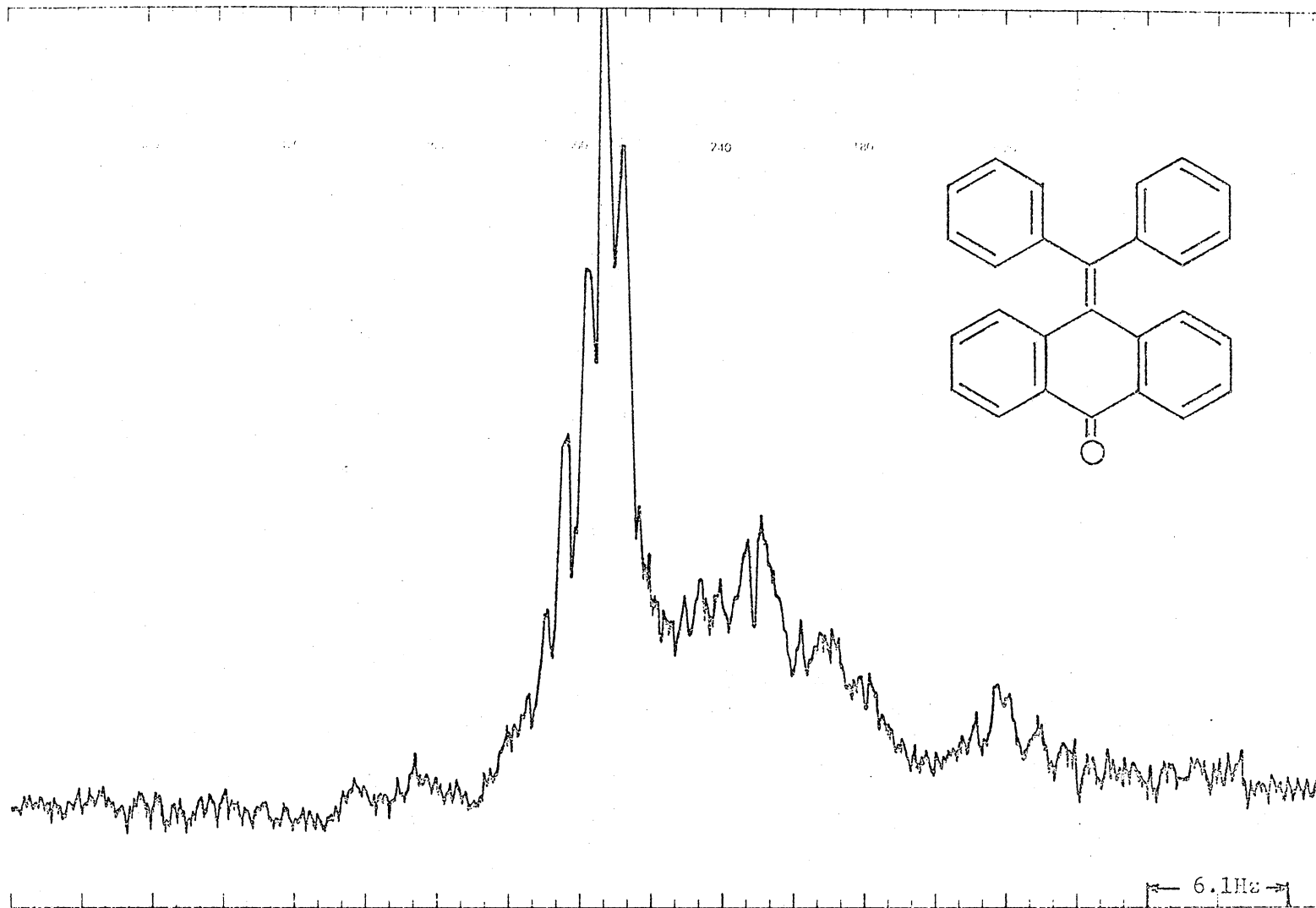


Figure 27. NMR Spectrum of Diphenylmethyleneanthrone in Decalin at 100°C; sweep width 9.92 ppm.

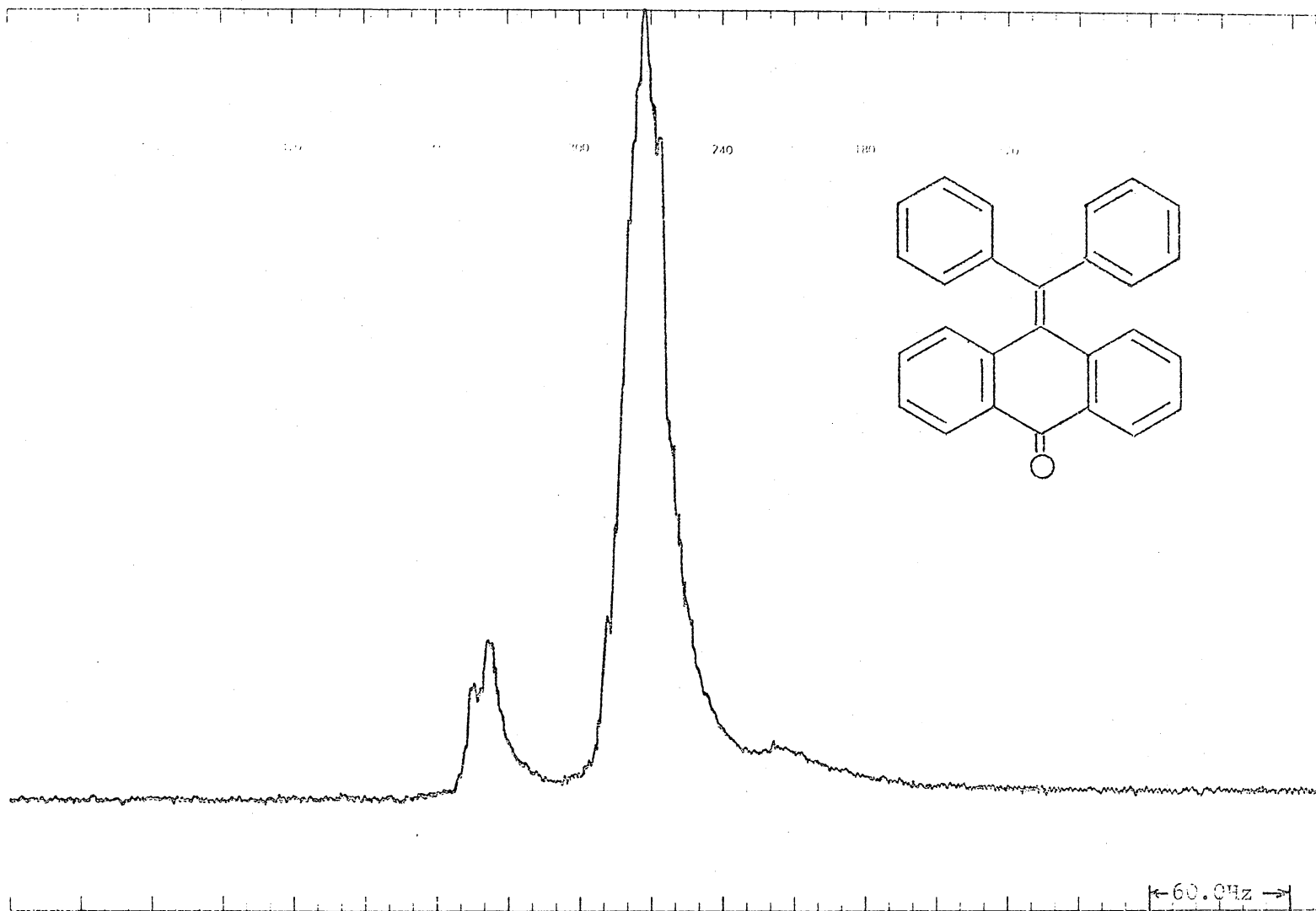


Figure 26. NMR Spectrum of Diphenylmethylenanthrone Melt; sweep width 9.00 ppm

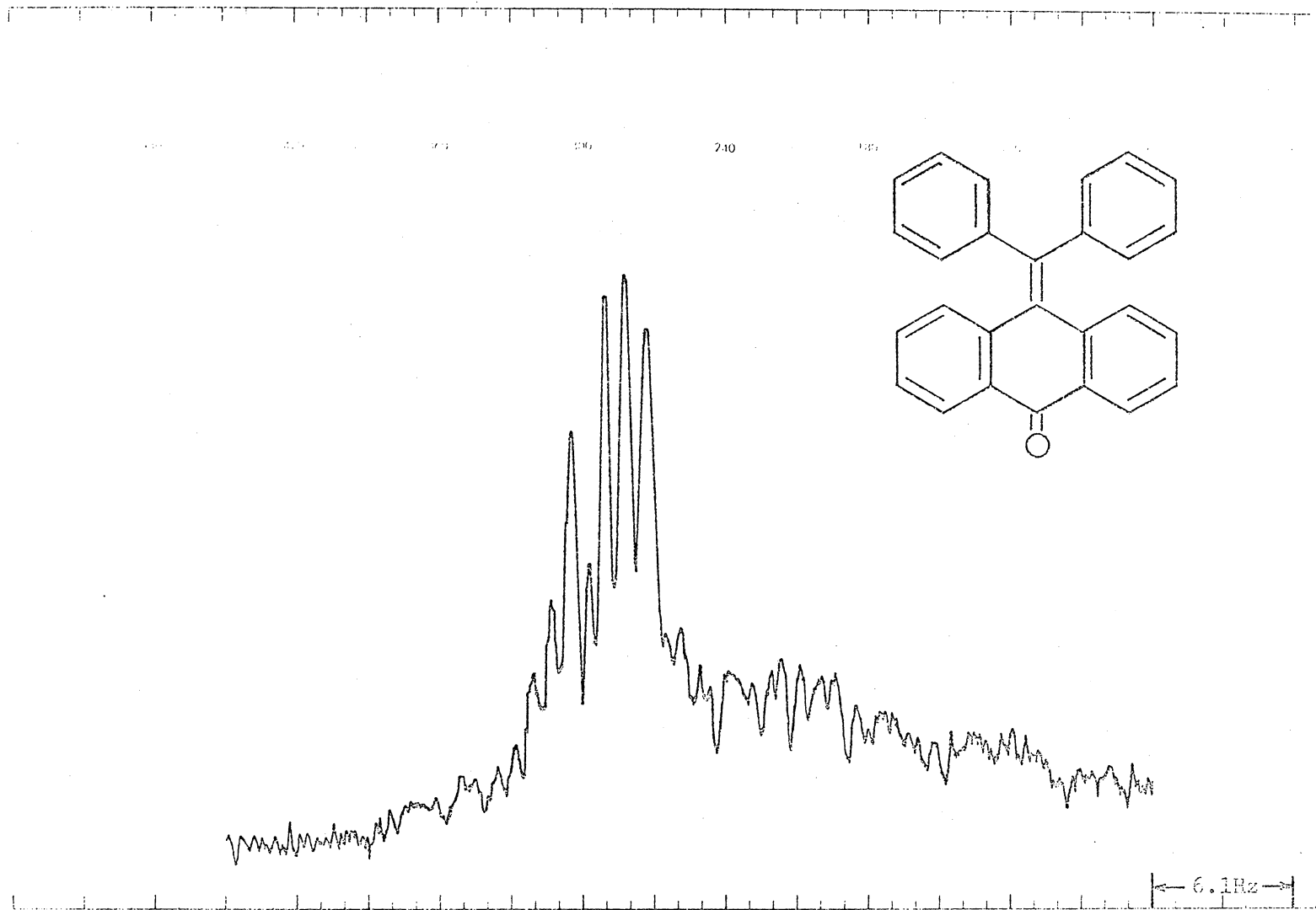


Figure 28. NMR Spectrum of Diphenylmethylenanthrone in Decalin at 180°C; sweep width 9.92 ppm.

## XII. BIBLIOGRAPHY

1. Agranat, I., Rabinovitz, M., Luckhurst, G. R., and Ockwell, J. N. J. Chem. Soc. (B), 294 (1970).
2. Allinger, N. L., and Stuart, T. W., J. Chem. Phys. 47, 4611 (1967).
3. Barnett, E. B., and Matthews, M. A., J. Chem. Soc. 123, 380 (1923).
4. Basu, R., Theoret. chim. Acta. (Berl.) 2, 215 (1964).
5. Becker, R. S., and Earhart, C. E., J. Am. Chem. Soc. 92, 5049 (1970).
6. Bergmann, E. D., Progress In Organic Chemistry, Vol. 3, Academic Press, Inc., New York (1955), p. 81.
7. Brockmann, H., and Muhlmann, R., Chem. Ber. 82, 348 (1949).
8. Bloembergen, N., Nuclear Magnetic Relaxation, W. A. Benjamin, Inc., New York (1961), p. 95.
9. Cizek, Jiri, Theoret. chim. Acta (Berl.) 6, 292 (1966).
10. Cohen, D., Millar, I. T., and Richards, K. E., J. Chem. Soc. (C), 793 (1968).
11. Drombrowski, L. J., Groncki, C. L., Strong, R. L., and Richtol, H. H., J. Phys. Chem. 73, 3481 (1969).
12. Edwards, T. G., and Grinter, R., Mol. Phys. 15, 357 (1968).
13. Flockhart, B. D., Scott, J. A. N., and Pink, R. C., Trans. Faraday Soc. 62, 730 (1966).
14. Grubb, W. T., and Kistiakowsky, G. B., J. Am. Chem. Soc. 72, 419 (1950).
15. Harnik, E., and Schmidt, G. M. J., J. Chem. Soc. 3295 (1954).
16. Hinze, J., and Jaffe, H. H., J. Am. Chem. Soc. 84, 540 (1962).
17. Hirota, F., and Nagakura, S., Bull. Chem. Soc., Japan 43, 1010 (1970).
18. Hirshberg, Y., J. Am. Chem. Soc. 78, 2304 (1956).

19. Ito, H., and I'Haya, Y., *Theoret. chim. Acta (Berl.)* 2, 247 (1964).
20. Jaffe, H. H., and Orchin, M., *Theory and Applications of Ultraviolet Spectroscopy*, John Wiley and Sons, Inc., New York (1962).
21. Klessinger, M., *Theoret. chim. Acta (Berl.)* 5, 236 (1966).
22. Kortum, G., and Bayer, G., *Chem. Ber.* 67, 24 (1963).
23. Kortum, G., and Koch, K. W., *Chem. Ber.* 100, 1515 (1967).
24. Kortum, G., and Krieg, P., *Chem. Ber.* 102, 3033 (1969).
25. Kortum, G., and Zoller, W., *Chem. Ber.* 103, 2062 (1970).
26. Kortum, G., Theilacker, W., and Braun, V., *Z. Physik. Chem. N. F.* 2, 179 (1954).
27. Kortum, G., Theilacker, W., and Schreyer, G., *Z. Physik. Chem. N. F.* 11, 182 (1957).
28. Kortum, G., Theilacker, W., Zeininger, H., and Elliehausen, H., *Chem. Ber.* 86, 294 (1953).
29. Koutecky, J., Cizek, J., Dubsy, J., and Hlavaty, K., *Theoret. chim. Acta (Berl.)* 2, 462 (1964).
30. Koutecky, J., Hlavaty, K., and Hochman, P., *Theoret. chim. Acta (Berl.)* 3, 341 (1965).
31. Kuboyama, A., and Wada, K., *Bull. Chem. Soc., Japan* 39, 1874 (1966).
32. Leibovici, C., and Deschamps, J., *Theoret. chim. Acta (Berl.)* 4, 321 (1966).
33. Lindner, P., and Martensson, O., *Theoret. chim. Acta (Berl.)* 7, 150 (1967).
34. Lorenz, R., Huber, J. R., and Wild, U., *Photochem. and Photobiol.* 10, 233 (1969).
35. Mallory, F. B., Wood, C. S., and Gordon, J. T., *J. Am. Chem. Soc.* 86, 3094 (1964).
36. Mataga, N., and Nishimoto, K., *Z. Physik. Chem.* 12, 335 (1957).

37. Michl, J., Koutecky, J., Becker, R. S., and Earhart, C. E., *Theoret. chim. Acta (Berl.)* 19, (1970).
38. Murrell, J. N., and McEwen, K. L., *J. Chem. Phys.* 25, 1143 (1956).
39. Nishimoto, K., and Forster, L. S., *Theoret. chim. Acta (Berl.)* 4, 155 (1966).
40. Nyburg, S. C., *Acta. Cryst.* 7, 779 (1954).
41. Nyburg, S. C., and Mills, J. F. D., *J. Chem. Soc.*, 308, 927 (1963).
42. Padova, M. R., *Ann. chim. Phys.* 19, 408 (1910).
43. Parr, R. G., *The Quantum Theory of Molecular Electronic Structure*, W. A. Benjamin, Inc., New York (1963).
44. Pilar, F. L., *Elementary Quantum Chemistry*, McGraw-Hill Book Company, New York (1968) Chaps. 18, 19.
45. Rabinovitz, M., Agranat, I., and Bergmann, E., *Tetrahedron Letters*, No. 18, 1265 (1965).
46. Sakamoto, K., and I'Haya, Y. J., *Theoret. chim. Acta (Berl.)* 13, 220 (1969).
47. Salem, L., *The Molecular Orbital Theory of Conjugated Systems*, W. A. Benjamin, Inc., New York (1966).
48. Schug, J. C., *Mol. Phys.* 19, 121 (1970).
49. Shimada, R., and Goodman, L., *J. Chem. Phys.* 43, 2027 (1965).
50. Singer, L. S., Lewis, I. C., Richerzhagen, T., Vincow, G., *J. of Phys. Chem.* 75, 290 (1971).
51. Steichen, J. C., M. S. Thesis, Virginia Polytechnic Institute, Blacksburg, Virginia, July (1969).
52. Stermitz, F. R., *Organic Photochemistry*, Marcel Dekker, Inc., New York 1, 248 (1967), ed. Chapman, O. L.
53. Streitwieser, A., Jr., *Molecular Orbital Theory for Organic Chemists*, John Wiley & Sons, Inc., New York (1961) p. 16.
54. Theilacker, W., Kortum, G., and Friedheim, G., *Chem. Ber.* 83, 508 (1950).

**The vita has been removed from  
the scanned document**

ELECTRONIC STRUCTURE OF PI-ELECTRON  
MOLECULES: HYDROCARBONS, QUINONES,  
THERMOCHROMIC ETHYLENES (NMR, ESR).

by

Peter Jeremy Schultz

(ABSTRACT)

The Pariser-Parr-Pople (PPP) method with configuration interaction including singly and doubly excited states (DCI) was used to calculate the electronic spectra of a variety of conjugated compounds. This method (PPP) of computing electronic wave functions has proven to be quite helpful in interpreting experimental data obtained from electronic absorption spectra. The wave functions of each molecule were assumed to meet the conditions of sigma-pi separability. Only the pi-electrons of carbon (or hetero) atoms were explicitly taken into consideration.

The configuration interaction procedure commonly includes interactions among singly excited configurations (MCI). The number of states increases formidably on including the doubly excited states. Generally it was impossible to include all the configurations. Several molecules with known electronic absorption spectra were analyzed to help determine how many configurations are needed and how they should be distributed between singly and doubly excited states. Consistently reasonable results were obtained when the total number of configurations was 80. A desirable combination of states was found to be about a 1:1 ratio of singly excited to

doubly excited states; furthermore, it was determined that configurations with more than 11.0 ev excitation energy do not have to be included.

Six hydrocarbons and four carbonyl compounds were treated. Agreement with experiment for benzene, naphthalene, anthracene, and trans-stilbene required an unusually low value for the one-center repulsion integral on carbon. The results for a series of p-quinones indicated that the inclusion of doubly excited states can substantially improve predictions when heteroatoms are present. Relatively minor changes in parameters were necessary in order to obtain reasonable agreement with experiment for p-benzoquinone, anthraquinone, p-naphthaquinone, benzophenone, cis-stilbene and dihydrophenanthrene intermediate.

The compounds 10,10'-bianthronylidene, 10,10'-bixanthenylidene, and diphenylmethylenanthrone which are thermochromic ethylenes were also treated. The interest in these compounds is as vivid as the colors they produce upon treatment by a variety of experimental procedures. Results were also obtained for a number of structures known to pertain to these systems. Which of the two configuration interaction procedures (MCI or DCI) was the better method for studying these large molecules was not established. Qualitatively, the results obtained by each procedure were the same. The calculations indicated that a single saturated bridge structure which is a valence isomer of the normal form was a probable structure for the colored form of a thermochromic

ethylene. The intense colors of sulfuric acid solutions were explained theoretically with a simple monoprotonated structure.

Magnetic resonance studies (NMR, ESR) were pursued to further investigate the thermochromic ethylenes. The studies involving acid solutions of the various compounds were particularly fruitful. The ESR spectrum of the hydrobianthrone radical was obtained when a pyridine solution of 10,10'-bianthranyl was refluxed. The formation of the bridge bond on the valence isomer of the ground state of 10,10'-bianthranylidene was predicted to occur in the process of quenching a conc. sulfuric acid solution on ice.